การผลิตแก๊สสังเคราะห์จากแกซิฟิเคชันร่วมของถ่านหินและชีวมวล

นางสาวสุภชิตา เกริกไกวัล

วิทยานิพนธ์นี้เป็นส่วนหนึ่งของการศึกษาตามหลักสูตรปริญญาวิทยาศาสตรดุษฎีบัณฑิต
สาขาวิชาเคมีเทคนิค ภาควิชาเคมีเทคนิค
คณะวิทยาศาสตร์ จุฬาลงกรณ์มหาวิทยาลัย
ปีการศึกษา 2555

SYNGAS PRODUCTION FROM CO-GASIFICATION OF COAL AND BIOMASS

Miss Supachita Krerkkaiwan

A Dissertation Submitted in Partial Fulfillment of the Requirements
for the Degree of Doctor of Philosophy Program in Chemical Technology
Department of Chemical Technology
Faculty of Science
Chulalongkorn University
Academic Year 2012

Thesis Title	SYNGAS PRODUCTION FROM CO-GASIFICATION OF COAL AND BIOMASS
By	Miss Supachita Krerkkaiwan
Field of Study	Chemical Technology
Thesis Advisor	Assistant Professor Prapan Kuchonthara, Ph.D.
Thesis Co-advisor	Professor Atsushi Tsutsumi, Ph.D.

Accepted by the Faculty of Science, Chulalongkorn University in Partial Fulfillment of the Requirements for the Doctoral Degree

…… Dean of the Faculty of Science
(Professor Supot Hannongbua, Dr. rer. nat.)

THESIS COMMITTEE

…… Chairman
(Associate Professor Kejvalee Pruksathorn, Dr. de L'INPT.)

…… Thesis Advisor
(Assistant Professor Prapan Kuchonthara, Ph.D.)

…… Thesis Co-advisor
(Professor Atsushi Tsutsumi, Ph.D.)

…… Examiner
(Associate Professor Pornpote Piumsomboon, Ph.D.)

…… Examiner
(Assistant Professor Prasert Reubroycharoen, Ph.D.)

…… External Examiner
(Suchada Butnark, Ph.D.)

สุภชิตา เกริกไกวัล: การผลิตแก๊สสังเคราะห์จากแกซิฟิเคชันร่วมของถ่านหินและชีวมวล. (SYNGAS PRODUCTION FROM CO-GASIFICATION OF COAL AND BIOMASS) อ.ที่ปรึกษาวิทยานิพนธ์หลัก: ผศ. ดร. ประพันธ์ คูชลธารา, อ.ที่ปรึกษาวิทยานิพนธ์ร่วม: Prof. Atsushi Tsutsuimi, Ph.D., 153 หน้า.

งานวิจัยนี้ศึกษากระบวนการไพโรไลซิสและแกซิฟิเคชันร่วมระหว่างถ่านหิน (ซับบิทูมินัส) และชีวมวล (ฟางข้าวและไม้กระถินยักษ์) ด้วยเตาปฏิกรณ์แบบเบดนิ่ง (drop-tube fixed bed reactor) โดยทำการศึกษาผลของอัตราส่วนระหว่างถ่านหินและชีวมวล, อุณหภูมิในการเกิดปฏิกิริยา และ ชนิดของชีวมวล ต่อร้อยละผลได้ของผลิตภัณฑ์, องค์ประกอบของแก๊สผลิตภัณฑ์ และคุณภาพของแก๊สผลิตภัณฑ์ พบว่า อันตรกิริยาระหว่างถ่านหินและชีวมวลก่อให้เกิดผลลัพธ์เชิงบวก (synergetic effect) ขึ้น ภายใต้สภาวะไพโรไลซิสและแกซิฟิเคชันด้วยไอน้ำ โดยส่งผลให้ได้ร้อยละผลได้ของผลิตภัณฑ์แก๊สเพิ่มขึ้น ในขณะที่ร้อยละผลได้ของน้ำมันทาร์และถ่านชาร์ลดลง โดยจะเห็นผลชัดเจนที่สุดที่อัตราส่วนระหว่างถ่านหินต่อชีวมวลเท่ากับ 1:1 โดยน้ำหนัก และอุณหภูมิในทำปฏิกิริยาเท่ากับ 800 องศาเซลเซียส นอกจากนี้ได้ทำการศึกษาอันตรกิริยาระหว่างถ่านชาร์จากถ่านหิน (coal char) และไอระเหยที่เกิดจากการไพโรไลซิสของชีวมวล (biomass derived tar) ในเตาปฏิกรณ์แบบเทอร์โมบาลานซ์ (rapid heating thermobalance reactor) โดยเตรียมถ่านชาร์จากถ่านหินที่ 3 สภาวะ ได้แก่ ไพโลไรซิสแบบช้า (Ex-char), ไพโรไลซิสแบบเร็ว (In-char) และการล้างด้วยกรด (Ac-char) พบว่า อัตราการเกิดปฏิกิริยาแกซิฟิเคชันด้วยไอน้ำของถ่านชาร์ลดลงอย่างมากเมื่อสัมผัสกับไอระเหยจากชีวมวล นอกจากนี้ยังได้ศึกษาผลเชิงเร่งปฏิกิริยาของถ่านชาร์จากถ่านหินต่อการสลายตัวของไอระเหยจากชีวมวลด้วยเตาปฏิกรณ์แบบเบดนิ่งสองขั้นตอน (two-stage fixed bed reactor) พบว่า ถ่านชาร์ที่เตรียมที่อุณหภูมิต่ำ จะแสดงผลเชิงเร่งต่อการสลายตัวของไอระเหยจากชีวมวลได้ดีกว่าถ่านชาร์ที่เตรียมที่อุณหภูมิสูง นอกจากนี้ยังพบว่า ถ่านชาร์จากถ่านหินจะแสดงผลเชิงเร่งได้ดีต่อการสลายตัวของไอระเหยที่มีโครงสร้างเป็นสารประกอบแอโรมาติกส์ขนาดใหญ่ จากผลดังกล่าวสามารถนำไปประยุกต์ใช้ในการออกแบบและดำเนินการ กระบวนการไพโรไลซิสและแกซิฟิเคชันร่วมระหว่างถ่านหินและชีวมวลได้อย่างมีประสิทธิภาพในอนาคต

ภาควิชา เคมีเทคนิค	ลายมือชื่อนิสิต
สาขาวิชา เคมีเทคนิค	ลายมือชื่อ อ.ที่ปรึกษาวิทยานิพนธ์หลัก
ปีการศึกษา 2555	ลายมือชื่อ อ.ที่ปรึกษาวิทยานิพนธ์ร่วม

5273907923: MAJOR CHEMICAL TECHNOLOGY
KEYWORDS: CO-GASIFICATION / COAL AND BIOMASS / VOLATILE-CHAR INTERACTION

SUPACHITA KRERKKAIWAN: SYNGAS PRODUCTION FROM CO-GASIFICATION OF COAL AND BIOMASS. ADVISOR: ASST. PROF. PRAPAN KUCHONTHARA, Ph.D., CO-ADVISOR: PROF. ATSUSHI TSUTSUMI, Ph.D., 153 pp.

In this work, the co-pyrolysis and co-gasification of Indonesian coal (sub-bituminous) and two types of biomass (rice straw and *Leucaena leucocepha*) were studied using a drop-tube fixed bed reactor. The synergetic effect in co-processing was manifested by the higher gas yield and lower tar yield compared to the predicted values from the experiments which used either coal or biomass alone. Results showed that the synergetic effect was found especially at a biomass and coal ratio of 1:1 and became more apparent when reaction temperature was increased. In addition, interaction between coal char and volatile derived from biomass was examined in a rapid heating thermobalance reactor. Three types of coal char were prepared i.e. slow pyrolyzed-coal char (Ex-char), fast pyrolyzed-coal char (In char) and acid washed-coal char (Ac-char) and three types of volatile sources were used (cellulose, xylan and rice straw). The results indicated that the steam gasification rate of Ex-char and In-char were significantly diminished by contacting with volatiles derived from all sources, especially from rice straw. However, in the case of Ac-char, the reduction of steam gasification rate with the appearance of volatiles was less dominant. It was due to the destruction of coal char structure and the loss of minerals on coal char surfaces. Moreover, the effect of coal char on the decomposition of biomass derived tar was also investigated in a two-stage fixed bed reactor. It was found that coal char exhibited the catalytic effect both on tar thermal cracking and tar steam reforming. Nevertheless, the catalytic role of char which was prepared under high pyrolysis temperature was less significant due to the loss of active structure on char. The obtained results will be useful for the effective design and operation of co-processing of coal and biomass.

Department : Chemical Technology Student's Signature .....
Field of Study : Chemical Technology Advisor's Signature .....
Academic Year : 2012 Co-advisor's Signature .....

ACKNOWLEDGEMENTS

I would like to express my deepest gratitude my supervisors, Asst. Prof. Prapan Kuchonthara and Prof. Atsushi Tsutsumi who reviewed this thesis during its preparation and offered many helpful suggestions, supervision and much encouragement throughout pass 3 years and 6 months of my research.

I would like to acknowledge Assoc. Prof. Kejvalee Pruksathorn, Assoc. Prof. Pornpote Piumsomboon, Asst. Prof. Prasert Reubroycharoen and Dr. Suchada Butnark for their participation on the dissertation chairman and members of thesis committee, respectively.

Sincerest appreciation also extends to The Royal Golden Jubilee Scholarship (Thailand Research Fund) for financial support of this research. Many thanks to Assoc. Prof. Chihiro Fushimi at Tokyo University of Agriculture and Technology and Dr. Hidetoshi Yamamoto at The University of Tokyo who offered the suggestions for my publications and many helpful about the experiment in Japan. And also thanks all Tsutsumi laboratory's member for their helpful advices, supports, encouragement and friendships during my period in Japan.

Finally, I wish to acknowledge the support of Dr. Sasithorn Sunphorka for suggesting about my thesis and encouragement of my beloved family who always beside me throughout Ph.D. period.

CONTENTS

PAGE

PAGE

PAGE

LIST OF TABLES

TABLE PAGE

LIST OF FIGURES

FIGURE PAGE

FIGURE PAGE

FIGURE PAGE

CHAPTER I

INTRODUCTION

1.1 Motivation

Gasification is a promising technology for producing gaseous fuel so-called "synthesis gas" from hydrocarbon-based materials. The produced gas can be applied for electricity generation and petrochemicals production such as methanol, dimethylether (DME) and Fisher-Tropsch oil. Coal, biomass, polymer/plastic and municipal wastes are typical sources for the gasification processes. Nowadays, coal is the main feedstock used for the gasification process because of its large reserve. Moreover, it is expected to be used as the energy resource for many decades ahead. However, coal utilization has been concerned about the environmental impacts. These problems were caused by the emission of toxic gases (H_2S, SO_x and NO_x) and the slagging problem from the fused-ash which was formed inside the gasifier. In contrast, biomass is a renewable energy resource which can be a substitute for coal to diminish the environmental impact and fossil fuel usage. Thailand is an agricultural based country with a vast supply of biomass resources. Most biomass including rice straw, rice husk, bagasse, palm oil waste and wood chips have been utilized for energy purposes such as combustion and gasification [1]. Unfortunately, gasification of biomass commonly confronts with several problems such as their seasonal harvesting rather than all year round availability, high transportation costs and lower fuel-qualification characters. Furthermore, the relatively high amount of tar in most biomass leads to corrosion in the piping and the decrease of overall gasification efficiency.

The co-utilization of coal and biomass is an interesting way to solve these problems. Recently, a number of studies have reported a synergetic effect in the co-processing of coal and biomass, in particular co-pyrolysis and co-gasification [2-9]. This synergy during the co-processing is probably due to the higher hydrogen and

carbon molar ratio (H/C) of biomass compared to coal, which could facilitate coal decomposition [2-4, 9]. Nevertheless, there is still a lack of any synergetic effect when using coal/biomass blends [10-14]. This obvious contradiction might depend on the operating parameters such as temperature, pressure, heating rate, type of reactor, type of coal, type of biomass and biomass blending ratio [2, 9, 10, 15-17]. In this study, the co-pyrolysis and co-gasification of Indonesian sub-bituminous coal and two types of biomass, rice straw (RS) and *Leucaena leucocepha* wood (LN), were carried out in a drop-tube fixed bed reactor. The samples (coal, biomass and coal/biomass blends) were instantly dropped. With this process, the heating rate of the particles was higher than other typical fixed-bed reactors. The effects of the biomass blending ratio, reaction temperature and biomass type on product distribution, gas composition and quality of the produced gas were studied. Their interaction in terms of the product distribution and gas composition were described by comparing between the experimental values obtained from the pyrolysis/gasification of coal or biomass alone and coal/biomass blends.

Moreover, volatile-char interaction between coal and biomass is an important key for ascribing the obvious synergetic effect. In order to establish an effective design and operation of co-pyrolysis/gasification, the volatile-char interaction is the one of essential considerations. In the previous studies, the volatile-char interaction on the steam gasification rate of Victorian brown coal have been investigated in a fluidized bed/fixed-bed reactor [18, 19] and in a bubbling fluidized bed reactor [20]. The volatiles released from coal pyrolysis as well as coal steam gasification showed the inhibition effect on the rate of char steam gasification because of the changing of char structure and char morphology. Furthermore, the reactivity of char has also been measured in a thermogravimetric analyzer (TGA) or thermobalance reactor to obtain the real time weigh loss of char and further analyze to the reactivity of char [21-23].

However, the effect of volatile on char reactivity by using the thermobalance reactor is still scarce, especially the operation at high heating rate. Fushimi et al. [24] who originated and modified the rapid heating thermobalance reactor into a two stage reactor (drop-tube/thermobalance fixed-bed reactor) investigated the effect of volatile on char reactivity concurrently to examine the effect of char on the volatile decomposition. The results previously reported that H_2 and the vapor phase of

levoglucosan had an inhibition effect on biomass char steam gasification resulting in the decrease of char steam gasification rate and gas evolution rate [24].

The effect of pyrolysis condition for char preparing step such as pyrolysis temperature, heating rate and holding time on char reactivity has been investigated in a number of studies. It was concluded that the reactivity of char was diminished when prepared at high pyrolysis temperature, slow heating rate and long holding time at the final pyrolysis temperature [25]. On the other hand, the alkali and alkaline earth metals (AAEM) on coal char surfaces was found to be the catalyst for coal char steam gasification [26]. However, the interaction of volatile and coal char which was prepared under the various conditions has not been studied yet. Therefore, three types of coal char were prepared in this study i.e. the slow pyrolyzed char (Ex-char), rapid pyrolyzed char (In-char) and the acid washed char (Ac-char) and three types of volatile sources such as cellulose, xylan and rice straw were selected.

Another point of view, the catalytic effect of char on tar reduction has been reported. Previously, the char was prepared from the pyrolysis of low-rank coal such as Brown coal [27, 28] and lignite [29] or the pyrolysis of biomass (charcoal) [30-32]. The attractiveness of char for tar reduction is that char production and tar reduction can be implemented simultaneously inside the gasifier by controlling the parameters and configurations [29]. Char exhibits some catalytic activities for tar reforming with its activity being, which was influenced by its surface area and the inherent mineral (Na, K, Ca and Mg) over char surfaces [27]. However, less attention has been paid to the catalytic effect of coal char on biomass derived tar. The knowledge about the interaction of coal char and biomass tar is expected to be useful for the design and operation of co-processing of coal and biomass.

Furthermore, the catalytic decomposition of biomass derived tar is relevant to its composition. Tar composition and structure have been reported to significantly rely on pyrolysis temperature [33, 34]. In this study, the catalytic effect of coal char on biomass derived tar reduction via thermal tar cracking and tar steam reforming was investigated, using a two-stage fixed bed reactor. The influences of biomass pyrolysis temperature were also explored.

1.2 Objectives

1. To study the synergetic effect between coal and biomass during co-pyrolysis/gasification at the various conditions.
2. To study the volatile-char interaction during co-pyrolysis/ and co-gasification

1.3 Scope of This Work

This work was separated into 3 parts. In part 1, the synergetic effect of coal and biomass during co-pyrolysis and co-gasification was carried out in a drop-tube fixed bed reactor. The effects of biomass to coal ratios (0:1, 1:3, 1:1, 3:1 and 1:0), reaction temperatures (600, 700 and 800^{O}C) and biomass types (rice straw and *Leucaena leucocepha*) on the synergetic effect in terms of product distribution, gas compositon and quality of the produced gas were investigated. In addition, the characterization of the pyrolytic products such as pyrolyzed char and tar was analyzed by BET, SEM, XRF and GC-MS methods. The steam gasification rate of the *in situ* pyrolyzed char was also determined in a rapid thermobalance reactor.

In part 2 and 3, the volatile-char interactions between coal char and biomass derived volatile were studied to clarify the obvious synergetic effect which was observed in part 1. In part 2, the volatile-char interaction study was explored in a thermobalance reactor which was modified to a drop-tube/thermobalance fixed bed reactor. The special function of this reactor is that the decrease of coal char weight can be promptly detected with the evolution of gas from the steam gasification of tar and char. Effect of the contact of volatiles on steam gasification rate of coal char was investigated together with the effect of coal char on the decomposition of tar derived from volatile sources. Three types of coal char i.e. slow heating pyrolyzed char (Ex-char), fast heating pyrolyzed char (In-char) and acid washed char (Ac-char) and three types of volatile source (cellulose, xylan and rice straw) were used in this part. The image of volatile-char interaction of each type of coal char was proposed.

In part 3, the catalytic effect of coal char on biomass derived tar decomposition was examined by using a two-stage fixed bed reactor. In this reactor, the temperature of biomass pyrolysis (upper part) and the catalytic cracking of char

(lower part) can be separately controlled by two electric furnaces. Two types of coal char including Ex-char and Ex-char800 were prepared. The Ex-char was prepared from coal pyrolysis at low temperature (600^{O}C) and Ex-char800 was prepared at high temperature (800^{O}C). The effect of pyrolysis temperature (600, 700 and 800^{O}C) on the catalytic cracking of tar over coal char surface (with and without external steam) was investigated.

CHAPTER II

THEORY AND LITERATURE REVIEWS

2.1 Gasification process

Gasification is the controlled partial oxidation of a carbonaceous material and it is achieved by supplying less oxygen than the stoichiometric requirement for complete combustion. Depending upon the processing design and operating conditions, low- or medium- value of producer gas, including combustible and non-combustible gases, is generated [35]. Gasification technology has been widely used to produce commercial fuels and chemicals. An impressive feature of this technology is its ability to produce a reliable high–quality syngas product that can be used for energy production or as a building block for chemical manufacturing process. The gasification process uses an agent such as air, oxygen, hydrogen or steam to convert carbonaceous materials into gaseous products. Figure 2.1 shows the gasification process with various agents and their products.

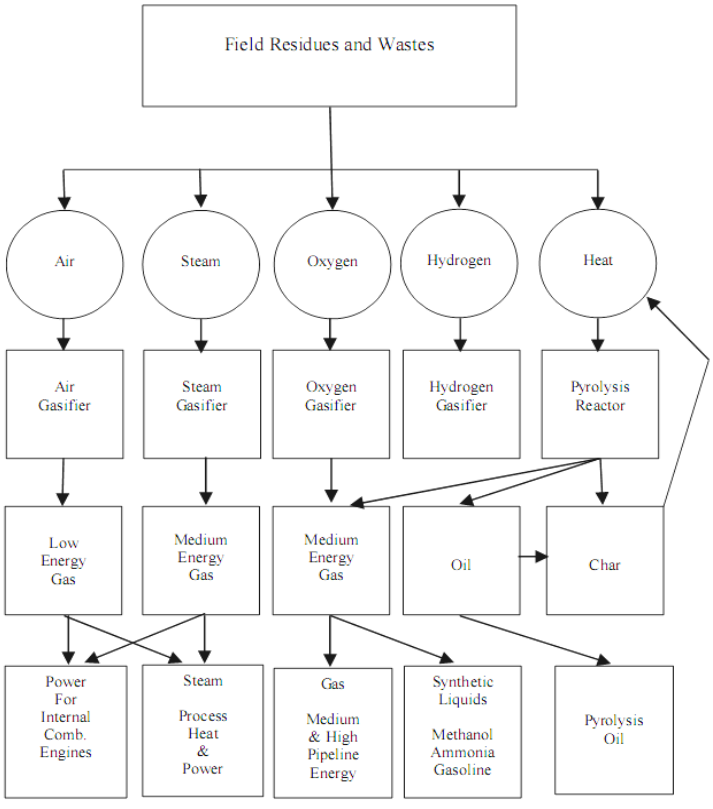

Figure 2.1 Gasification process with different gasifying agents and their products [35]

2.1.1 Feedstock

2.1.1.1 Coal

Coal retains its leading position as the predominant gasifier feedstock (51%). Petroleum provides 25% of feedstocks, with natural gas increasing to 22% due to the Pearl GTL in Qatar. All 11 plants currently under construction will be coal-fired. The syngas capacity of 40,432 MW that is in the planning stages for the 2011-2016 period, more than 70% is expected to be coal fed, with petcoke to account for almost all of the remaining 30% capacity growth [36]. World gasification plants and planed growth for 3 years ahead is shown in Figure 2.2. World gasification summary in 2011 classifying by the feedstock is shown in Table 2.1. It also showed that the major syngas production of the world was produced from coal gasification.

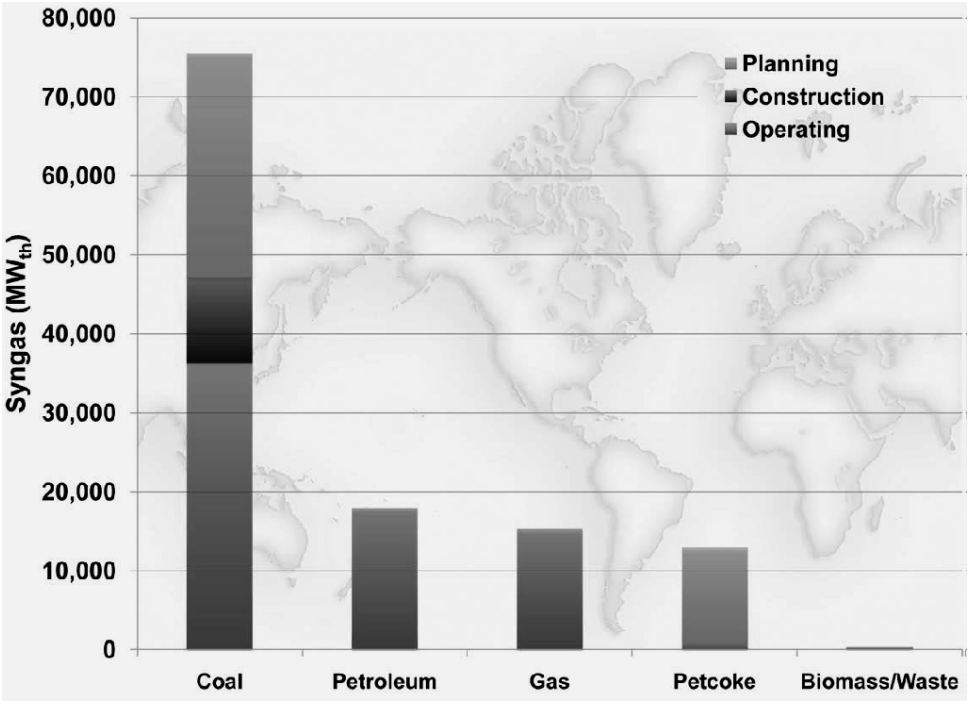

Figure 2.2 World gasification capacity and planned growth in 2010 [36]

Table 2.1 Summary of gasification industry classified by type of feedstock in 2011 [36]

Feedstock		Operating 2010	Construction 2010	Planned 2011-2016	Totals
Coal	Syngas Capacity (MW_{th})	36,315	10,857	28,376	75,548
	Gasifiers	201	17	58	276
	Plants	53	11	29	93
Petroleum	Syngas Capacity (MW_{th})	17,938			17,938
	Gasifiers	138			138
	Plants	56			56
Gas	Syngas Capacity (MW_{th})	15,281			15,281
	Gasifiers	59			59
	Plants	23			23
Petcoke	Syngas Capacity (MW_{th})	911		12,027	12,938
	Gasifiers	5		16	21
	Plants	3		6	9
Biomass/Waste	Syngas Capacity (MW_{th})	373		29	402
	Gasifiers	9		2	11
	Plants	9		2	11
Total Syngas Capacity (MW_{th})		70,817	10,857	40,432	122,106
Total Gasifiers		412	17	76	505
Total Plants		144	11	37	192

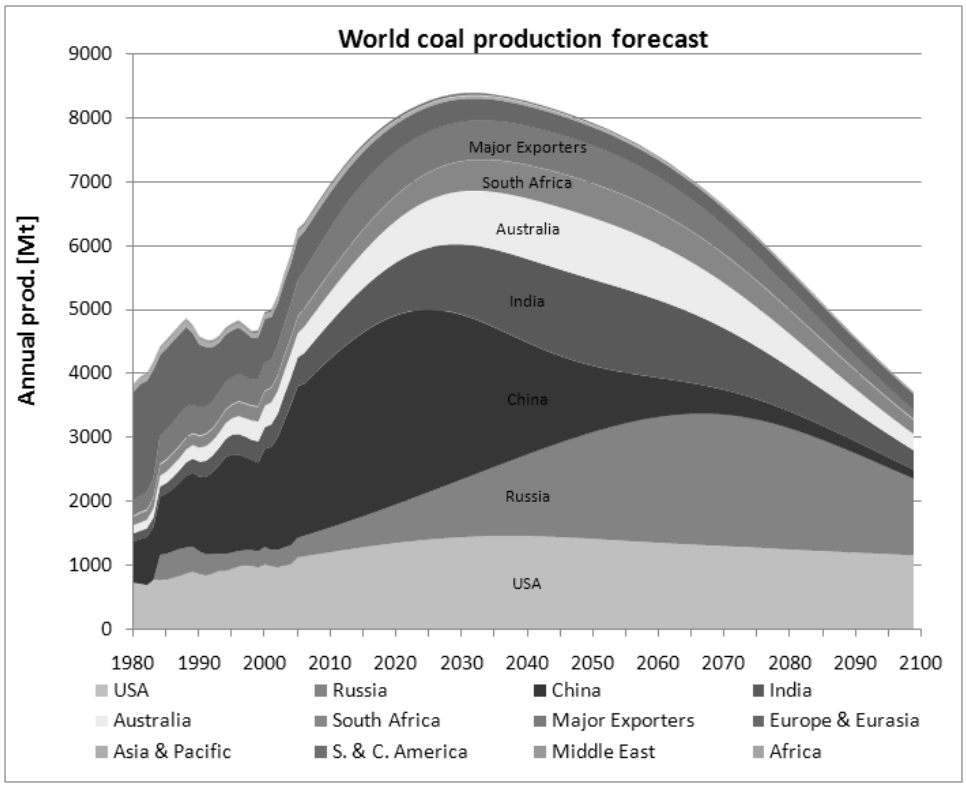

Figure 2.3 World coal production and forecast from 1980 to 2100 [37]

The forecast of coal production of the world classified by the region is shown in Figure 2.3. It can be seen that at present, coal mostly produced from the Australia and Asia region. But in the future coal will be produced from Russia and North America region. It reveals that coal is still the major feedstock for gasification process because of its large amount of reserve and can be used as fuel for many decades ahead.

The composition of coal is very complex and the types of coal considerably differ. The detailed petrographic composition of the organic part of coals, often characterized by a maceral analysis, has little influence on most gasification processes. Important for gasification are the age of coal, its cracking properties, its water content and its ash properties [38]. The classification of coal is presented in Table 2.2.

Table 2.2 Classification of coals [38]

Class	**Volatile matter (wt%)**	**Fixed carbon (wt%)**	**Heating value (HHV) (MJ/kg)**
Anthracite	<8	>92	36 - 37
Bituminous	8 - 22	78 - 92	32 - 36
Sub-bituminous	22 - 27	73 - 78	28 - 32
Brown coal (lignite)	37 - 35	65 - 73	26 - 28

2.1.1.2 Biomass

Biomass feedstock for energy may be based on existing food/feed crops (such as sugarcane sucrose or corn starch for ethanol; soybeans for biodiesel); on residues from existing food/feed crops (bagasse from sugarcane, corn stover); on residues and waste from forest (wood) products; and on organic municipal solid waste (MSW). However, the potential for dedicated “energy crops” is the most important to be considered and each region may have a different set of options. The use of wastes will not present any conflict (land availability) with food production [39]. The global distribution of land by region and used in 2009 is shown in Figure 2.4. Overall, approximately 10% was dedicated to produce arable crops, over a quarter was used for pasture (to produce meat, milk and wool), and forestry accounted for ~30% is a

broad category that includes all other uses, including barren land and built-up areas [40]. Note that the Arable means the area under temporary agricultural crops, Pasture is the permanent fields and pastures either cultivated or growing wild. Forest is the areas spanning more than 0.5 hectares with trees higher than 5 meters. The other lands are the land cannot classify as Agricultural land and Forest area, includes built-up related, barren land, other wooded land, etc.

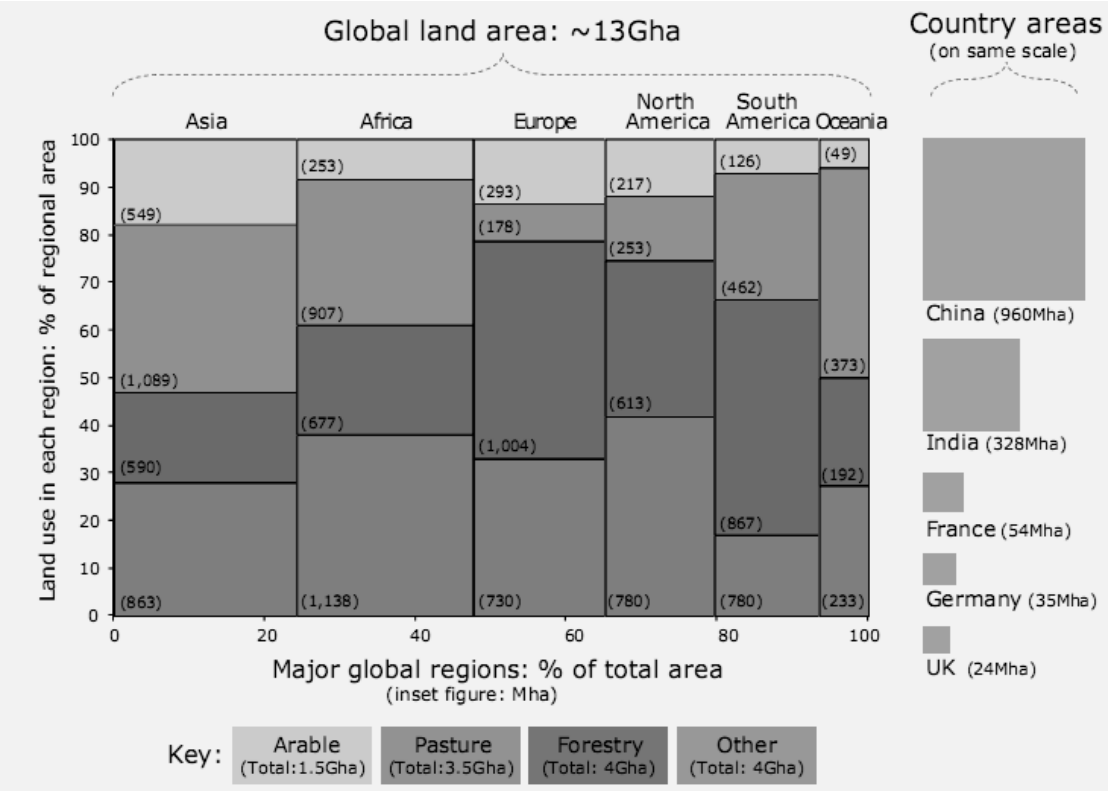

Figure 2.4 Global distribution of land by region and used in 2009 [40]

The biomass sources are categorized in Table 2.3. At the global level, the categories most often included energy crops, forestry, residues from forestry, residues from agriculture and wastes [41]. The conversion process of biomass to energy is also summarized in Figure 2.5. There are two main processes i.e. thermochemical conversion and biochemical conversion processes. Each type of the conversion process shows the different process operation and provides the different product distribution and quality as shown in Figure 2.5.

Table 2.3 Sources and categories of biomass feedstocks [40-42]

	Classification		**Biomass source**
Energy crops	Conventional crops		Annual crops: cereals, Oil seed rape, sugar beet
	Perennial energy crops		Short rotation coppice (willow or poplar); plantation tree crops e.g. eucalyptus; energy grasses: switch grass
Primary residues	Forestry and forestry residues		Short rotation forestry
			Wood chips from branches, tips and poor quality crops
	Agricultural crop residues		Straw from cereals, oil seed rape and other crops
	Secondary residues	Sawmill co-product	Wood chips, sawdust and bark from sawmill opearations, stemwood,
		Arboricultural arising	wood chips from municipal tree surgery operations
Wastes	Tertiary residues	Waste wood	Clean and contaminated waste wood
		Organic waste	Paper/card, food/kitchen, garden/plant and textiles wastes
		Sewage sludge	From wasted-water treatment works
		Animal manures	Manures and slurries from cattle, pigs, sheep and poultry
		Landfill gas	Captured gases from decomposing

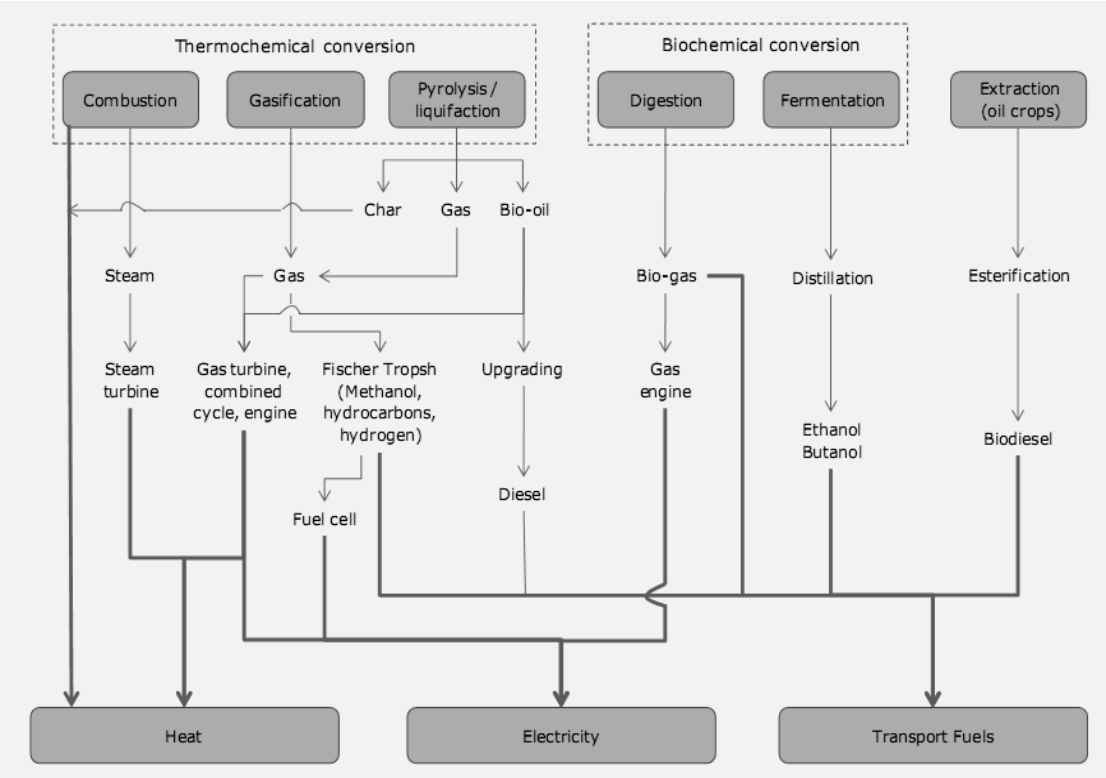

Figure 2.5 The overall biomass conversion process [43]

Thermochemical processes preferentially use dry feedstock and include combustion, gasification and pyrolysis. Combustion involves the complete oxidation of biomass to provide heat. This may be used directly or may be used to produce steam and generate electricity. Gasification involves the partial oxidation of the biomass at high temperature (>500^{O}C) and yields a mixture of CO and H_2 (syngas) along with some CH_4, CO_2, water and small amounts of N_2 and heavy hydrocarbons [44]. The quality of the gas depends on the temperature of the gasification process: a higher temperature process will yield more syngas with fewer heavy hydrocarbons. Pyrolysis involves heating biomass in the absence of oxygen at temperature up to 500^{O}C and produces an energy-dense bio-oil along with some gaseous and char products.

Biochemical conversion pathways use microorganisms to convert biomass into methane or simple alcohols, usually in combination with some mechanical or chemical pretreatment step. Anaerobic digestion is a well established technology and is suited to the conversion of homogenous wet wastes that contain a high proportion

of starches and fats. Fermenting sugars and starches to alcohols using yeast is also fully mature technology. Woody biomass can also potentially be used as feedtock for both anaerobic digestion and fermentation processes but requires an additional pretreatment step in order to release the sugar that these feedstocks contain. At present, these technologies are being demonstrated but are not yet fully mature.

2.1.2 Coal and biomass situation in Thailand

The production of energy in Thailand, 2009 classified by type of fuels is shown in Table 2.4. It can be seen that the growth percentage of coal decreased from the previous data, whilst, the renewable energy including biomass is increasing. It can be estimated that in the future the renewable energy will become the substitute energy resources for the fossil fuels.

Table 2.4 Energy production in Thailand classified by type of fuels [45]

ENERGY PRODUCTION	QUANTITY (ktoe)			GROWTH (%)	
	2008	2009	2010^{p}	2009	2010^{p}
Energy Production	62,695	64,890	71,429	3.5	10.1
• Commercial Energy	42,509	44,263	49,148	4.1	11.0
- Crude Oil	7,320	7,585	7,655	3.6	0.9
- Lignite	4,743	4,775	4,771	0.7	(0.1)
- Natural Gas	24,969	26,525	31,061	6.2	17.1
- Condensate	3,900	3,792	4,467	(2.8)	17.8
- Hydro and Others*	1,577	1,586	1,194	0.6	(24.7)
• Renewable Energy and Other **	21,188	20,627	22,281	2.2	8.0

Thailand has coal reserve more than 2,000 Mtons, accounted as measured reserve at 1,100 Mtons and most of coal sources are at the northern part. The coal rank will be at lignite, sub-bituminous, bituminous and some of anthracite but at a small amount found in Loei of the northeast region. Thailand has imported the high quality coal, mostly of Bituminous due to the exported coal source of this region are of bituminous production with a good quality. In 2001, more than a half of total coal

import value was of bituminous, followed by anthracite, coke and semi-coke respectively. The highest import is from Indonesia about 65 percent, the rest are imported from Vietnam, Myanmar, Australia, China, Laos and others in order. Coal selection depends on coal quality and transport distance, therefore coal will be imported from our neighboring countries for purchasing the good quality coal at reasonable prices [46]. The reserved amounts of lignite in the northern of Thailand is about 2 Gton, in 2010, is estimated for electricity production for 100 years ahead with the present production rate [47].

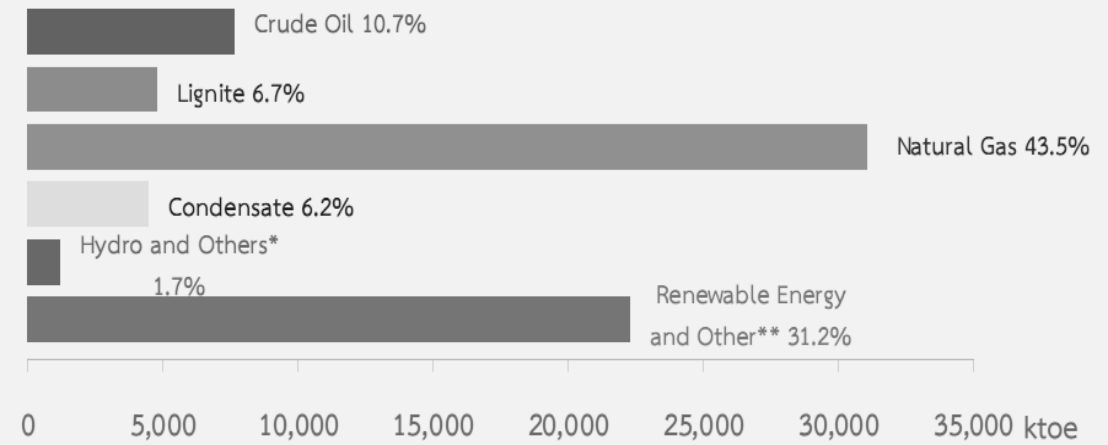

* Others include geothermal, solar cell and wind power.

** Including fuel wood, charcoal, paddy husk, bagasse, agricultural waste, garbage, biogas, biofuel, black liquor and residual gas from production processes.

p: preliminary data.

Figure 2.6 Energy production in Thailand, 2010 [45]

Domestic coal applications are limited in direct combustion and as raw material in production process and thermal uses in 2 production sectors as power sector and industrial sector. Majority of coal consumption will be in power generation sector by 81 percent and the rest are used by industrial sector by 19 percent, rank by ascending consumption of cement, paper, fiber, food, lime, tobacco, metal, battery and others. In 2010, lignite/coal consumption totally 35 million tons, increasing by 1.2% from that in 2009 (based on the heating value), divided into consumption of lignite at 18 million tons and of imported coal of 17 million tons [48].

Renewable energy consumption in Thailand (2009) is summarized in Figure 2.7. Biofuel, mainly produced from biomass, showed the higher consumption from 602 to 804 ktoe from 2008 to 2010. It indicates that in the future the demand of renewable energy resources such as biomass is continuously increasing.

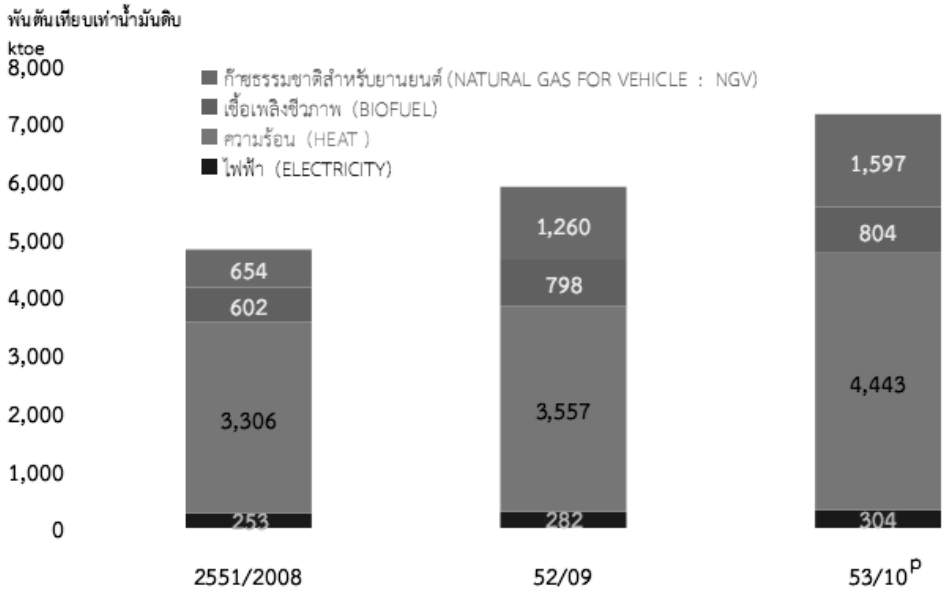

Figure 2.7 Consumption of renewable energy resources in Thailand (2009) [45]

The total capacity of electricity generation by using alternative energy in Thailand is shown in Figure 2.8.

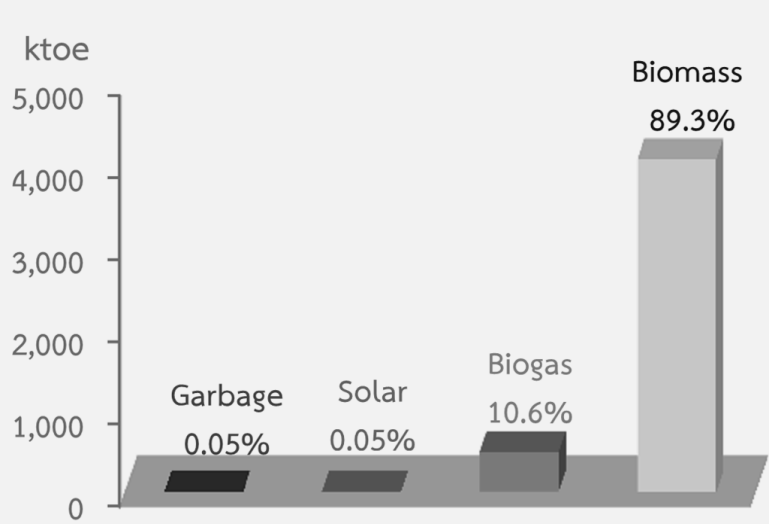

Figure 2.8 Total capacity of electricity generation by using alternative energy in Thailand (2011) [49]

It showed that the total capacity of electricity from the alternative energy resource was 2,157 MW, up 14.7% from the previous year. Biomass power plants were the greatest share 82.6% of the total installed capacity, followed by biogas, small hydro power, solar energy, garbage, and wind energy shared 7.3%, 4.4%, 4.2%, 1.2%, and 0.3% respectively [49]. Sugarcane and rice straw are the highest potential biomass in 2011, as can be seen in Table 2.5.

Table 2.5 Energy potential of solid biomass in Thailand (2011) [49]

Biomass		**Total production (ktoe)**	**Percentage (%)**
Industrial	Top, Trashier	7,760.81	20.592
Sugarcane	Bagasse	5,374.55	14.260
Rice	Paddy husk	2,485.42	6.595
	Straw	12,541.68	33.277
Maize	Stalk, Top, Leaves	1,558.84	4.136
	Cob Maize	346.18	0.919
Cassava	Stalk	978.47	2.596
	Root	760.37	2.018
	Frond	837.74	2.223
Oil Palm	Fiber	900.16	2.388
	Shell	1,079.03	2.863
	Empty bunches	851.59	2.260
Coconuts	Husk	231.60	0.615
	Frond, empty bunches	216.97	0.576
Groundnuts	Shell	4.62	0.012
Cotton	stalk	2.28	0.006
Soybeans	Stalk, leaves, shell	68.41	0.182
Sorghum	Leaves, stem	31.49	0.084
Charcoal		658.59	1.747
Para rubber	Fuel wood	304.48	0.080
	Frond, leaves	98.33	0.261
	Saw dust	28.41	0.075
Pineapple	stalk	568.81	1.509

2.1.3 Chemical Reactions

The gasification of solid fuels such as coal and biomass proceeds primarily via a two-step process, pyrolysis followed by gasification (Figure 2.9). Pyrolysis, also known as devolatilization, is the decomposition of the feedstock by heat. It is endothermic reaction. The main product from pyrolysis step is volatile product (more than 75 – 90 %) which is separated into the non-condensable gases and condensable liquids. The remaining solid, called char, contains high carbon content.

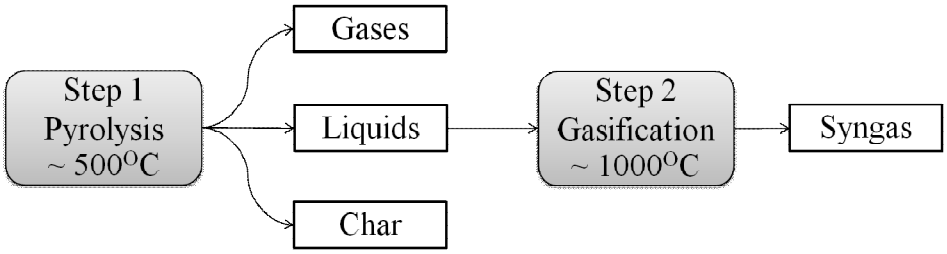

Figure 2.9 Gasification step [50]

The volatile hydrocarbons and char are subsequently converted into synthesis gas (syngas) in the second step, called gasification. During the process of gasification of solid fuels, the principal chemical reactions are those involving carbon (C), carbon monoxide (CO), carbon dioxide (CO_2), hydrogen (H_2), water (or steam) and methane (CH_4) [38]. These are:

Combustion reactions

$$C + \tfrac{1}{2}O_2 = CO \qquad \text{-111 MJ/kmol} \qquad (2.1)$$

$$CO + \tfrac{1}{2}O_2 = CO_2 \qquad \text{-283 MJ/kmol} \qquad (2.2)$$

$$H_2 + \tfrac{1}{2}O_2 = H_2O \qquad \text{-242 MJ/kmol} \qquad (2.3)$$

Boudouard reaction

$$C + CO_2 = 2CO \qquad \text{+172 MJ/kmol} \qquad (2.4)$$

Water gas reaction

$$C + H_2O = CO + H_2 \qquad \text{+131 MJ/kmol} \qquad (2.5)$$

Methanation reaction

$$C + H_2 = CH_4 \qquad \text{-75 MJ/kmol} \qquad (2.6)$$

The reactions with free oxygen are all essentially complete under gasification conditions reactions following Eqs. (2.1) to (2.3). However those reactions are not related to the determination of the composition of syngas at equilibrium. Three heterogeneous (i.e. gas and solid phase) reactions (2.4) to (2.6) are sufficient to determined the syngas composition.

In general, we are concerned with situations where the carbon conversion is also essentially complete. Under this circumstance, we can reduce equations (2.4) to (2.6) by following two homogeneous gas reactions:

CO shift reaction

$$CO + H_2O = CO_2 + H_2 \qquad \text{-41 MJ/kmol} \tag{2.7}$$

and

steam methane reforming

$$CH_4 + H_2O = CO + 3H_2 \qquad \text{+206 MJ/kmol} \tag{2.8}$$

Reactions (2.1), (2.4), (2.5) and (2.6) describe the four ways in which a carbonaceous or hydrocarbon fuel can be gasified. Reaction (2.4) is important for the production of pure CO when gasifying pure carbon with an oxygen/CO_2 mixture. Reaction (2.5) plays a predominant role in the water gas process. Reaction (2.6) is the basis of all hydrogenating gasification processes. But most gasification processes rely on a balance between reaction (2.1) (partial oxidation) and (2.5) (water gas reaction).

For real fuels, including coal which also contains hydrogen, the overall reaction can be written as:

$$C_nH_m + {}^{n}\!/\!_{2}\,O_2 = nCO + {}^{m}\!/\!_{2}\,H_2 \tag{2.9}$$

where,

- for gas, as pure methane, m=4 and n=1, hence m/n=4
- for oil, m/n ≈2, hence m=2 and n=1
- for coal, m/n≈1, hence m=1 and n=1

A simplified reaction sequence for coal or biomass gasification can be also described as in Figure 2.10.

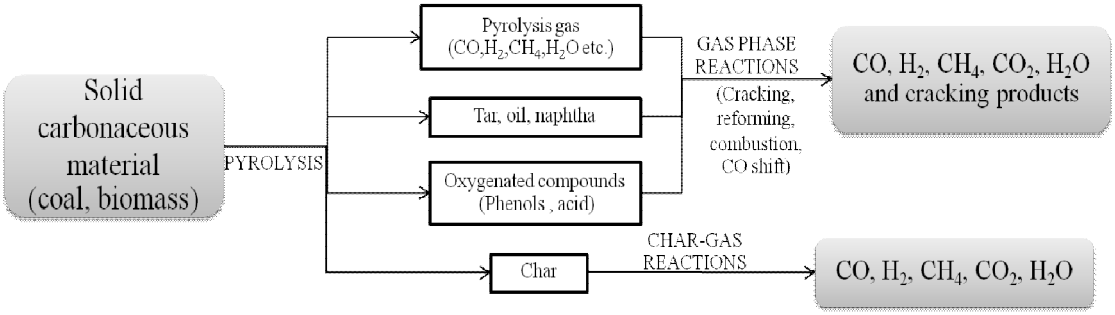

Figure 2.10 Reaction sequence for gasification of coal or biomass [51]

The first step, pyrolysis or devolatilization step, takes place already at low temperature (350 -800 ^{O}C) and in parallel with the heating up of the coal particles. The heating rate of the coal particles influences the way in which the devolatilization takes place. The rate of devolatilization is dependent not only on the heating rate but also on the particle size and the rate of gasification by the water gas reaction and also influence by on the reaction temperature and the partial pressure of steam. The devolatilization of coal produces a variety of species such as tar, hydrocarbon liquid and gases including CH_4, CO, H_2, H_2O and HCN. This material reacts with the oxidant surrounding the coal particle. The extent rate of reaction between solid fuel and oxidant depends on the amount of volatile produced.

In combustion environment, where there is an overall excess of oxygen, the combustion of the volatiles is complete. There is a recirculation of synthesis gas in many gasifiers, not only in fluidized-bed but also in entrained-flow reactors. Combustion of solid fuel occurs in the vicinity of the burner. There are the combustion flue gas, which consists mainly of carbon dioxide, water vapor and nitrogen, produce along with the generating heat. The carbon dioxide and water vapor have a moderate effect which resulting in the reducing of temperature. On the other hand, the recycled gas contains significant quantities of carbon monoxide and hydrogen for the case of gasification that will cause locally high temperatures.

The slowest reaction in gasification governs the overall conversion rate which are the heterogeneous reactions with carbon such as water gas, Boudouard and hydrogenation as presented above in equations (2.4) to (2.6). The rates of reaction for the water gas and Boudouard reactions with char are comparable and are several orders of magnitude faster than the hydrogenation reaction [52].

2.1.4 Gasification reactor (Gasifier)

In the practical realization of gasification process a broad rank of reactor types has been used. The gasification reactor types can be grouped into 3 categories: moving-bed gasifier, fluidized-bed gasifier and entrained-flow gasifier [53] as shown in Figure 2.11.

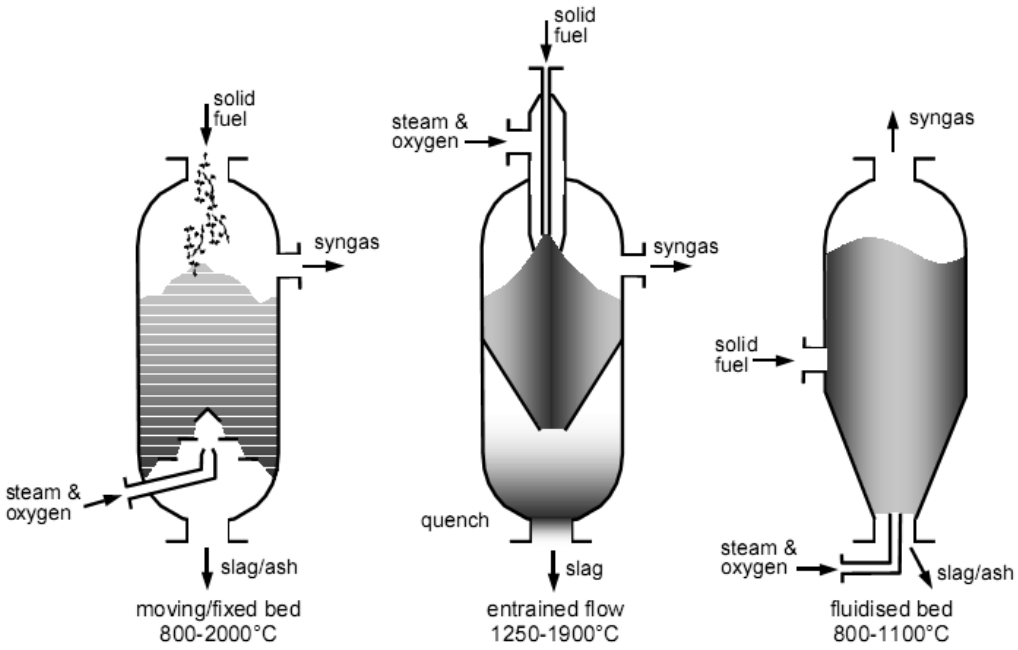

Figure 2.11 Typical gasifier types [53]

Moving-bed gasifier (sometimes called fixed-bed gasifier) are characterized by a bed in which the coal moves slowly downdraft under gravity as it is gasified by a blast that is generally in a counter-current blast to the coal. In such a counter-current arrangement, the hot synthesis gas from the gasification zone is used to preheat and pyrolyze the downward flowing coal. With this process the oxygen consumption is very low but pyrolysis products are present in the synethesis gas. The outlet temperature of the synthesis gas is generally low, even if high, slagging temperatures are reached in the middle of the bed. Moving-bed processes operate on the lump coal. An excessive amount of fines, particularly if the coal has strong caking properties, can block the passage of the up-flowing syngas. The flow arrangement of two types fixed bed gasifer is shown in Figure 2.12.

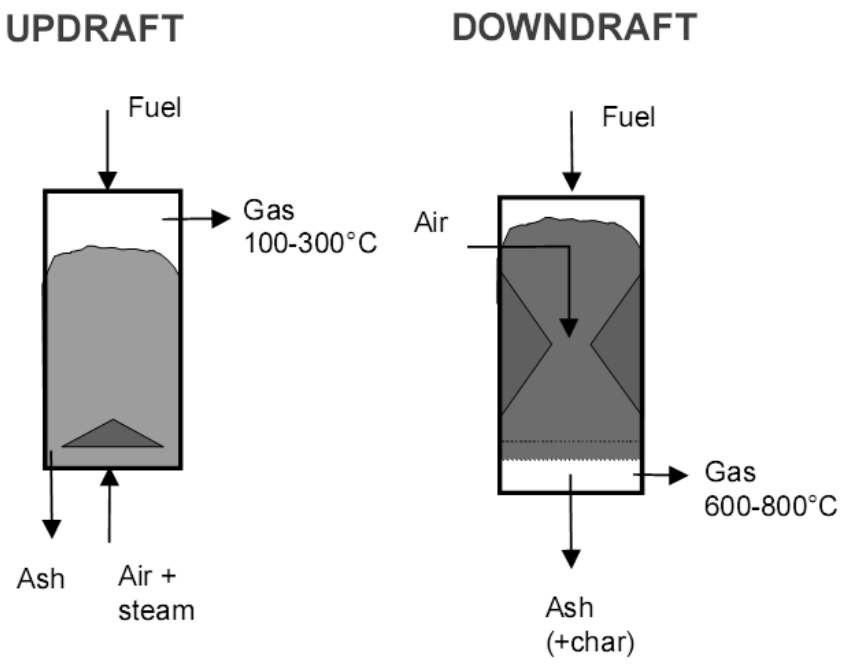

Figure 2.12 Conventional fixed-bed gasifier types [54]

Fluidized-bed gasifiers offer extremely good mixing between feed and oxidant, which promotes both heat and mass transfer. This ensures an even distribution of material in the bed, and hence a certain amount of gasifying agent may reflect on the limitation of carbon conversion of fluidized-bed processes. The operation of fluidized-bed gasifiers is generally restricted to temperatures below the softening point of the ash since ash slagging will disturb the fluidization of the bed. Some attempts have been made to operate into the ash softening zone to promote a limited and controlled agglomeration of ash with the aim of increasing carbon conversion. Sizing of the particles in the feed is critical; material that is too fine will trend to become entrained in the syngas and leave the bed overhead. This is usually partially captured in a cyclone and returned to the bed. The lower temperature operation of fluidized-bed processes means that they are more suited for gasifying reactivity feedstocks such as low-rank coals and biomass.

Entrained-flow gasifiers operate with feed and blast in co-current flow. The residence time in these processes is too short (a few second). The feed is ground to a size of 100 μm or less to promote mass transfer and allow transport in the gas. Given the short residence time, high temperature and required to ensure a good conversion

and therefore all entrained-flow gasifiers do not have any specific technical limitations on the oxygen consumption to levels where alternative processes may have an economic advantage. The characteristics of gasifier types are summarized in Table 2.6.

Table 2.6 Characteristics of different categories of gasification process [55]

Category	**Moving-bed**		**Fluidized-bed**		**Entrained-flow**
Ash conditions	Dry	Slagging	Dry ash	Agglomerating	Slagging
Typical processes	bottom Lurgi	BGL	WinKler, HTW,CFB	KRW, U-gas	BGL
Feed characteristics					
Size	6 – 50 mm	6 – 50 mm	6 – 10 mm	6 – 10 mm	<100 μm
Acceptability of fine particles	Limited	Injection	Good	Better	Unlimited
Acceptability of Caking coal	Yes	Yes	Possibly	Yes (with stirrer)	Yes
Preferred coal rank	Any	High	Low	Any	Any
Operating characteristics					
Outlet gas temperature(^{O}C)	Low (425–650)	Low (425–650)	Moderate (900–1050)	Moderate (900–1050)	High (1250–1600)
Oxidant demand	Low	Low	Moderate	Moderate	High
Steam demand	High	Low	Moderate	Moderate	Low
Other characteristics	HC in gas	HC in gas	Lower C-conversion	Lower C-conversion	pure gas, high C conversion

Interestingly, there is a greater variety of arrangements for the gasification of coal or biomass/waste. Figure 2.13 shows a number of other arrangements that are either well established or continue to be developed [56].

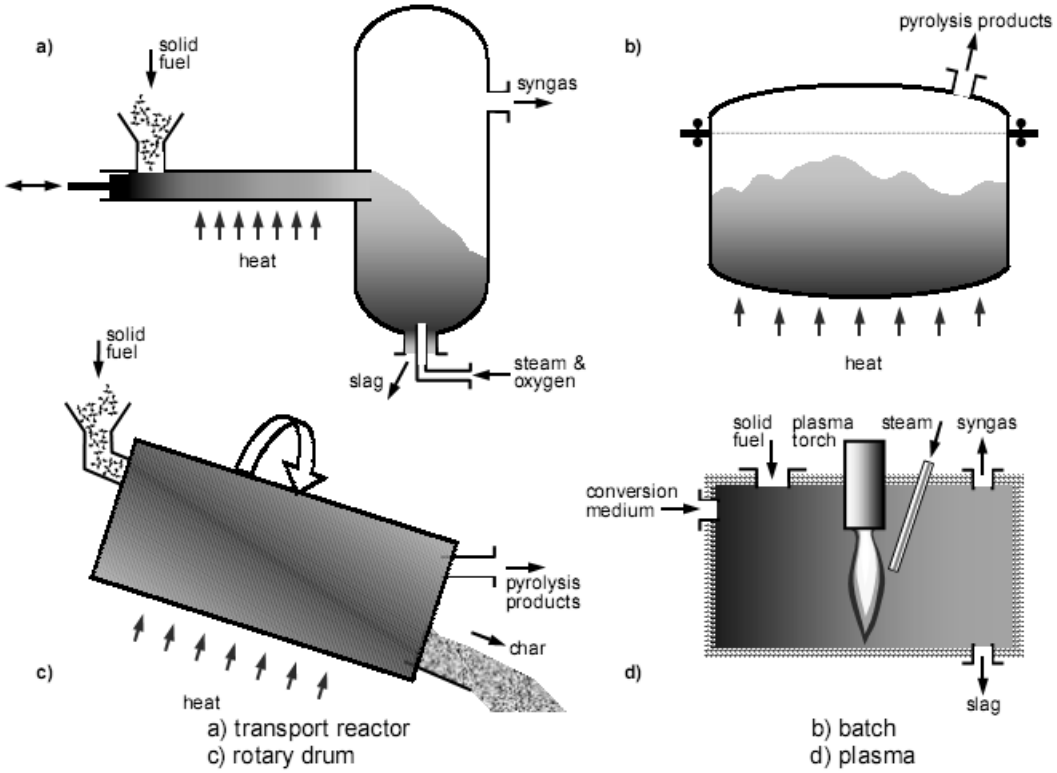

Figure 2.13 Alternative gasifier types [56]

2.1.5 Application of synthesis gas

The composition of syngas will vary based on many factors, including reactor type, feedstock and processing conditions. The option of the produced syngas is shown in Figure 2.14. There are two main purposes for syngas either power generation or chemical production. The characteristics of syngas for any applications are summarized in Table 2.7.

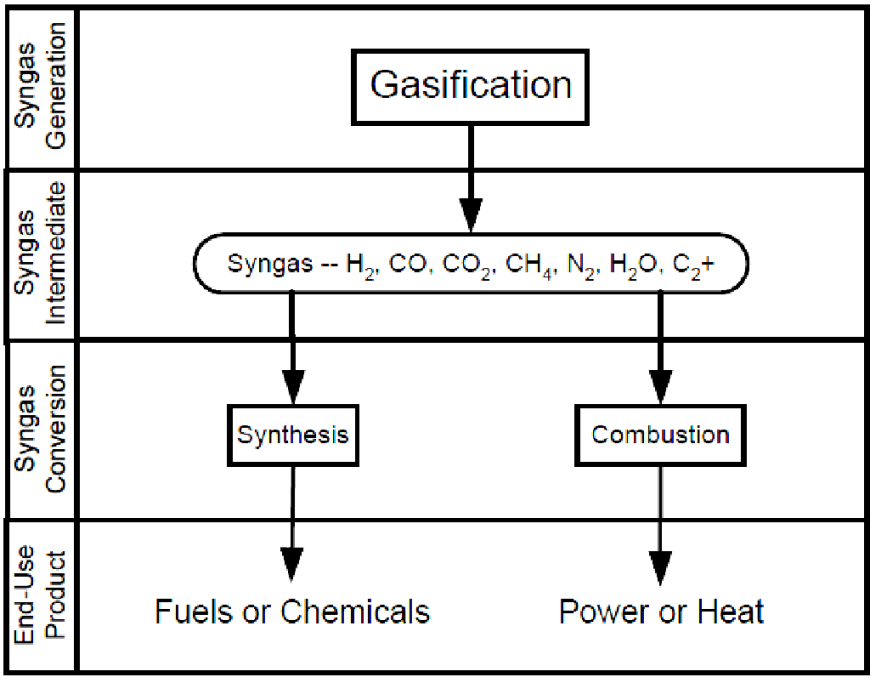

Figure 2.14 Syngas application options [50]

2.1.5.1 Application for gaseous fuel

Power generation can be accomplished via gasification of coal or biomass, followed by a combustion engine, combustion turbine, steam turbine or fuel cell. These systems can produce both heat and power (CHP-combined heat and power) and can achieve greater system efficiencies in the range of 30 to 40 %. The power generation scheme employed establishes syngas specifications. There is more latitude with regard to syngas composition for engine combustion than for turbine combustion. Gas turbines have emerged the best means for transforming heat to mechanical energy and are now key component of the most efficient electric generating system. To ensure maximum flexibility for industrial or utility applications, syngas heating value requires to be above 11 MJ/m^3. As indicated in Table 2.7 below, the high hydrocarbon content corresponds to the higher heating value for the syngas. IGCC (Integrated Gasification Combined-Cycle) with Carbon Capture and Storage (CCS) technology allows coal or biomass to be used to generate power as cleanly as natural gas. The schematic image of IGCC plant is shown in Figure 2.15.

Table 2.7 Characteristics of the syngas for different application [50]

	Synthetic fuel	**Methanol**	**Hydrogen**	**Gaseous fuel**	
	FT Gasoline and Diesel			Boiler	Turbine
H_2/CO	0.6 [a]	~2.0	High	Unimportant	Unimportant
CO_2	Low	Low [c]	Not important [b]	Not critical	Not critical
Hydrocarbon	Low [d]	Low [d]	Low [d]	High	High
N_2	Low	Low	Low	Note [e]	Note [e]
H_2O	Low	Low	High[f]	Low	Note [g]
Contaminant	<1 ppm Sulfur low particulates	<1 ppm Sulfur low particulates	<1 ppm Sulfur low particulates	Note [k]	Low particulates Low metal
Heating Value	Unimportant [h]	Unimportant	Unimportant [h]	High [l]	High
Pressure, bar	~20-30	~50 (liquid phase) ~140 (vapor phase)	~28	Low	~400
Temperature, ^oC	200-300 [j] 300-400	100-200	100-200	250	500-600

(a) Depends on catalyst type.

(b) Water gas shift will have to be used to convert CO to H_2, CO_2 in syngas can be removed at same time as CO_2 generated by the water gas shift reaction.

(c) Some CO_2 can be tolerated if the H_2/CO ratio is above 2.0; if excess H_2 is available, the CO_2 will be converted to methanol.

(d) Methane and heavier hydrocarbons need to be recycles for conversion to syngas and represent syngas inefficiency.

(e) N_2 lowers the heating value, but level is unimportant as long as syngas can be burned with a stable flame.

(f) Water is required for the water gas shift reaction.

(g) Can tolerate relatively high levels; steam sometimes added to moderate combustion temperature to control NO_x.

(h) As long as H_2/CO and impurities levels are met, heating value is not critical.

(i) Efficiency improves as heating value increases.

(j) Depends on catalyst types

(k) Small amounts of contaminants can be tolerated.

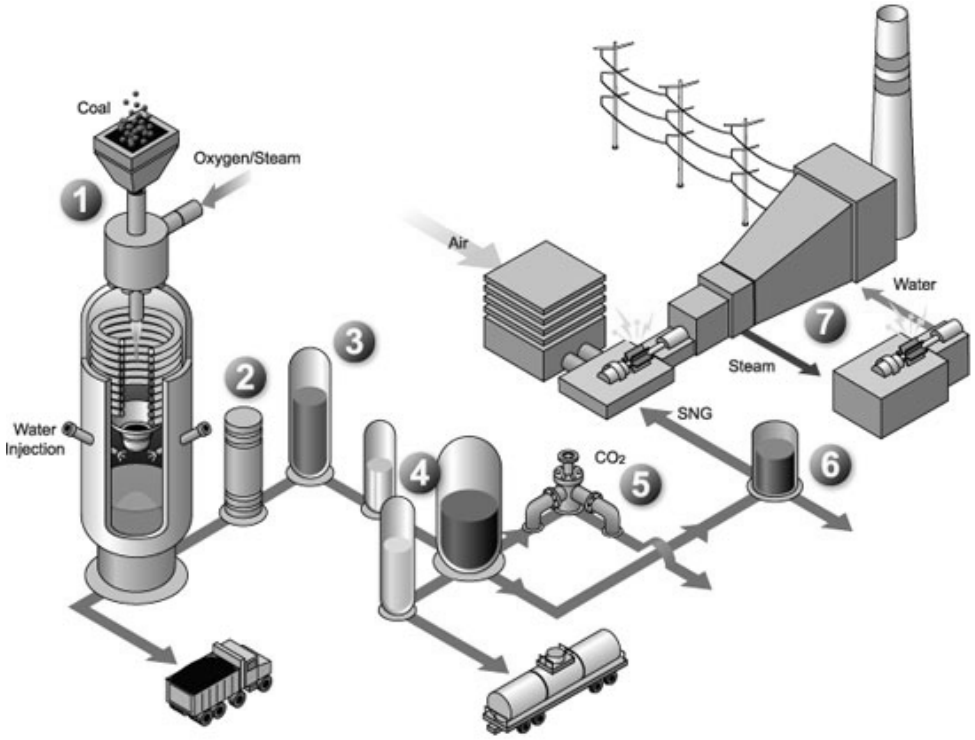

Figure 2.15 Integrated Gasification Combined-Cycle (IGCC) [7]
(1) Gasification unit, (2) Particulate scrubber (3) Steam shift vessel (4) Contaminate absorber, (5) Saline geologic reservoir, (6) Methanation unit (7) Steam turbine

2.1.5.2 Hydrogen production

Hydrogen is currently produced in large quantities via steam reforming of hydrocarbons over a Ni catalyst at $800^{O}C$. This process produces a syngas that must be further processed to produce high purity hydrogen. The syngas conditioning required for steam reforming is similar to that which would be required for a gasification derived syngas, however, tars and particulates are not as much of a concern. To raise the hydrogen content, the product syngas is fed to one or more water gas shift (WGS) reactors, which convert CO to H_2. The gas stream leaving the first WGS stage has CO content of about 2%; in a second stage this is reduced further to about 5000 ppm. The remaining CO can be removed by a pressure swing adsorption (PSA).

2.1.5.3 Methanol synthesis

The formation of methanol from syngas is taking place according to the following two main equations, methanol synthesis (Eq. 2.10) and water Gas shift reaction (Eq. 2.7) as shown above.

$$CO + 2H_2 = CH_3OH \tag{2.10}$$

The methanol synthesis is exothermic, a higher methanol yields are obtained at lower temperature and higher pressure. Usually, CO is preferred over CO_2 as a reactant by all copper catalysts, and one aims at producing syngas with the highest possible CO and lowest possible CO_2 content, securing the theoretically optimal stoichiometric number (SN) as following $\quad SN = \frac{[H_2]-[CO_2]}{[CO]-[CO_2]} = 2.0 \tag{2.11}$

This is the stoichiometric amount of hydrogen required for methanol synthesis. For kinetic reasons, however, a certain minimum quantity of CO_2 (2.5 to 3.5 vol%) must be present in practice to attain a high CO conversion. As a function of the CO_2 content in the syngas, the CO conversion rises rapidly to a maximum, where after it drops slightly up to a CO_2 concentration of about 12 vol%. Above 12 vol% CO_2 is droped more steeply. Using several commercial copper-based catalysts, it could be proven that no methanol can be produced using syngas without CO_2 and from which all water was withdrawn. At high CO_2 concentrations, it reduces the catalyst activity, however, by inhibiting methanol synthesis [57]. Figure 2.16 shows a simplified process flow depicting the use of LPMEOH™ with IGCC for MeOH and power co-production.

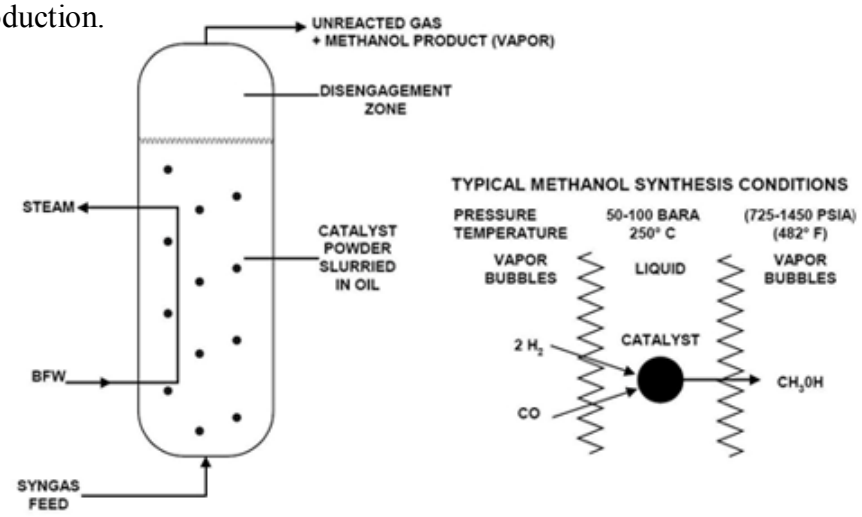

Figure 2.16 LPMEOH™ with IGCC for MeOH and power co-production [58]

2.1.5.4 Fisher-Tropsch synthesis

Synthetic fuels such as gasoline and diesel can be produced from synthesis gas via the Fischer-Tropsch (FT) process. There are several commercial FT plants in South Africa producing gasoline and diesel, both from coal and natural gas, and a single plant in Malaysia feeding natural gas. The FT synthesis involves the catalytic reaction of H_2 and CO to form hydrocarbon chains of various lengths (CH_4, C_2H_6, C_3H_8, etc.). The FT synthesis reaction can be written in the general form following,

$$(n/2 + m)H_2 + mCO \rightarrow C_mH_n + mH_2O \qquad (2.12)$$

when only paraffins are formed, and 2m when only olefins are formed. Iron catalyst has water-gas shift (WGS) activity, which permits the use of low H_2/CO ratio syngas. Gasifier product gases with a H_2/CO ratio around 0.5 to 0.7 is recommended as a feed to the FT process when using iron catalyst. The WGS reaction adjusts the ratio to match requirements for the hydrocarbon synthesis and produce CO_2 as the major by-product. On the other hand, cobalt catalysts do not have WGS activity, and the H_2 to CO ratio required is then (2m + 2)/m. Water is the primary by product of FT synthesis over a cobalt catalyst. The general diagram of FT process is shown in Figure 2.17.

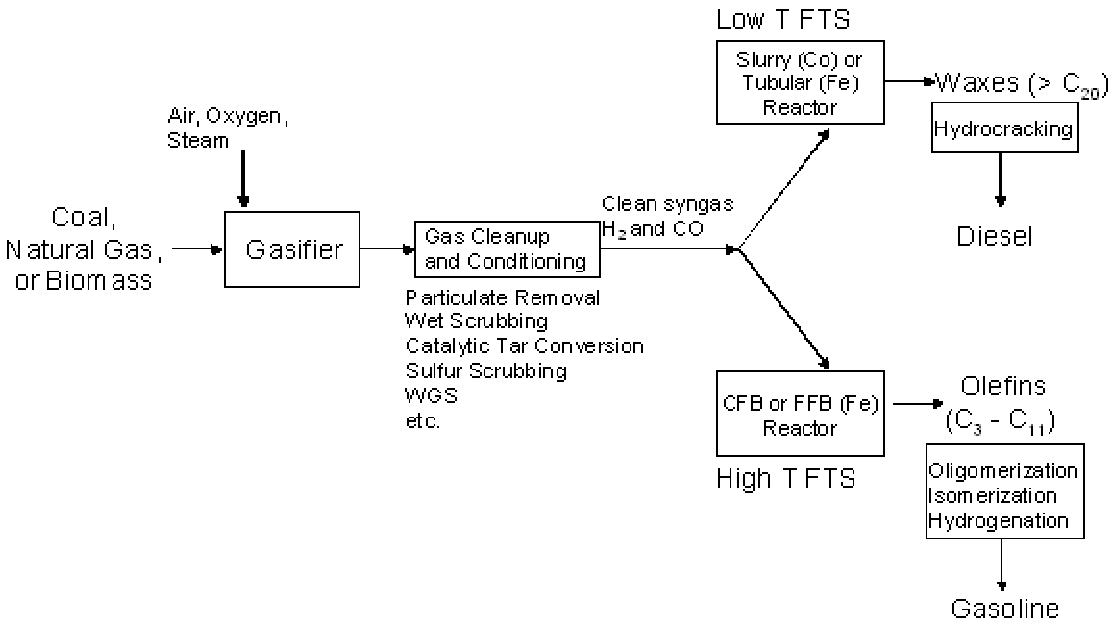

Figure 2.17 Production of liquid fuels by Fisher-Trosch process [59]

2.2 Co-utilization of coal and biomass

2.2.1 Challenge and advantages

Co-gasification of coal and biomass is a relatively new area of research. Preliminary results from several pilot studies have shown promising results in terms of quality of the syngas and reduced environmental impact. Although coal is the world's most plentiful fossil fuel and is extensively used in power generation, it has had a serious impact on the environment as evidenced by acid rain caused by SO_x, and NO_x emissions. Emissions of the greenhouse gas CO_2 during coal combustion have also become a major global concern. Biomass has lower energy content than coal. However its use for energy production can significantly contribute to the reduction of net CO_2 emissions. These two fuels, when co-gasified, exhibit synergy with respect to overall emissions, including greenhouse gas emissions, without sacrificing the energy content of the product gas.

Biomass, whether as a dedicated crop or a waste-derived material, is renewable. However, the availability of a continuous biomass supply can be problematic. For example, crop supply may be decreased by poor weather or by alternative uses, and the availability of a waste material can fluctuate depending on variations in people's behavior. With co-gasification, adjusting the amount of coal fed to the gasifier can alleviate biomass feedstock fluctuations. This approach may also allow biomass feedstocks to benefit from the same economies of scale as achieved with coal gasification that may be necessary for the economic production of fuels, chemicals and hydrogen.

2.2.2 Reviews of co-pyrolysis and co-gasification of coal and biomass

Recently, a number of studies have reported a synergetic effect in the co-processing of coal and biomass, in particular co-pyrolysis and co-gasification [2-9]. For co-pyrolsyis, the synergetic effects, in terms of the decreased char and increased tar yields, were observed in many types of reactor such as a free fall reactor [2], a high-frequency furnace [16], the special chamber with rapid heating rate reactor [15] and fixed-bed reactor [3]. The previous study also revealed that at higher biomass blending ratio and the relatively lower temperature (~600 ^{O}C) are more in favor of the obvious synergies during the co-pyrolysis of coal and biomass which tested in a free

fall reactor [2]. In addition, the intrinsic and morphological structure of the residual char obtained from co-pyrolysis was developed resulting in the increase of char gasification rate [16]. The chars obtained from co-pyrolysis of coal and biomass also has been prepared for the smokeless solid fuels because of its low volatile and sulfur contents [6]. In addition the devolatilization behavior during co-pyrolysis of coal and pine wood was deducted by using pyrolysis GC/MS (py-GC/MS) and TGA analysis [60]. It revealed that the liquid products derived from the co-pyrolysis contained the lower aromatics and higher phenol compounds compared to the case of pure coal pyrolysis [60].

Nevertheless, some studies have reported a lack of any significant synergetic effect when using coal/biomass blends [10-14]. This apparent discrepancy might depend on the operating parameters used, such as temperature, pressure, heating rate, type of reactor, type of coal, type of biomass and biomass blending ratio [2, 9, 10, 15-17]. In a conventional thermobalance reactor (or typical fixed-bed reactor), the devolatilization of coal and biomass particles takes place at different time due to the slow heating rate of ~10 ^{O}C min^{-1} [13, 61]. Moreover, the rapid heating rate in a fluidized bed reactor could shorten the time lag of devolatilization and the contact time between the pyrolytic products from coal and biomass is relatively short [14], which likely explains why no synergetic effect was observed in those studies.

Moreover, the gasification rate of the chars obtained from co-pyrolysis of coal and straw with CO_2 and steam was investigated. It was reported that the gasification rate of char derived from co-pyrolysis significantly increased compared to the gasification rate of coal pyrolysis alone because of the relatively high potassium content in the co-char [7]. This result agreed with CO_2 gasification rate the char obtained from co-pyrolysis of coal and biomass with biomass to coal ratio of 1 : 4 [16].

The previous co-gasification of coal and biomass studies were carried out both in the lab scaled and pilot plant. The synergetic effect in terms of product gas yield, carbon conversion and cold gas efficiency were observed in a dual fluidized-bed reactor [62, 63], bench-scale fluidized bed reactor [8] and downdraft fixed-bed reactor[4]. These studies were operated at the atmospheric pressure. The synergetic effect in their study was pronounced when increasing temperature and steam to fuel

ratio. The maximum calorific value of the produced gas that can be achieved was about 13.77 – 14.39 MJ/m^3 when operating at 800^{O}C and biomass blending of 50wt% [62]. Aigner et al. also studied co-gasification of coal and biomass in a dual fluidized bed gasifier. They mentioned that their process performed well in 100kW dual fluidized bed gasifier and the further cleaning process for the flue gas is not necessary because of the relatively low amount of NH_3 and H_2S after blended biomass with coal [63].

The upgrading of low-grade coal (black coal) and refused coal into the high quality solid fuels for gasification process was investigated by mixing with pine chip [8]. The higher low heating value of gas product (LHV) increased 23% and 18 % for pine chip/low-grade coal and pine chip/refused coal blends, respectively [64]. Kumabe et al. reported that the cold gas efficiency (CGE) was increased from 65 to 85% for the co-gasification of coal and biomass in a downdraft fixed-bed gasifier. The application of the produced gas was dependent on biomass blending ratio in the feedstock. At low biomass ratio, the produced gas was favorable for the production of methanol whilst the produced gas was suitable for dimethylether (DME) when increasing biomass ratio in the total weight of feed [4]. Li et al. also studied the stabilization of co-gasification process of coal and biomass in a bench-scale fluidized bed and reported that a continuously stable operation could be gained when the biomass ratio was no more than 33wt% resulting in the highest gasification efficiency was about 60.92% [65]. In addition, co-gasification at high pressure (15 Mpa) has been studied in a bench scaled-fluidized bed reactor [66]. It revealed that the synergetic effect in terms of the increased CO and H_2 in syngas was observed when blending a small amount of biomass (about 10 wt%) with coal and a petroleum coke. High-pressure co-gasification of coal (sub-bituminous and bituminous) and sawdust has also been explored in a pilot-scale fluidized bed reactor with pressure 3.03 Mpa [67]. It was reported that the transport properties of coal/biomass blend was improved compared with feed coal alone.

2.3 Reviews of volatile-char interactions

Volatile-char interaction during co-pyrolysis and co-gasification of coal and biomass is an important consideration for the effective design and operation. From the previous studies, the volatile-char interaction during co-processing of coal and biomass has not been clearly mentioned. However, there are a number of literatures have been reported about the effect of volatiles on the reactivity of char in the gasification of coal or biomass alone. In addition, the effect of char as a catalyst for tar reduction has also been studied. The details of those studies will be presented below.

2.3.1 Inhibitory effect of volatiles on char reactivity

During steam gasification of char obtained from the pyrolysis of Victorian brown coal, the non-catalytic gasification underwent in parallel with the catalytic gasification by the mineral species on char surfaces [20]. The presence of H_2 or the H-radicals from the thermal cracking of volatiles could inhibit the steam gasification rate of char for non-catalytic gasification [20]. This result showed an agreement with the inhibition effect of the steam gasification of biomass derived char by hydrogen. Fushimi et al. reported that the increase of partial pressure of hydrogen could inhibit the steam gasification rate of biomass char and more significant inhibition effect was observed when feeding the volatiles from the pyrolysis of levoglucosan [24]. Therefore, the inhibition of volatiles on char gasification rate is very important and strongly influenced on the progression of char gasification. However, the catalytic effect of AAEM such as Na, K, Ca and Mg on char surfaces could be accelerated the steam gasification of char itself [68, 69]. In parallel with the catalytic gasification of char, the volatilization of AAEM was promoted by the contact of volatile. The volatilization of Na and K was more promoted by volatiles than the volatilization of Mg and Ca on coal char [70, 71]. Potassium has been reported as a catalyst for coal char steam gasification [69, 72]. The deactivation of K on coal char by volatiles can be reduced by addition some calcium species on char surfaces resulting in the increase of char steam gasification rate [72]. Kinetic of CO_2 gasification with the presence of CO and steam gasification with the presence of H_2 were proposed by Hung et al [73]. They revealed that the Langmuir-Hinshelwood (L-H) kinetic equation was applicable

to describe the inhibition effect of CO and H_2 on char gasification and the active site for CO_2-char and H_2O-char gasification was separated.

The evolution of char structure with the presence of volatiles (mostly H-radicals) was investigated in a one-stage fluidized bed reactor. The result showed that H-radicals from the volatiles could penetrate into coal char matrix and promoted condensation reaction resulting in the production of larger aromatic hydrocarbon [18]. Mechanism for steam gasification of the low-rank fuels with the presence of volatiles was summarized by Kajitani et al. as is shown in Table 2.8 [74].

Table 2.8 Mechanism for steam gasification of low-rank fuels [74]

	(I) Non-catalytic gasification	**(II) Catalytic gasification**
	$C + H_2O \rightarrow CO+H_2$	$C+H_2O \rightarrow CO+H_2$
		$CM–M+H \rightarrow CM–H + M$
(i) Dissociative adsorption of steam	$C_f + H_2O \rightarrow C(H) + C(OH)$	$M+ H_2O \rightarrow M(H) + M(OH)$
	$C_f + C(OH) \rightarrow C(O) + C(H)$	$C+ M(OH) \rightarrow C(O) + M(H)$
(ii) Dissociative adsorption of Hydrogen	$C(H) \leftrightarrow C_f+1/2H_2$	$M(H) \leftrightarrow +M +1/2\ H_2$
(iii) Desorption of carbon monoxide	$C(O) \rightarrow CO$	$C(O) \rightarrow CO$
(iv) Adsorption of free radicals from volatiles	$C_f+H \rightarrow C(H)$	$M+H \rightarrow M(H)$
(v) Volatilization of catalyst (Na)		$M(H) \rightarrow CM–H+ M_{gas}$
		$M \rightarrow M_{gas}$
(III) Condensation of aromatics ring		
Smaller aromatics ring system + nH → Bigger aromatics ring system (≥6 fused ring)		
(IV) Deposition of coke from volatiles		
Volatiles → C + Gases		

Note: C_f, M and CM donated the active site of carbon in char, the active site of the catalyst, which is AAEM (especially Na or K), and char matrix, respectively.

2.3.2 Catalytic effect of char on tar reduction

Recently, the catalytic effect of char on tar reduction has been investigated in many literatures. Most of these literatures used the char derived from the pyrolysis of biomass, called charcoal because of its high porosity and high content of minerals, such as AAEM. Gillbert et al. investigated the minimization of tar over hot char bed during the pyrolysis of biomass in a new fixed bed gasifier. It revealed that the carbon in the condensable phase reduced more than 66% compared to the absence of char. Moreover, the decrease of heavy condensates was observed when temperature was increased from 500 to 800^{O}C [31]. The catalytic effect of charcoal, which produced from the pyrolysis of pine wood, on tar reduction during pyrolysis was also mentioned by Sun et al. They reported that the catalytic effect of charcoal would be dominant for the cracking temperature of 500 – 600^{O}C but the thermal effect was more significant at 650 – 700^{O}C [29]. The decomposition of model compound of tar such as phenol and naphthalene over the biomass char was also conducted comparing with the using of other catalyst bed (dolomite, olivine and spent fluid catalytic cracking catalyst (FCC)) [30]. It reported that the biomass char was an effective catalyst for tar reduction that provided the highest naphthalene conversion among the other types of catalyst and could be continuously produced during the gasification process [30].In addition, wood char has been used as the catalyst for the decomposition of methane to increase the H_2 composition in the syngas obtained from biomass gasification. It revealed that wood char was suggested to be the cheapest and greenest catalyst for CH_4 conversion providing the CH_4 conversion of 70% at 100^{O}C and it also can be reproduced in the system [75].

A few of studies interested to investigate the catalytic effect of coal char on the coal gasification and coal pyrolysis. Zhang et al. studied the effect of char on tar reforming during coal pyrolysis by feeding char and raw coal simultaneously [27]. The catalytic effect of char was observed by means of the increase of tar conversion. Preparing coal char with the presence of steam provided the high surface area of char causing the extensive catalytic behavior on tar reduction [27]. Tar reforming of the nascent tar during the pyrolysis of brown coal with the presence of nascent char was investigated. It mentioned that not only the effective structure of coal char but the inherent mineral on coal char such as Na and Ca were also the significant parameter

affecting the improvement of tar steam reforming [76]. Mechanism of the catalytic effect of char on the decomposition of some aromatics was proposed by Hosokai et al [77]. They revealed that the aromatics were decomposed over the charcoal by coke formation resulting in the decrease of the catalytic activity of char. However, the gasification of the formed coking simultaneously occurred to produce gaseous products. Therefore, for maintaining the activity of char, the rate of coke steam gasification should be equivalent or greater than the rate of coke formation [77]. Unfortunately, no literature has been investigated the catalytic effect of coal char on the decomposition of biomass derived tar. This volatile-char interaction will be useful for the operating and design the co-processing between coal and biomass.

CHAPTER III

EXPERIMENTAL APPARATUS

AND ANALYTICAL METHOD

3.1 Materials

3.1.1 Fuel samples and chemicals

Indonesian sub-bituminous coal and two types of biomass i.e. rice straw and *Leucaena leucocepha*, were used for test the synergetic effect study. Hereafter, the Indonesian coal, rice straw and *Leucaena leucocepha* were referred as coal, RS and LN, respectively. All of the samples were ground and sieved into the same particle size of 150-250 μm. Coal/biomass blends were prepared by physical mixing at the different biomass blending ratios of 0, 25, 50, 75 and 100wt%, respectively.

In the volatile-char interaction study, three types of volatile sources were used i.e. cellulose (Merk, Co.), xylan from birch wood (Sigma-Aldrich, Co.) and rice straw. Cellulose and xylan were sieved to particle size of 75 – 106 μm while rice straw was sieved to particle size of 75 – 180 μm.

All fuel samples and the chemicals were oven-dried at 110 ^{O}C for 1 h to remove the effect of moisture content, and then stored in a desiccators before testing.

3.1.2 Coal char

In the volatile-char interaction study, four types of coal char were prepared at the various pyrolysis conditions. The nomenclature of all prepared coal chars was given in Table 3.1

Table 3.1 Nomenclature of the prepared coal chars and preparation condition

Name	Sources	Temperature (^{O}C)	Heating rate (^{O}C/min)	Holding time (min)	Reactor	remark
Ex-char	Raw coal	600	27	60	Conventional fixed bed	-
Ac-char	Ex-char	600	27	60	Conventional fixed bed	acid washing
Ex-char800	Raw coal	800	27	60	Conventional fixed bed	-
In-char	Raw coal	600	1980	1	Thermo balance	-

3.2 Equipment

3.2.1 Conventional fixed bed reactor for char preparation

A conventional fixed bed reactor is illustrated in Figure 3.1. It consists of quartz reactor (19 mm-ID and 58 cm-heating zone length), electric furnace with temperature controller (Nabertherm RS 8013001M), Iced-tar trap and inert N_2 cylinder with mass flow controller. There is a quartz wool filter was located at the middle of the reactor to support coal or coal char.

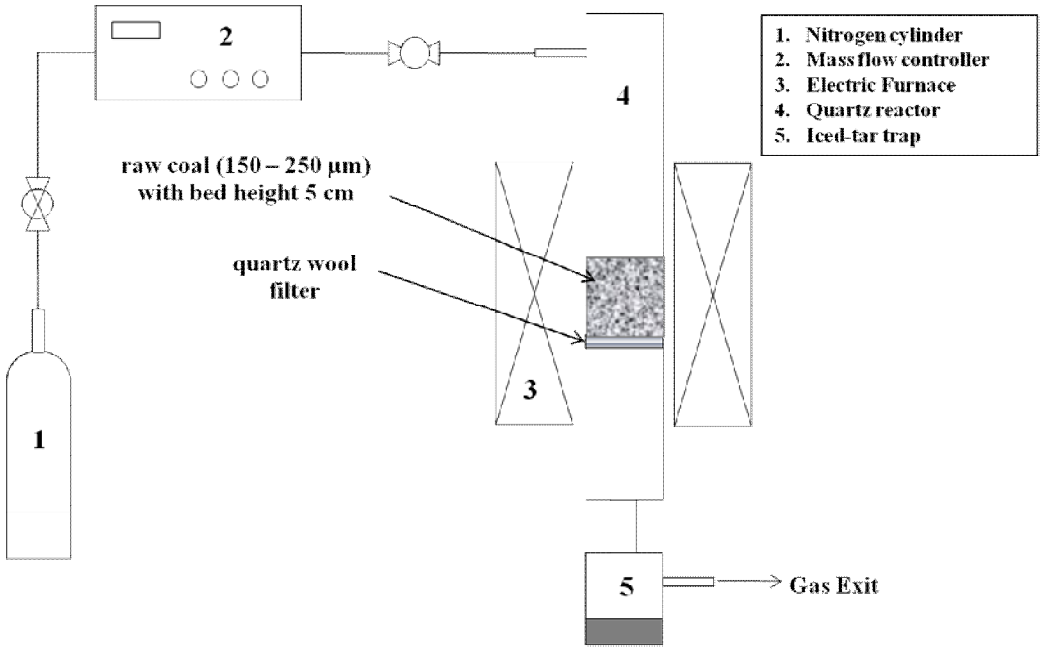

Figure 3.1 Schematic image of a conventional fixed bed reactor

3.2.2 Drop-tube fixed bed reactor

A schematic of drop-tube fixed bed reactor is shown in Figure 3.2. A main reactor tube and almost all parts are similar with the conventional fixed bed reactor. The additional parts are steam temperature controller, distilled water reservoir, HPLC pump and sample feeder.

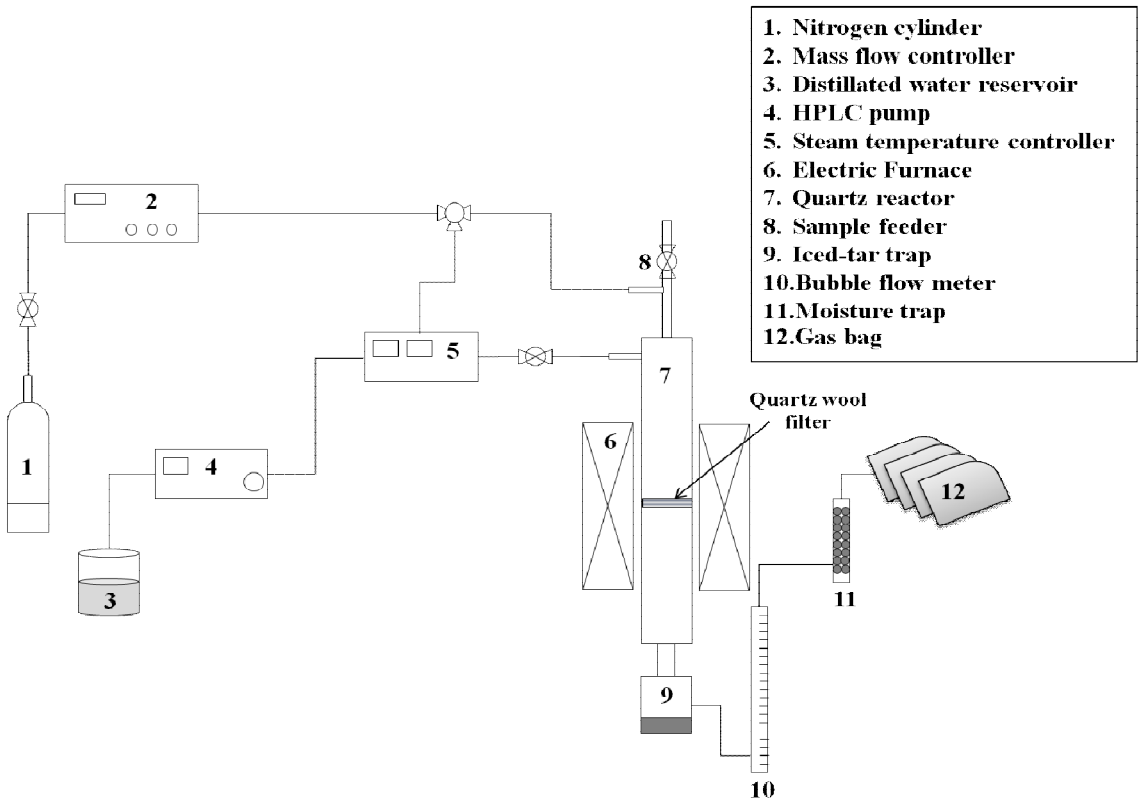

Figure 3.2 Schematic image of a drop-tube fixed bed reactor

Figure 3.3 A drop-tube fixed bed reactor

3.2.3 Thermobalance reactor

A schematic of thermobalance reactor is illustrated in Figure 3.4 The thermobalance reactor consists of quartz 25 mm-ID outer tube, 13 mm-ID inner tube, an infrared gold image furnace and balance sensor (TG-9000HC; ULVAC-RIKO Inc.).

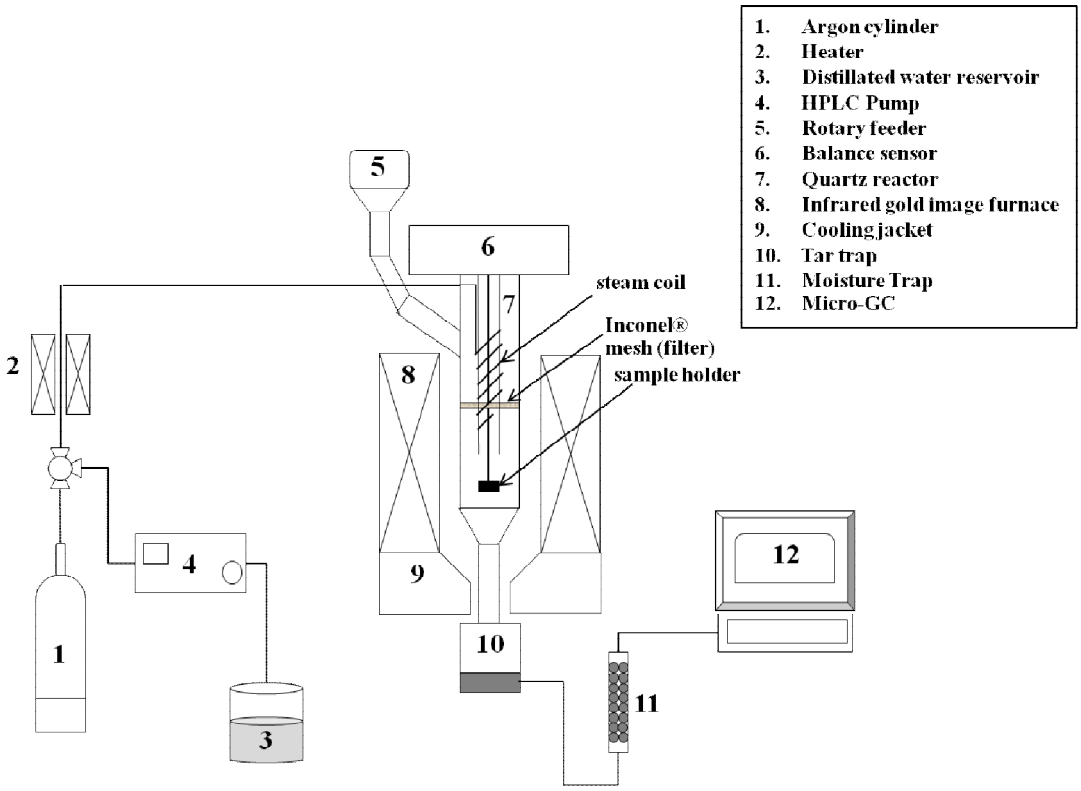

Figure 3.4 Schematic image of a thermobalance reactor

A ceramic basket with platinum mesh filter is suspended with the balance controller. For investigating the effect of volatile resource on coal char reactivity, the thermobalance reactor has been modified as a two-stage reactor (drop-tube/thermobalance fixed bed reactor) which divided to the top and bottom stage by an Inconel® wire mesh filter. The conceptual image of the drop-tube/thermobalance fixed bed reactor is shown in Figure 3.5. At the top stage, the volatile sources were fed by a rotary feeder (Dust departure α, Alpha Corporation). Steam was generated by a steam generator which was heated at 300 ^{O}C by an electric heater and introduced into the reactor through a coil at the bottom stage.

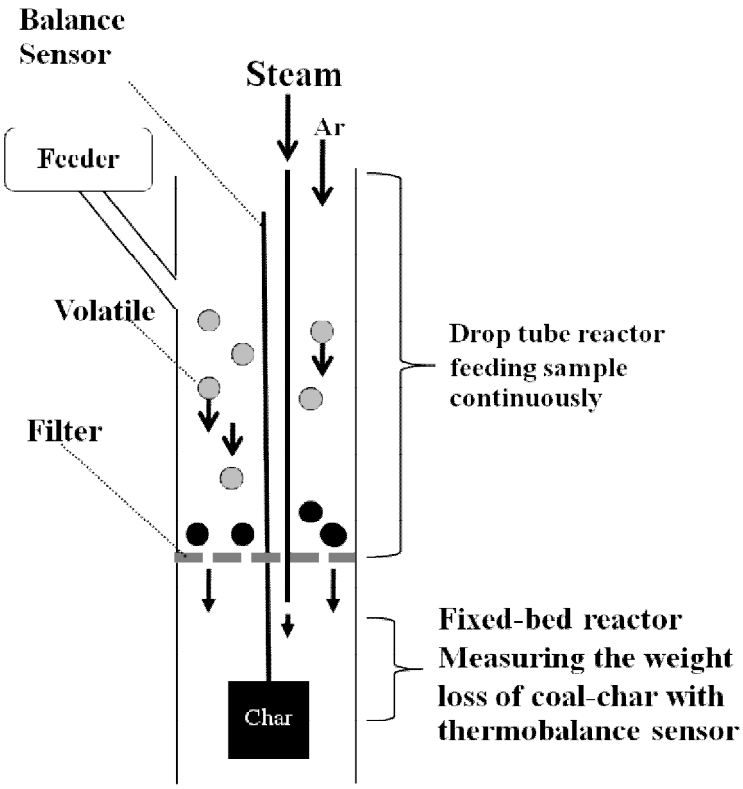

Figure 3.5 Conceptual image of a drop-tube/thermobalance fixed bed reactor

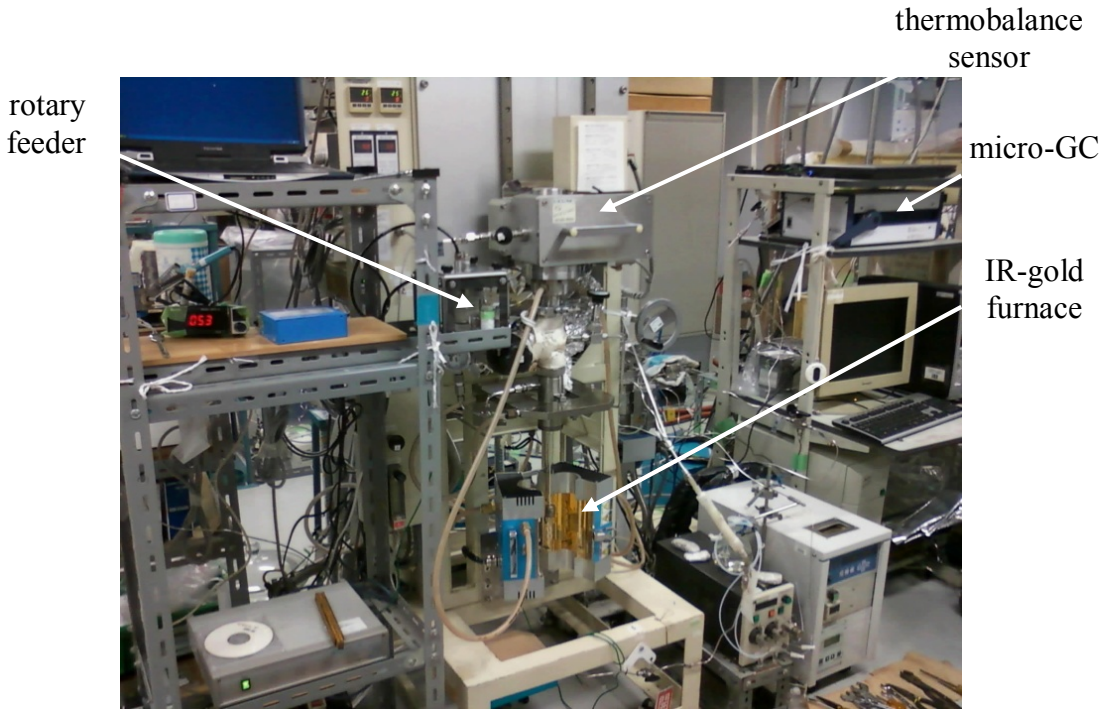

Figure 3.6 A Thermobalance reactor

3.2.4 Two-stage fixed bed reactor

A schematic image of a two-stage fixed bed reactor is shown in Figure 3.7. The two-stage fixed bed reactor consists of two quartz reactors (inner tube with 9 mm-ID and 60 cm-length and outer tube with19 mm-ID and 89 cm-length), two external electric furnaces (Carbolite model MTP 12) with temperature controller, N_2 cylinder with mass flow controller, Iced-tar trap, moisture trap, steam temperature controller, distilled water reservoir, HPLC pump and sample feeder. The heating zone was located in the middle of the outer tube with the length of 67 cm.

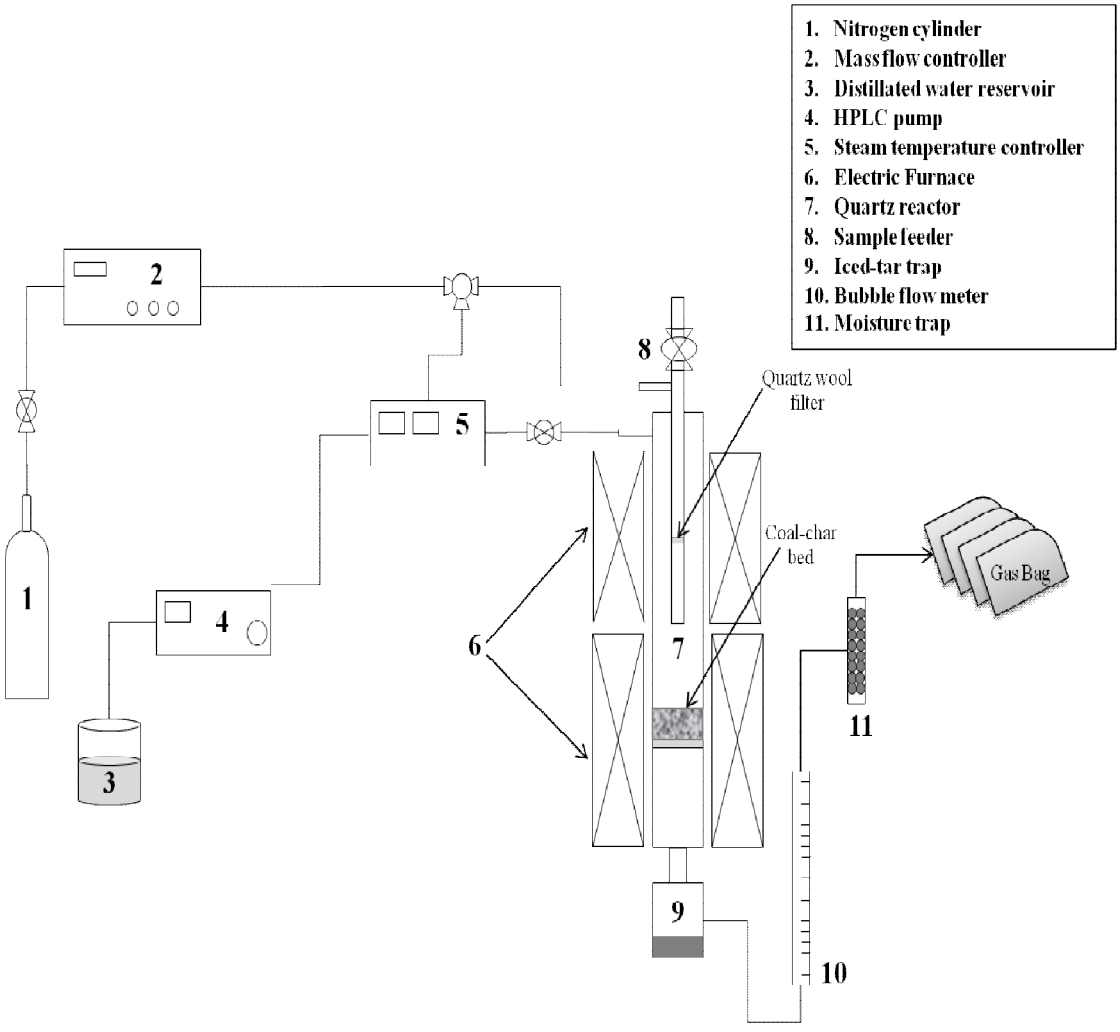

Figure 3.7 Schematic image of a two-stage fixed bed reactor

The reactor is divided in 2 zones; upper zone, called “pyrolysis”, and lower zone, called “volatile-char contacting”, the conceptual image of this reactor is shown in Figure 3.8.

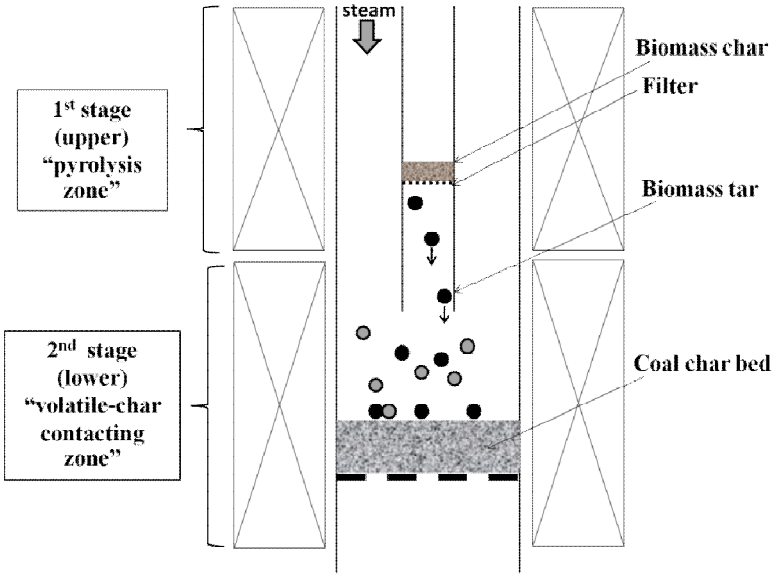

Figure 3.8 Concept of a two-stage fixed bed reactor

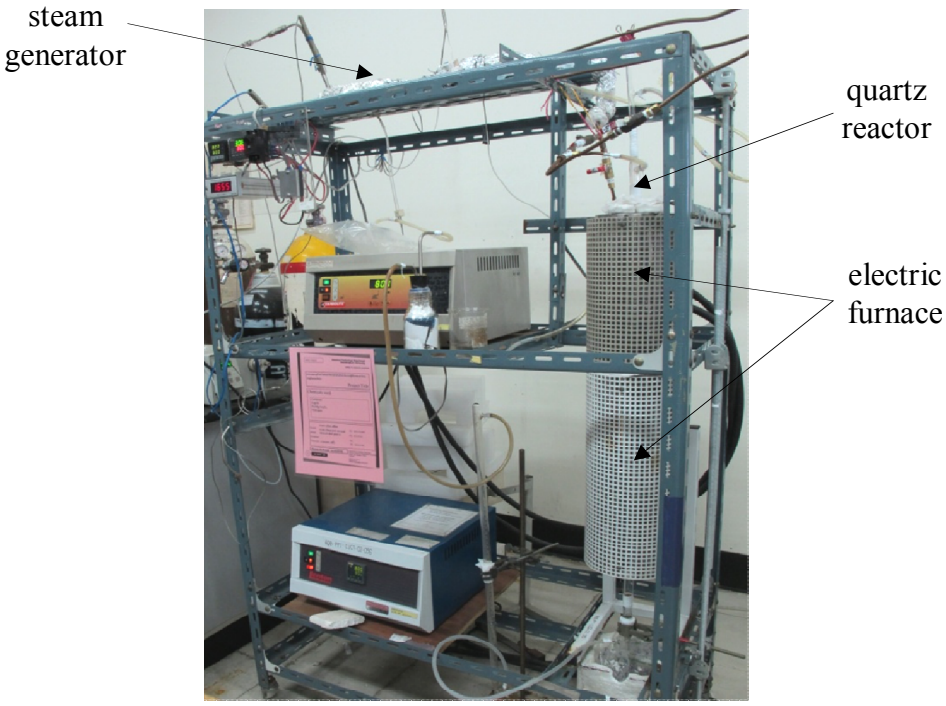

Figure 3.9 A two-stage fixed bed reactor

3.3 Experiment procedure

3.3.1 Coal char preparation

3.3.1.1 In conventional fixed bed reactor

Seven grams of Indonesian coal (sub-bituminous coal, particle size: 150 - 250 μm) was put inside the reactor tube of conventional fixed bed reactor (Figure 3.1). Before heating up, the reactor was purged by the inert N_2 with flow rate of 120 ml/min for 90 min. The oxygen content inside the reactor was checked by sampling 3 gas samples for analyzing by gas chromatography. It should be less than 0.1 v/v% of the oxygen content in air sample. Then the furnace was heated up from 30 to 600 ^{O}C (or 800 ^{O}C) with heating rate about 27 ^{O}C/min and kept maintain at 600 ^{O}C (or 800 ^{O}C) for 60 min. Ex-char and Ex-char800 were collected and kept in a desiccator until using. Char yield of both Ex-char and Ex-char800 were about 60 wt%.

An acid washed-coal char, called "Ac-Char" was prepared by washing the Ex-char with 0.1 M sulfuric acid solution for at least 16 h under inert Ar atmosphere and then washed with double-distilled water and partially dried at low temperature (<35 °C), a detail of method was explained elsewhere [78].

3.3.1.2 In thermobalance reactor

A rapid pyrolyzed-coal char, called "In-char", was prepared inside a thermobalance reactor as shown in Figure 3.4. Twenty milligrams of raw coal was put in a sample basket. Temperature program of thermobalance reactor was set in 2 heating steps. First, slow heating (a heating rate of 15 ^{O}C/min) from room temperature (25 ^{O}C) to 115 ^{O}C, held for 15 min to completely remove moisture in the samples and, second, rapid heating to 600 ^{O}C (a heating rate of 1980 ^{O}C/min), held for 1 min. The inert Ar gas was used as the carrier gas with the total flow rate of 150 ml/min.

3.3.2 Co-pyrolysis and co-gasification

3.3.2.1 In drop-tube fixed bed reactor

Pyrolysis and steam gasification of pure coal, pure biomass and coal/biomass blend were carried out in a drop-tube fixed bed reactor as illustrated in Figure 3.2. Before the temperature was increased, inert alumina ball (2-mm in diameter) was added into the reactor tube with the bed height of 2 cm. The inert N_2 with a total gas

flow rate of 120 ml/min was purged for 60 min to confirm that the oxygen content in reactor was less than 0.1 v/v%. After purging, the temperature was heated up to 800 ^{O}C and held for 1 h. Then, four grams of sample was instantly dropped into the reactor. The fast pyrolysis immediately took place within short residence time. Char was produced over quartz wool filter and weighed for further calculating char yield. Some of heavy tars were condensed by an iced-tar trap which filled with isopropanol and round glass beads with 6 mm in diameter to enhance its capability of recovering condensable compound. The chemical structure of condensed-tar was further characterized with a GC-MS analyzer. Main produced gases were collected by 2-l of gas bag and further quantitatively analyzed with a TCD-gas chromatograph. The reaction time was 1 h, changing a gas bag every 15 minutes after the sample was dropped. In case of steam gasification, distillated water was pumped by HPLC pump with flow rate of 0.14 μl/min and flow pass through the steam heater to generate steam. The steam was fed into the reactor tube after the temperature reached to 800 ^{O}C with the steam content of 60 v/v%.

3.3.2.2 In thermobalance reactor

Steam gasification of pure coal, pure biomass and coal/biomass blend were also examined in a thermobalance reactor as illustrated in Figure 3.4. Ten milligrams of raw sample (pure coal, pure biomass and coal/biomass blends) was placed into the ceramic basket. First heating up to 115 ^{O}C and held it for 15 min to evaporate water inside the sample. In the second heating up to 800 ^{O}C (a heating rate of 1980^{O}C/min) under Ar inert atmosphere, the rapid pyrolysis took place and pyrolyzed char was produced immediately. After that steam from the steam generator, which was heated by a heater at 200 ^{O}C, was introduced into the reactor and steam gasification of char took place under this condition. The weight loss of the sample was continuously recorded with time interval of 0.4 s along the reaction time of 80 min.

3.3.3 Volatile-char interaction study in a thermobalance reactor

The effect of volatile resource on coal char reactivity was examined in a thermobalance reactor which illustrated in Figure 3.4. At the pyrolysis zone (top stage), the volatile sources including cellulose, xylan and rice straw were prepared in

a rotary feeder. At the volatile-char contacting zone (bottom stage), 10 mg of coal char was placed inside the ceramic basket. Inert Ar with total flow rate of 150 ml/min was purged inside the reactor for 120 min to confirm that the oxygen content inside the reactor was less than 200 ppm. Before heating up, temperature program was set into 2 steps; first, heating up to 115 ^{O}C with slow heating rate of 15 ^{O}C/min and holding for 15 min to evaporate water inside the sample and, second, heating up to 800 ^{O}C with rapid heating rate of 1980 ^{O}C/min.

After checking the oxygen content, the temperature program was run to the set point. The volatile was fed into the top stage with a constant feed rate and the rapid pyrolysis took place immediately. The produced solid from the volatile resource was put over the inconel® mesh filter only the volatile was pass through the filter and contacted with coal char in the bottom stage. At the same time, steam from the steam generator, heated at 200 ^{O}C by an electric heater, was introduced into the reactor through a coil at the bottom stage. Char steam gasification was progress with the presence of volatile. The feed rate and feeding time of cellulose, xylan and rice straw was 12 - 13 mg/min for 85 min, 25 mg/min for 30 min and 18-19 mg/min for 30 min, respectively.

The weight loss of coal char in the ceramic basket was continuously recorded with time interval of 0.4 s along the reaction time of 90 min. Tar and water were condensed in an ice-tar trap and then the non-condensable stream passed through the moisture capturing plot filled with silica gel. Gas production rate during steam gasification was analyzed by TCD-micro gas chromatograph (TCD-micro GC, Inficon) equipped with MS-5A and Pora Plot Q column. After steam gasification of char, char was burnt by introducing air into the reactor. After char combustion, blank experiment was done using exactly the same procedure to compensate the output drift of the thermobalance reactor.

3.3.4 Volatile-char interaction study in a two-stage fixed bed reactor

The effect of coal char on biomass derived tar decomposition was investigated in a two-two stage fixed bed reactor which illustrated in Figure 3.7. In the pyrolysis of rice straw, before the reactor was heated up, fifty milligrams of coal char or inert bed (inactive alumina) with bed height of 2 cm was added into the lower zone. The reactor

was then purged by inert N_2 gas with a total gas flow rate of 110 ml/min for 60 min. After purging, oxygen content inside the reactor was checked by sampling 3 gas samples and analyzed by TCD-GC. The oxygen content in reactor should be lower than 0.1 v/v%. After oxygen checking, both electric furnaces were heated up to the desired temperature and gas evolution of coal char bed during this period was collected.

After the temperature reached to the set point, one hundred-twenty milligrams of rice straw was instantly dropped into the inner tube and then pyrolysis took place immediately. The rice straw char was located over the quartz wool filter in the inner tube whist only rice straw tar was passed through the filter. After that, the produced tar contacted with coal char bed which located at the lower zone.

Some of heavy tars were condensed in an iced-tar trap which filled with isopropanol and round 6 mm-glass beads to enhance its capability of recovering condensable compound. The gaseous products were collected by 2-liter gas bag and further quantitatively analyzed. The reaction time was 1 h, changing a gas bag every 15 minutes after the sample was dropped. In case of steam gasification, steam was fed into the outer tube of reactor after the temperature reached to the set point. Steam content was about 60 v/v%.

3.4 Data analysis

In co-pyrolysis and co-gasification, the calculation yield (Y_{cal}) of coal/biomass blend was obtained by Eq. (3.1) to compare with the experimental value;

$$Y_{cal} = X_b \times Y_b + (1 - X_b) \times Y_c \tag{3.1}$$

where X_b is the mass fraction of biomass in the mixture, Y_b and Y_c are the product yield obtained from the experiment of pure coal or biomass. In addition, low heating value (LHV) of the produced gas from steam gasification of coal, biomass and coal/biomass blends were calculated following equation [79];

$$\mathrm{LHV(MJ/m^3)} = \left(\frac{\mathrm{CO} \times 126.35 + \mathrm{H_2} \times 107.98 + \mathrm{CH_4} \times 358.18}{1000} \right) \tag{3.2}$$

where, CO, H_2 and CH_4 are the molar percentages of each component of the product gas, respectively.

The weight of sample inside the ceramic basket which obtained from the thermobalance reactor can be calculated in order to provide the rate of char steam gasification by assuming to obey the first-order kinetics. The rate constant (k_i) of char steam gasification was calculated by Eq. (3.3)

$$\frac{1}{1-X_{char}}\frac{dX_{char}}{dt} = -k_i \tag{3.3}$$

where X_{char} is the conversion of char during steam gasification. The conversion was calculated by Eq. (3.4)

$$X_{char} = \frac{X - X_p}{1 - X_p} \tag{3.4}$$

where X and X_p are the conversion to volatile at time (t) and the conversion to volatile in pyrolysis, respectively.

3.5 Characterization method

3.5.1 Gas chromatography (GC)

The produced gas (mainly H_2, CO, CH_4 and CO_2) from the drop-tube fixed bed reactor and two-stage fixed bed reactor was quantitatively analyzed by gas chromatograph (Shimadzu GC-2014) with a thermal conductivity detector (TCD) using Unibeads C column (3.00 mm I.D × 2000 mm length).

Table 3.2 Condition of Gas chromatography

	Conditions
Carrier gas	Ar
Column type	Unibeads C packed column
Injector temperature (^{O}C)	120
Column temperature (^{O}C)	60 for 2 min and 120 for 9 min
Detector type	Thermal conductive dectector (TCD)
Detector temperature (^{O}C)	180

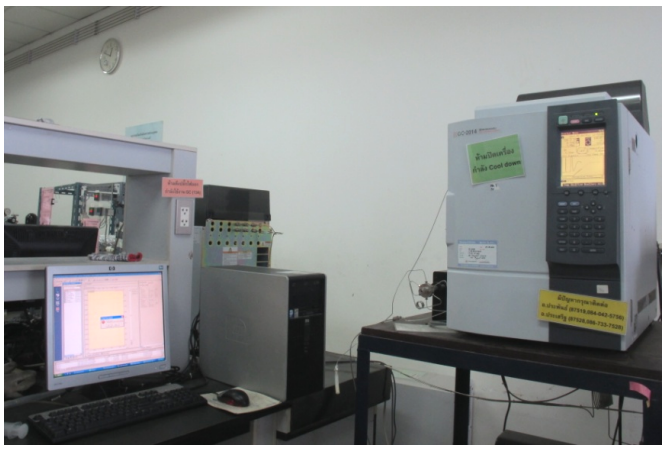

Figure 3.10 Shimadzu GC-2014

3.5.2 micro-Gas chromatography (micro-GC)

The produced gas (mainly H_2, CO, CH_4 and CO_2) from the thermobalance reactor was analyzed by TCD-micro gas chromatograph (TCD-micro GC, Inficon). H_2, O_2, N_2, CO and CH_4 were analyzed with MS-5A column while CO_2 was analyzed with Pora Plot Q column**.**

3.5.3 Gas chromatography/Mass spectrometry (GC-MS)

Some of condensed tar in the ice-tar trap was analyzed to determine the chemical composition by using a GC-MS (a Varian Model Saturn 2200 equipped with a capillary column, 0.25 mm-OD × 0.25 mm-film thickness × 30 m-length, DB-5ms, J&W Scientific) with helium as the carrier gas. The molecular weight scan range was 50 – 650 m/z with a 5 min of solvent cut time. The column was held at 50 °C for 3 min, and then the temperature was increased to 220 °C at heating rate of 20 °C/min and held for 40 min.

Figure 3.11 Varian Model Saturn 2200 GC-MS

3.5.4 CHN and S analysis

All fuel samples and coal chars were analyzed with a CHN analyzer (LECO CHN-2000), Figure 3.12. Sulfur content was estimated by bomb washing method following ASTM 3177.

Figure 3.12 LECO CHN-2000 analyzer

3.5.5 Brunauer-Emmitt-Teller (BET) analysis

The specific surface area, pore volume and pore size of the pyrolyzed chars were measured by N_2 adsorption at -196^{O}C using the Brunauer-Emmitt-Teller, BET method (model Quantachrome, Autosorb-1) by degassing of sample before adsorption at 300 ^{O}C for 6 h.

3.5.6 Scanning electron microscopy (SEM)

The morphology of produced chars was also characterized by scanning electron microscopy (SEM, model JEOL, JSM-5410LV) method.

3.5.7 X-ray fluorescence (XRF)

Alkali and alkaline earth metallic species (AAEM) and other minerals in fuel samples and coal chars were characterized by X-ray fluorescence (XRF) technique (Philips model PW2400). The elements are consists of Na, K, Mg, Ca, and Si was calculated by the theoretical formulas “fundamental parameter calculations” method.

CHAPTER IV

SYNERGETIC EFFECT DURING CO-PYROLYSIS AND CO-GASIFICATION OF COAL AND BIOMASSS

In this chapter, co-pyrolysis and co-gasification of Indonesian sub-bituminous coal and two types of biomass i.e. rice straw (RS) and *Leucaena leucocepha* wood (LN) was studied using a drop-tube fixed bed reactor as described in Chapter III. The results are divided into 3 sections; (i) the characteristics of raw materials (coal and two types of biomass), (ii) synergetic effect during co-pyrolysis and (iii) synergetic effect during co-gasification. In section 4.2, the effect of biomass to coal ratios, reaction temperatures and biomass types on product distribution and gas composition were discussed together with the characterization of the pyrolyzed-char and tar, by BET, SEM, XRF and GC-MS techniques. In addition, char steamfffffff gasification rate of the pyrolyzed char, which *in situ* pyrolyzed in a thermobalance reactor, was determined. In the last section (4.3), the effect of biomass to coal ratio and reaction temperature on carbon conversion, gas composition, H_2/CO molar ratio and heating value of the produced gas during co-steam gasification were presented.

4.1 Characteristics of fuel samples

Proximate, ultimate analyses and gross heating value of coal, RS and LN are shown in Table 4.1. It can be confirmed that the coal sample used in this study is sub-bituminous coal because its characters such as high moisture, low sulfur content and moderate heating value (19 – 22 kJ/g) are consistent with the coal classification in ASTM D388. Comparing with coal, two types of biomass (RS and LN) have the higher volatile matter, H/C and O/C molar ratio and lower gross heating value. This is due to the different molecular structure and thermal behavior between biomass and coal. Biomass is the lignocellulosic material which composes of cellulose, hemicellulose and lignin. Cellulose and hemicellulose are predominantly decomposed to the volatiles, including non-condensable gases and condensable products, over the temperature range of 200 to 500 ^{O}C [80]. On the other hand, coal mainly comprises of

the polyaromatic hydrocarbons (PAHs) which is decomposed at higher temperature compared to the biomass. In addition, the mineral analysis of all showed that these biomasses have high amount of K and Ca than that of coal (Table 4.2). These metals have been reported as the catalytic species in the decomposition of coal [72, 81]. Rice straw seems to have the highest Si content among all samples. These different characters between coal and biomass are supposed to discover some distinct results in terms of product yield and gas composition during the co-pyrolysis and co-gasification of coal and biomass which will be discussed in the next section.

Table 4.1 Proximate and ultimate analyses of fuel samples

Sample	**Indonesian coal (Coal)**	**Rice straw (RS)**	***Leucaena leucocepha* (LN)**
Proximate analysis (wt%, as received)			
Moisture	12.41	6.43	8.89
Ash	8.39	11.22	2.59
Volatile matter	36.84	61.95	62.21
Fixed carbon	42.36	29.25	26.31
Ultimate analysis (wt%, daf)			
Carbon	72.13	45.30	48.39
Hydrogen	6.67	6.93	7.11
Nitrogen	1.40	0.92	0.29
Sulfur[a]	0.22	0.14	0.14
Oxygen (by difference)	19.58	46.71	44.07
H/C molar ratio	1.11	1.84	1.76
O/C molar ratio	0.20	0.77	0.68
Gross heating value (kJ/g)	22.66	14.95	12.76

[a] by Bomb washing method (ASTM 3177)

Table 4.2 Element analysis of fuel samples by X-ray fluorescence (XRF)

Sample	Indonesian coal (Coal)	Rice straw (RS)	*Leucaena leucocepha* (LN)
Elemental analysis (wt%, db)			
Sodium (Na)	0.034	0.064	0.219
Potassium (K)	0.126	1.892	0.823
Calcium (Ca)	0.788	0.844	1.108
Magnesium (Mg)	0.171	0.139	0.186
Silicon (Si)	4.00	11.81	1.00
Iron (Fe)	1.645	0.075	0.165

4.2 Synergetic effect during co-pyrolysis

4.2.1 Effect of biomass to coal ratio

Effect of biomass to coal ratio on product yield obtained from the pyrolysis of coal/RS and coal/LN blends at 800 ^{O}C is shown in Figure 4.1. Consider the product yield of pure coal and pure biomass (RS and LN), it could be seen that coal and biomass gave entirely different product yields corresponding to their main chemical components. At the same pyrolysis temperature (800 ^{O}C), RS and LN gave higher gas yield and lower yield of tar and char compared to coal. This is correlated to their macrostructures since biomass is contained of cellulose, hemicellulose and lignin that are linked together with relatively weak ether (R-O-R) bonds. On the contrary, coal is composed of dense polycyclic aromatic hydrocarbons (PAHs), which form strong bonds. Therefore, it is resistant to thermal decomposition compared to the ether bond in biomass [2]. Consequently, the biomass is more simply decomposed to the lighter products than the coal.

In cases of coal/biomass blends, closed symbols represented the product yield obtained from the experiment and open symbols represented the predicted yield which was calculated by Eq. (3.1) in Chapter III. It was observed that the experimental product yields obtained from the pyrolysis of the coal/biomass blends were somewhat different from the predicted values which were deviating the most at biomass to coal ratio of 1:1 (w/w).

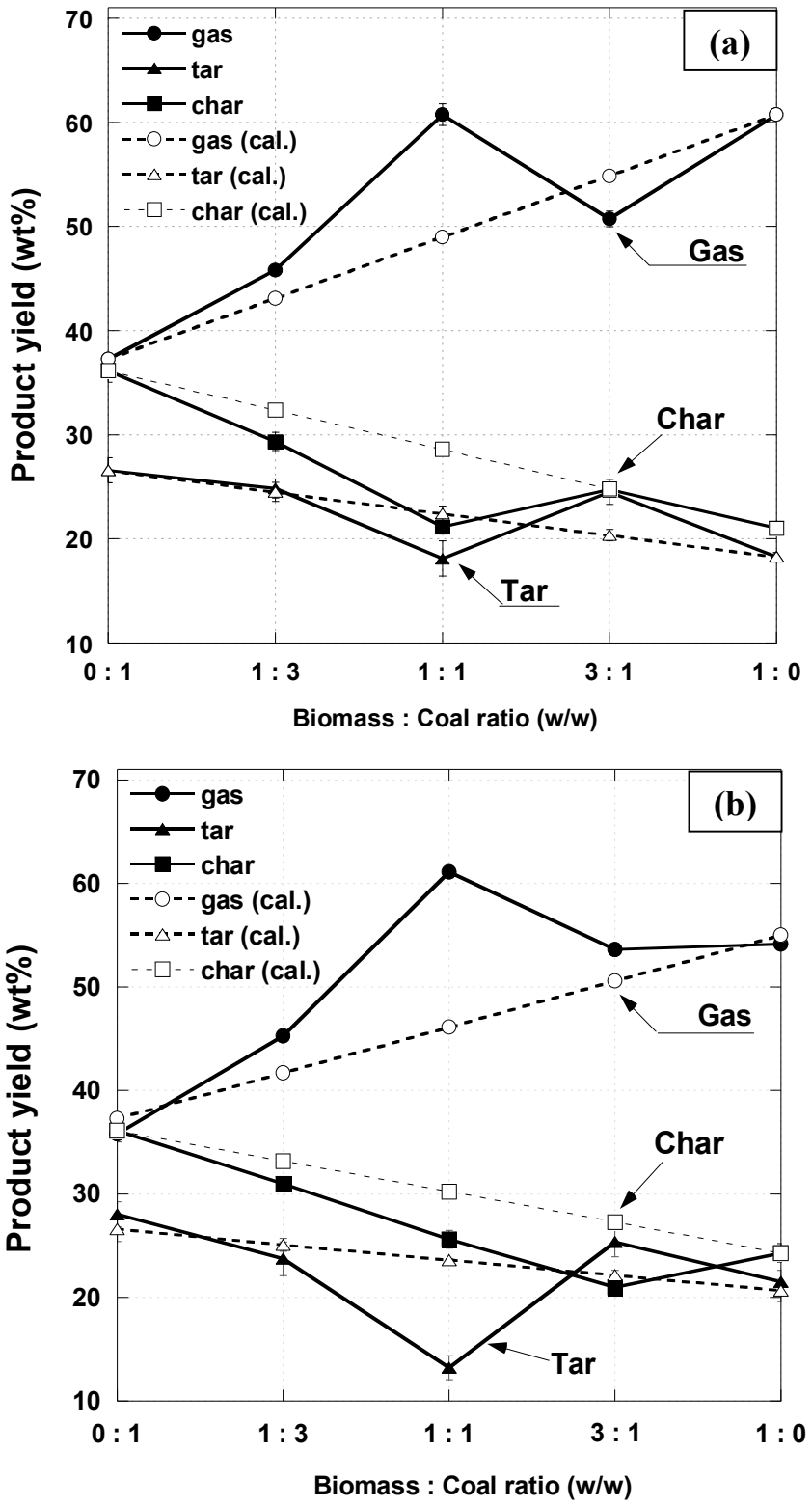

Figure 4.1 Effect of biomass to coal ratio on product yield from the pyrolysis of (a) coal/RS and (b) coal/LN blends at 800 ^{O}C

At RS to coal ratio of 1:3 and 1:1 (w/w), the experimental gas yield was higher whilst tar and char yields are lower than the predicted values (Figure 4.1a). Similarly with the pyrolysis of coal/LN blends (Figure 4.1b), the deviation between the experimental and predicted values was remarkable at LN to coal ratio of 1:1 (w/w). This can be attributed to the fact that the H/C and O/C molar ratios of RS and LN are about 1.8 and 3.4 times higher than coal (Table 4.1). Hence, a larger amount of H and OH radicals could be produced and acted as hydrogen donors, promoting the cracking of aromatic compounds in the coal [16]. This caused to the suppression of the secondary tar/char formation which is formed during the co-pyrolysis of coal and biomass via the secondary reactions, such as condensation, repolymerization and/or cross-linking reactions [9, 12, 82].

As stated above, the synergetic effect was most noticeable at the biomass to coal ratio of 1:1 (w/w), which agrees with the co-pyrolysis of lignite and straw in a free fall reactor in the previous study [2]. It was reported that a clear synergy occurred under high biomass to lignite blending ratios was probably because the biomass provided adequate hydrogen donors for promotion the lignite pyrolysis by hydrogenation. However, at a biomass to coal ratio of 3:1 (w/w), it was clear that the synergetic effect was reduced or abolished in this study reported here both in the cases of coal/RS and coal/LN blends. This is probably due to the production of excess volatile components [83].

Additionally, the observed synergetic effect during the co-pyrolysis of coal with RS or coal with LN blends could be ascribed by the roles of alkali and alkaline earth metallic species (AAEMs). As stated in section 4.1 (Table 4.2), it was found that the biomass contains more AAEM species than coal, especially potassium (K). The K content in RS and LN was 15.0 and 6.5 times higher than those in the coal, respectively. Potassium has been reported to act as a catalyst for the secondary decomposition of char and char gasification [7, 83, 84]. Kajitani et al. [84] proposed that the potassium from the cedar bark was volatilized and then condensed over the coal char surface and so improved its reactivity during co-pyrolysis. The reactivity of char obtained from the coal/biomass blends in steam gasification was also investigated in this study and discussed in section 4.2.

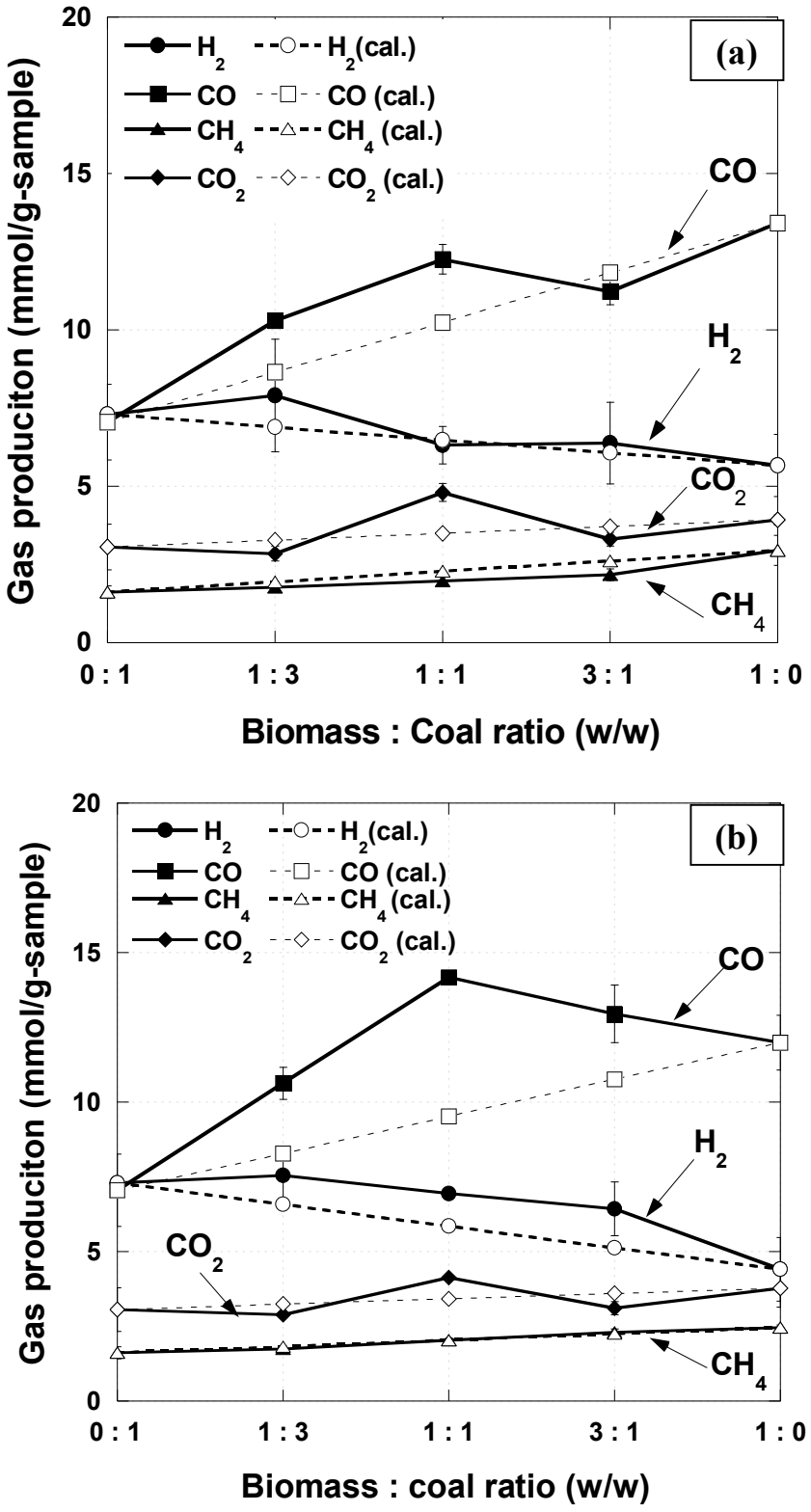

Figure 4.2 Effect of biomass to coal ratio on gas production from the pyrolysis of (a) coal/RS and (b) coal/LN blends at 800 ^{O}C

Gas production from the pyrolysis of coal/RS and coal/LN blends at 800 ^{O}C is shown in Figure 4.2. It was found that, for the RS to coal ratio of 1:3 and 1:1 (w/w), the observed experimental yields of CO were higher than the predicted values (Figure 4.2a). This could be due to the OH radicals which were released from biomass. The radicals formed during co-pyrolysis can attack the aromatic rings in coal and also react with aliphatic species and intermingle with carbon atoms to form CO [16]. The increase of CO production was also clearly observed in the cases of LN to coal ratio of 1:1 (w/w), as can be seen in Figure 4.2b. In addition, the slightly higher experimental yields of H_2 and CO_2 compared to the predicted yields were found in both cases of coal/RS and coal/LN blends. In contrast, no obvious synergy was observed for CH_4 production, although this may due to the relatively low net levels of CH_4 production compared to the other gaseous species. The magnitude of the increase of gas production (CO, H_2 and CO_2) in both coal/RS and coal/LN was relevant with biomass type which will be further discussed in section 4.2.3.

4.2.2 Effect of reaction temperature

The effect of pyrolysis temperature on the synergetic effect in terms of product yield and gas production from the co-pyrolysis of coal/RS and coal/LN blends is shown in Figure 4.3 and Figure 4.4, respectively. Note that the bold symbols represented the product yields obtained from the experiment and the dash line referred to the predicted values which were calculated from the pyrolysis of coal or biomass alone at each pyrolysis temperature. For coal/RS blend, at low temperature (600 and 700 ^{O}C), the product yields obtained from the experiment were quite similar to the predicted values. However, the synergetic effect in terms of the increased gas and decreased tar and char yields was manifested at a higher pyrolysis temperature (800 ^{O}C), as can be seen in Figure 4.3a. Consider in the coal/LN blend in Figure 4.3b, it was found that the synergetic effect in terms of product yields was noticed at 700^{O}C resulting in the increase of gas and decrease of char yields compared to the predicted yields. At higher temperature, the synergetic effect in terms of the increased gas and the decreased tar and char were more pronounced. This is probably because the amount of H and OH species were more released from the biomass at high temperature and played the synergetic role with coal. In addition, the volatilization of

K was promoted at high pyrolysis temperature to generate more volatile K from the biomass. This abundant of the volatile K species were likely condensed over the char surfaces and became a catalyst for tar and char decomposition.

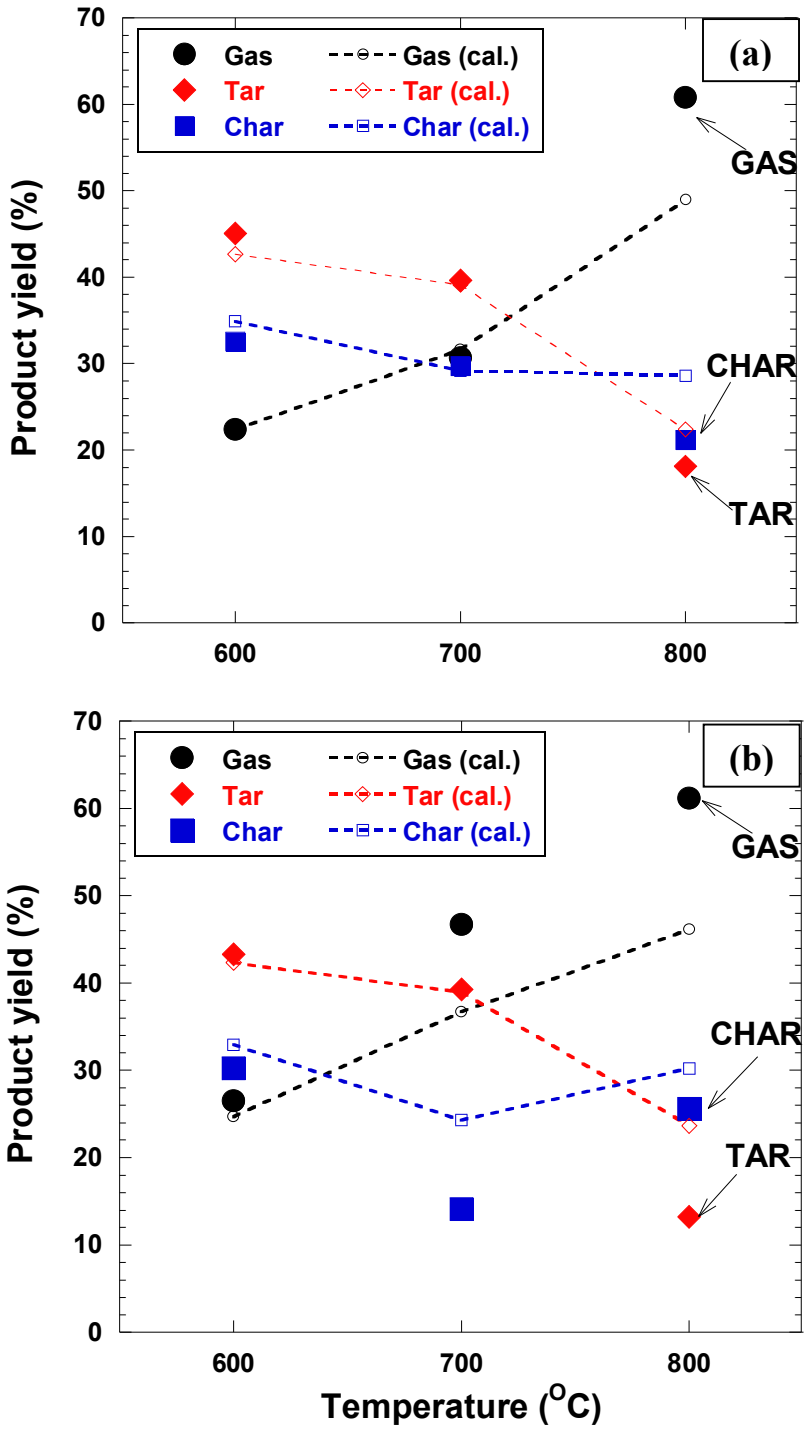

Figure 4.3 Effect of temperature on product yield from the pyrolysis of (a) coal/RS and (b) coal/LN blend with biomass to coal ratio of 1:1 (w/w)

The effect of pyrolysis temperature on gas production of the co-pyrolysis is shown in Figure 4.4. It was found that the increase of CO production compared to the predicted values was observed starting at 700 ^{O}C and 800 ^{O}C for coal/RS blend and coal/LN blend, respectively. Among all gaseous production, the CO production was most remarkably increased at the pyrolysis temperature of 800^{O}C both for coal/RS and coal/LN. The increment of CO production was relevant to the increase of OH species which more released at high pyrolysis temperature. In addition, the decreased H_2 production was observed at almost all pyrolysis temperatures. It might be due to the consumption of H_2 species during the decomposition of the aromatic or/and aliphatic hydrocarbons during the co-pyrolysis. The pyrolysis temperature was not significantly influenced on the production of CO_2 and CH_4 as the presented similar levels of their productions both in cases of coal/RS and coal/LN blends. From the result, it can be stated that pyrolysis temperature is an important factor that can be determined the synergetic results during co-pyrolysis of coal and biomass.

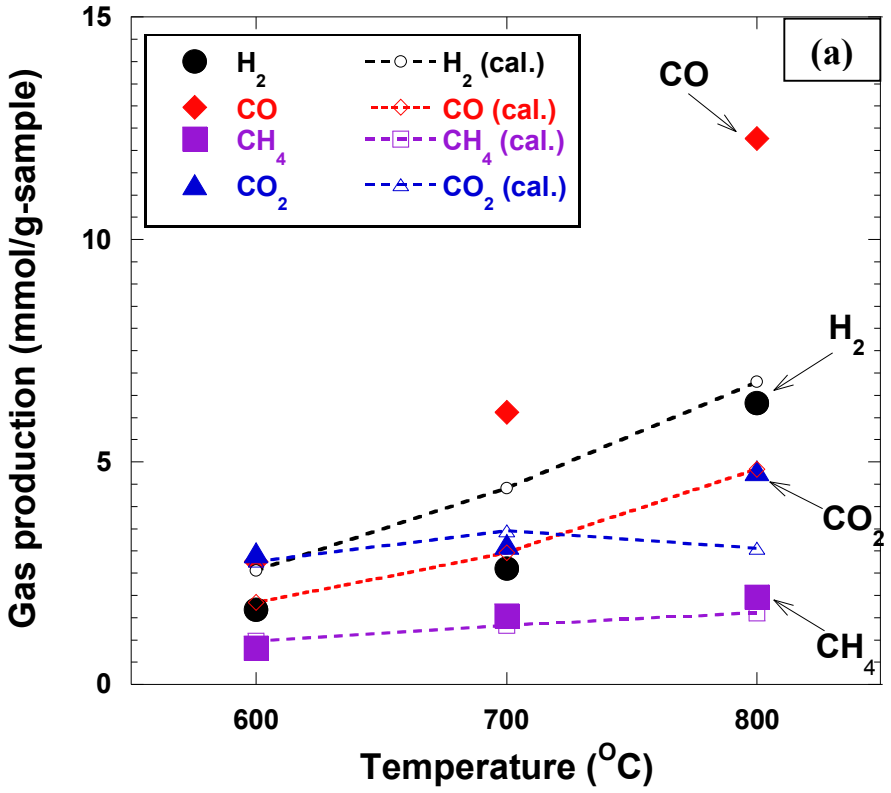

Figure 4.4 Effect of temperature on gas production from the pyrolysis of (a) coal/RS and (b) coal/LN blend with biomass to coal ratio of 1:1 (w/w)

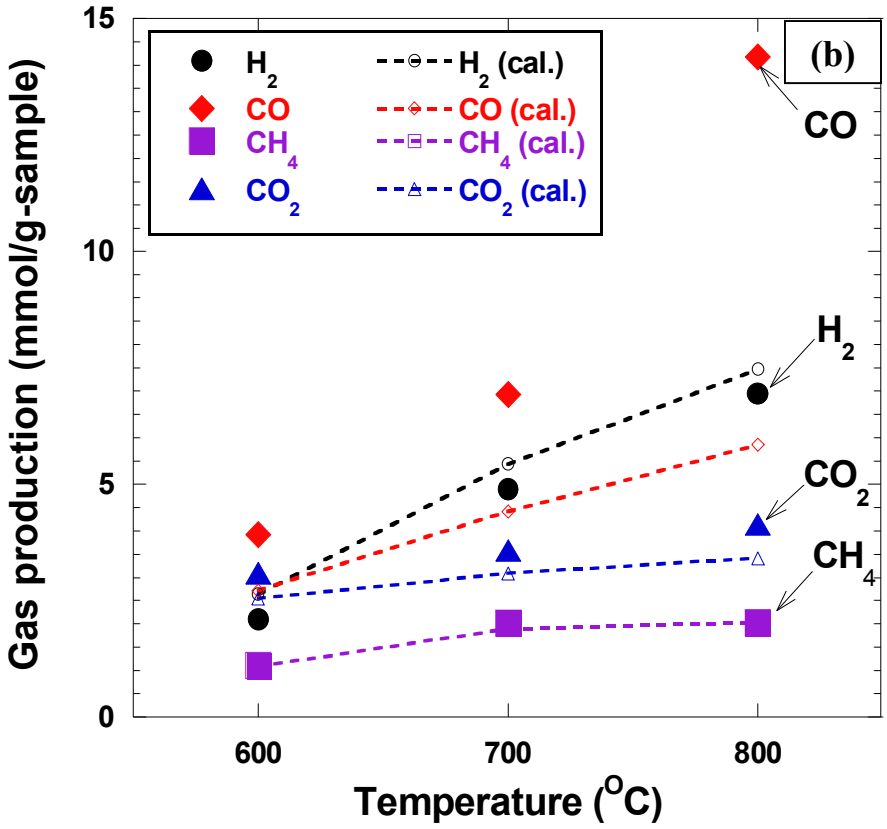

Figure 4.4 (cont.) Effect of temperature on gas production from the pyrolysis of (a) coal/RS and (b) coal/LN blend with biomass to coal ratio of 1:1 (w/w)

4.2.3 Effect of biomass type

Figure 4.5 shows the deviation of product yields from the co-pyrolysis of coal/biomass at the weight ratio of 1:1 (w/w). Note that the positive and negative values represented the increment and the reduction of the experimental yields deviating from the predicted values, respectively. For coal/RS blend, it was found that the increased gas yield might be related to the decrease of char yield. However, for coal/LN blend, the increased gas yield corresponded to the decreased tar yield, as can be seen in Figure 4.5. It can imply that the interaction between coal and biomass during co-pyrolysis depends on the biomass type. As mentioned in section 4.2.1, the increased gas yield could be attributed to the improvement of coal decomposition by the released OH and H radicals and the AAEM species, especially K, from the biomass. The amount of generated OH and H radicals from RS and LN were presumably similar since they have comparable H/C molar ratios (Table 4.1) and the

content of cellulose and hemicelluloses [85, 86]. However, the AAEM content of RS and LN were different, and in particular the K content in RS was 2.3 times higher than that in LN (Table 4.2).

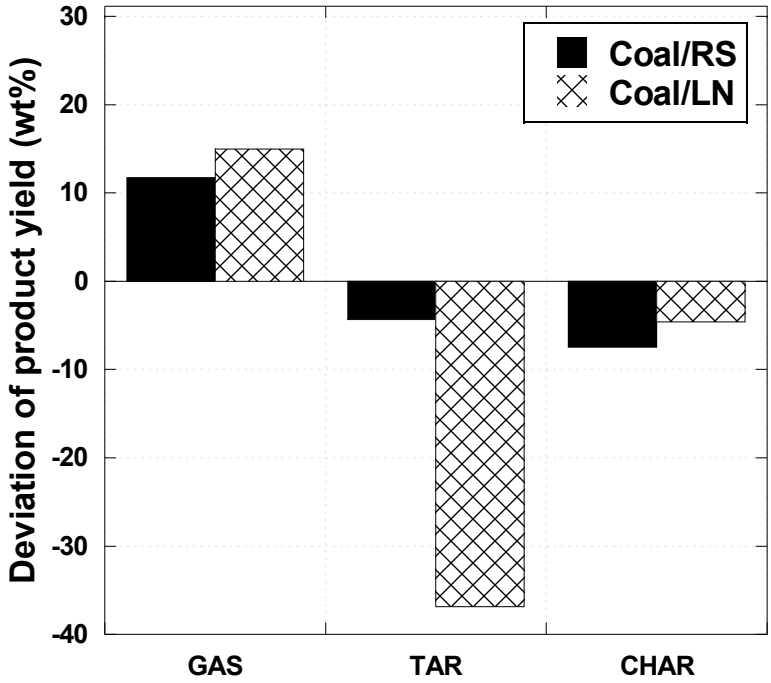

Figure 4.5 Deviation of product yield from co-pyrolsysis of coal/biomass blend at 800 ^{O}C with biomass to coal ratio of 1:1 (w/w)

During pyrolysis, some of the K is released as a volatile (gas phase) and plays a catalytic role in the pyrolysis and gasification [24] whilst the rest of K is remained in the char (solid phase). The mineral analysis of char revealed that around 43wt% of the K remained in the RS-char compared to only ~10wt% in the LN-char. This would be owing to the moderately high Si content in the RS-char that promotes the absorption of K to form potassium silicate (K_2SiO_3) [87, 88]. Considering the same biomass weights, the amount of released (volatile) K from LN was comparable to that from RS (~ 0.7 - 1 wt%) while the retained K in the LN char was lower. Volatile K, with a high sufficient mobility to be deposited on the coal char surfaces, was speculated to play a significant role in co-pyrolysis through promotion of both secondary decomposition and gasification of the nascent char with the steam produced during pyrolysis (pyrolytic steam) [26]. From the previous study [89], RS has been shown to produce greater amounts of pyrolytic steam compared to LN. It

could account for the remarkable decrease in the char formation levels as can be seen in the pyrolysis of the coal/RS blends. For LN/coal blend, volatile K was expected to present in a different form due to the difference in the volatile compounds between RS and LN. It promoted the decomposition of nascent tar resulting in lower tar yield. This explanation could be confirmed by the different amount of the retained K in the chars obtained from the co-pyrolysis. This result will be shown and described in section 4.2.4.

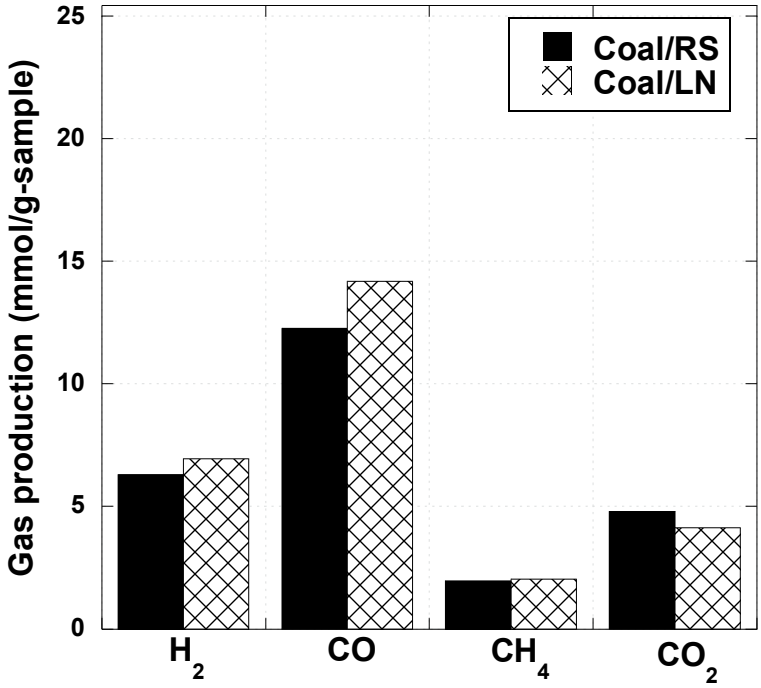

Figure 4.6 Gas production from the co-pyrolsysis of coal/biomass blend at 800 ^{O}C with biomass to coal ratio of 1:1 (w/w)

Gas production from the pyrolysis of RS/coal and LN/coal blends is shown in Figure 4.6. It was found that almost gas products (H_2, CH_4 and CO_2) from both coal/RS and coal/LN were comparable, except the CO production. The CO production obtained from the pyrolysis of coal/LN blend was slightly higher than that coal/RS blend. This might be due to the dominant decomposition of tar in the coal/LN pyrolysis. The effect of biomass type on the characterization of the pyrolytic products will be shown in the next section.

4.2.4 Characterization of the pyrolytic product

4.2.4.1 Char structure and morphology

Char after pyrolysis was characterized with SEM and BET technique. The SEM image of all pyrolyzed chars is shown in Figure 4.7. It could be seen that pure coal char appeared to have a smooth surface of dense hydrocarbon with small pores, while pure biomass char had more porous structure with larger pores. This was attributed to the higher volatile matter content in the biomass (Table 4.1). In the char derived from the coal/biomass blends, the morphology clearly changed into a loose packed and more porous structure compared to pure coal char (Fig. 4.7(e) and (g)). These transformations are probably related to the increased reactivity of the char derived from the coal/RS and coal/LN blends as will be discussed in next section.

Furthermore, the BET surface area and pore volume of chars derived from the co-pyrolysis of coal and biomass were higher than the predicted values which calculated from the values of pure coal and biomass (Table 4.3). Therefore, the change in the BET surface area and pore volume of the char from the co-pyrolysis was consistent with the change in their morphology, as mentioned above. Interestingly, the char obtained from the pyrolysis of coal/RS blend gave the higher BET surface area and pore volume than that from either coal (1.07 and 1.11 times, respectively) or RS (1.64 and 1.36 times, respectively). It could be used to explain that the higher reactivity of the coal/RS blend char with steam since the surface area and pore volume are important parameters to control the reactivity of char [62].

Table 4.3 The physical properties of the pyrolyzed char

Char sample	Coal	RS	LN	Coal/RS blend 1 : 1		Coal/LN blend 1 : 1	
				Exp.	Cal.	Exp.	Cal.
BET surface area (m^2 /g)	233.81	152.09	119.19	250.28	192.95	210.89	176.50
Pore volume (cm^3 /g)	0.157	0.129	0.087	0.175	0.143	0.146	0.122
Pore size (Å)	26.85	34.05	29.14	27.99	30.45	27.74	28.00

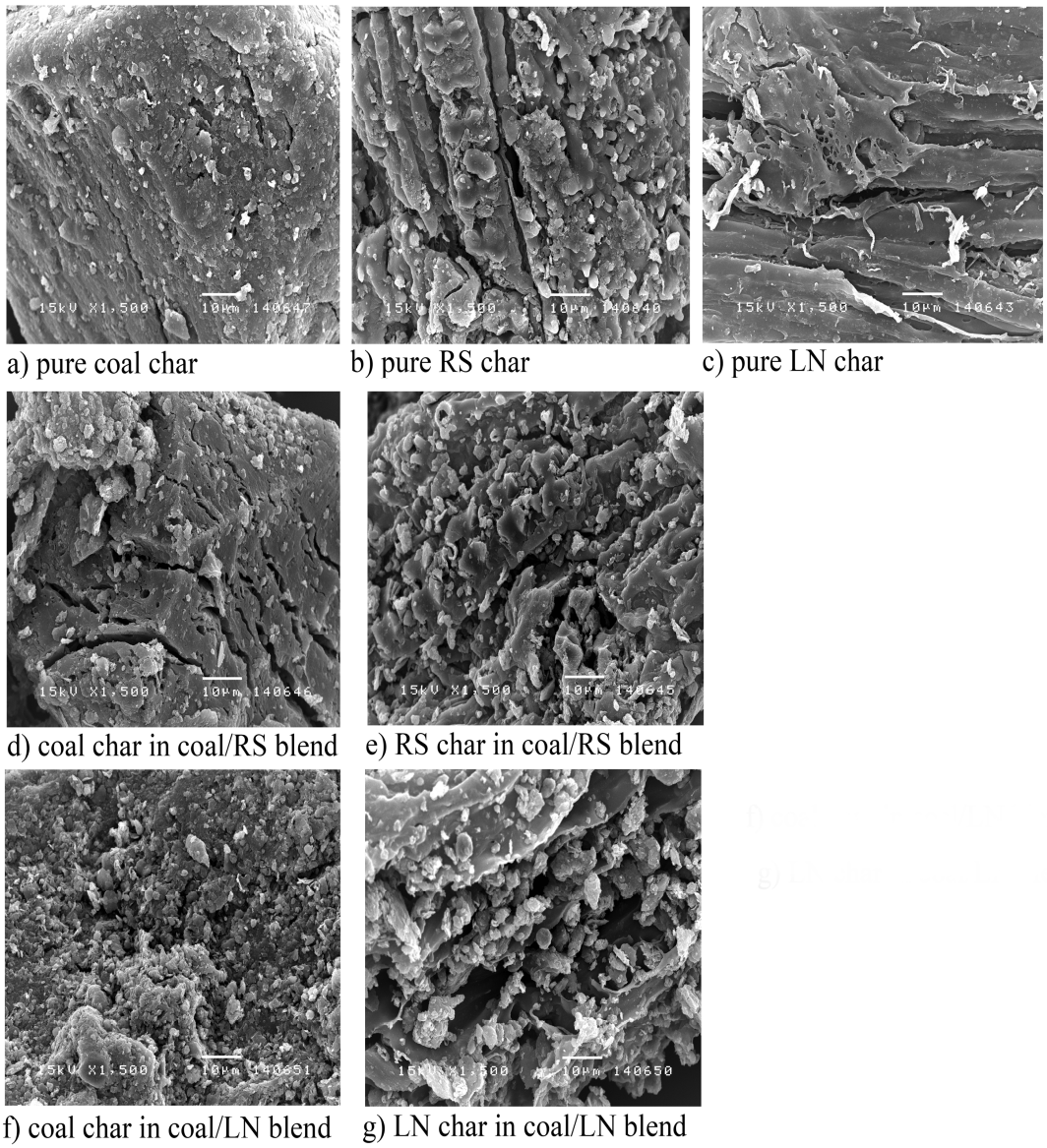

a) pure coal char b) pure RS char c) pure LN char

d) coal char in coal/RS blend e) RS char in coal/RS blend

f) coal char in coal/LN blend g) LN char in coal/LN blend

Figure 4.7 SEM images of the pyrolyzed-char obtained from the pyrolysis of (a) pure coal, (b) pure RS, (c) pure LN, (d) coal/RS blend (coal char section), (e) coal/RS blend (RS char section), (f) coal/LN blend (coal char section) and (g) coal/LN blend (LN section)

4.2.4.2 *In situ* Char steam gasification

The reactivity of *in situ* pyrolyzed char was carried out in the thermobalance reactor, as mentioned in Chapter III. The relative mass of pure coal and pure biomass char were plotted with time and compared to the coal/biomass blends. Note that the initial time (0 s) was defined as the weight change of the sample during the initial pyrolysis before the temperature reached 800 ^{O}C. The decrease in the relative mass of the char over time in the coal/RS and coal/LN blends during steam gasification at 800 ^{O}C is shown in Figure 4.8. The relative mass loss over time of the pure coal was remarkably different from that of pure RS or LN. Coal exhibited an essential decrease of relative mass to ~0.4 during the initial pyrolysis, and then gradually decreased during steam gasification to a relative mass of 0.05 at 5000 s. In contrast, both RS and LN showed a much larger initial weight loss during pyrolysis (95% conversion in pyrolysis, X_p) and were the almost completely decomposed (nearly 100% of conversion) within 2000 s (RS) or 500 s (LN) of steam gasification period. The coal/biomass blends with the weight ratio of 1:1 revealed the lower weight decrease than that predicted data for both RS and LN. The derived overall rate constants (k) of the *in situ* pyrolyzed char steam gasification, calculated by applying the first-order kinetic equation rate, are shown in Table 4.4.

Table 4.4 Overall rate constant (k) of char steam gasification in cases of coal and biomass blends

Overall rate constant (k) [a]	RS : Coal = 1 : 1	LN : Coal = 1 : 1
Experimental value	1.031 (R^2 = 0.99)	1.112 (R^2 = 0.95)
Predicted value [b]	0.442 (R^2 = 0.91)	0.805 (R^2 = 0.95)

[a] The overall rate constant followed the first-order kinetic rate equation

[b] calculate from the data of pure coal and pure biomass

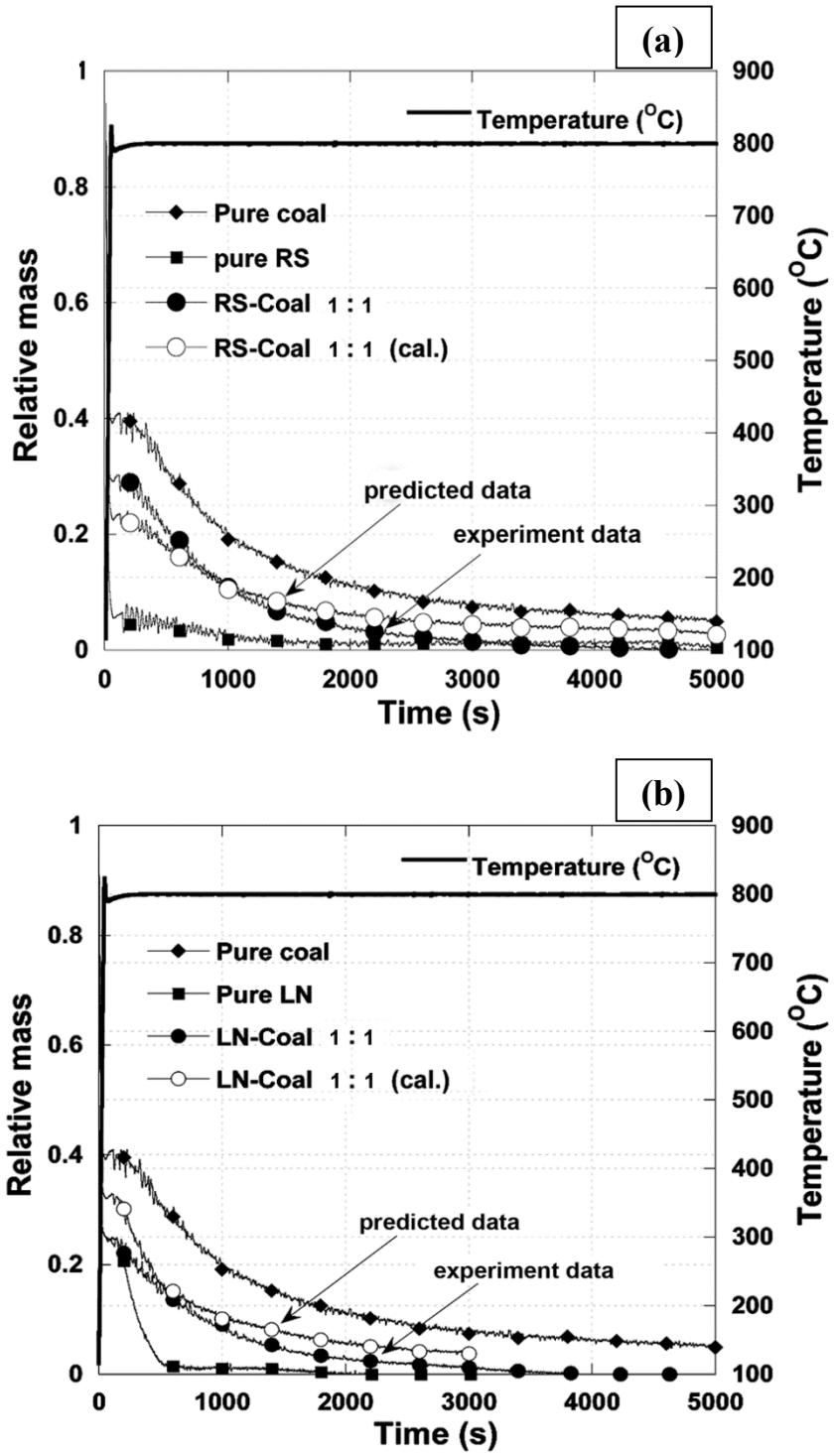

Figure 4.8 Relative mass vs time of the chars obtained from *in situ* pyrolysis of coal, biomass and coal/biomass blends (a) for coal and RS and (b) for coal and LN during steam gasification at 800 ^{O}C

The chars obtained from the pyrolysis of coal/biomass blend had the higher overall rate constants (k) than the calculated values, indicating the synergetic effect between coal and the biomass (RS or LN) in terms of the rate of char steam gasification. This synergy can be described by the development of char structure as mentioned in the previous section. In addition, the mineral analysis of the obtained chars from co-pyrolysis was also characterized by XRF technique. It was found that the amount of the retained AAEMs, in particular K, on the chars derived from co-pyrolysis was higher than the predicted contents, as can be seen in Table 4.5. This indicates that there would be some interaction between the released K from the biomass and the produced chars during the pyrolysis of coal/biomass blend. The increment of retained K on the char was directly relevant to the improvement of char reactivity [84]. Consequently, the improvement of the steam gasification rate of char, which was observed in this study, can be described by the development of char structure and the synergy of the retained K on the char during coal and biomass blending system.

Comparing the two types of biomass, the magnitude of the difference between the experimental and the predicted k values was larger for coal/RS blend than for the coal/LN blend (Table 4.4). This was due to the promotion of char steam gasification by the association of char structure and AAEM roles in the case of coal/RS blend which described in section 4.2.3.

Table 4.5 Mineral analysis of the pyrolyzed char

Char sample	Coal	RS	LN	Coal/RS blend 1 : 1		Coal/LN blend 1 : 1	
				Exp.	Cal[a].	Exp.	Cal[a].
Mineral analysis (wt%, db)[b]							
Sodium (Na)	0.10	0.11	0.10	0.16	0.10	0.19	0.10
Potassium (K)	0.55	2.72	1.45	2.31	1.63	1.38	1.00
Calcium (Ca)	3.20	1.85	5.38	1.26	2.53	1.56	4.29
Magnesium (Mg)	0.24	0.25	0.66	0.42	0.24	0.48	0.45

[a] calculate from the data of pure coal and pure biomass

[b] by X-ray fluorescence (XRF)

4.2.4.3 Pyrolytic tar composition

The chemical structure of the pyrolytic tar released during pyrolysis at 800 ^{o}C was characterized by GC-MS over the scanning time range of 5-30 min. Figure 4.9 shows the GC-MS patterns of tar derived from the pyrolysis of coal, biomass and coal/biomass blend with biomass to coal ratio of 1:1. It was found that tar derived from coal pyrolysis mainly consisted of the aromatic hydrocarbons (1, 2, 3 and 4 rings) and their isomeric structures such as naphthalene, fluorene, phenanthrene, anthracene, pyrene and fluoranthene. These structures are hardly decomposed due to the high energy bond of the resonance -C=C- in their aromatic ring (more than 1000 kJ/mol). This result agrees with a previous study which reported that the tar derived from coal pyrolysis contained with PAHs and long chain aliphatic hydrocarbons (C_{50}) [22]. However, the long chain aliphatic hydrocarbons could not be detected in this study because their molecular weight is over the limit of the scanning range (m/z) of the MS (max. m/z = 650).

For the coal/RS blend (Figure 4.9a), the tar component was significantly different from that obtained from both coal and RS. The peaks of phenolic and oxygenated compounds disappeared whilst the aromatic compounds such as naphthalene, anthracene and pyrene were observed instead. Presumably, the oxygenated compounds in the original RS-tar condensed over the coal char to initiate oxygenated-coke species. Concurrently, the volatile K would be interacted with carbon to form the phenolate groups (K-O-C) over the char surfaces. This phenolate group has been reported to play a catalytic role in char steam gasification [4, 18, 23].

The GC-MS pattern of the pyrolytic tar derived from coal/LN blend presented similar peaks of aromatic compounds with lower peak intensity compared to that derived from coal and LN (Figure 4.9b). With respect to the mechanism of heavy tar decomposition over an alumina bed, it has been reported that nascent tar was firstly decomposed to form coke over acidic sites of alumina and then the coke acted as a catalyst for heavy tar decomposition by the accompanying AAEM species [24]. Accordingly, during the pyrolysis of the coal/LN blend, it is supposed that the porous structure of the coal char might promote the condensation of nascent tar, resulting in coke forming over the coal char particles [25]. Consequently, the volatile K from LN would have been deposited leading to the formation of catalytic sites for heavy tar

decomposition. If so, this would provide a potential reason for why the coal/LN blend tar yield was significantly decreased (section 4.2.3).

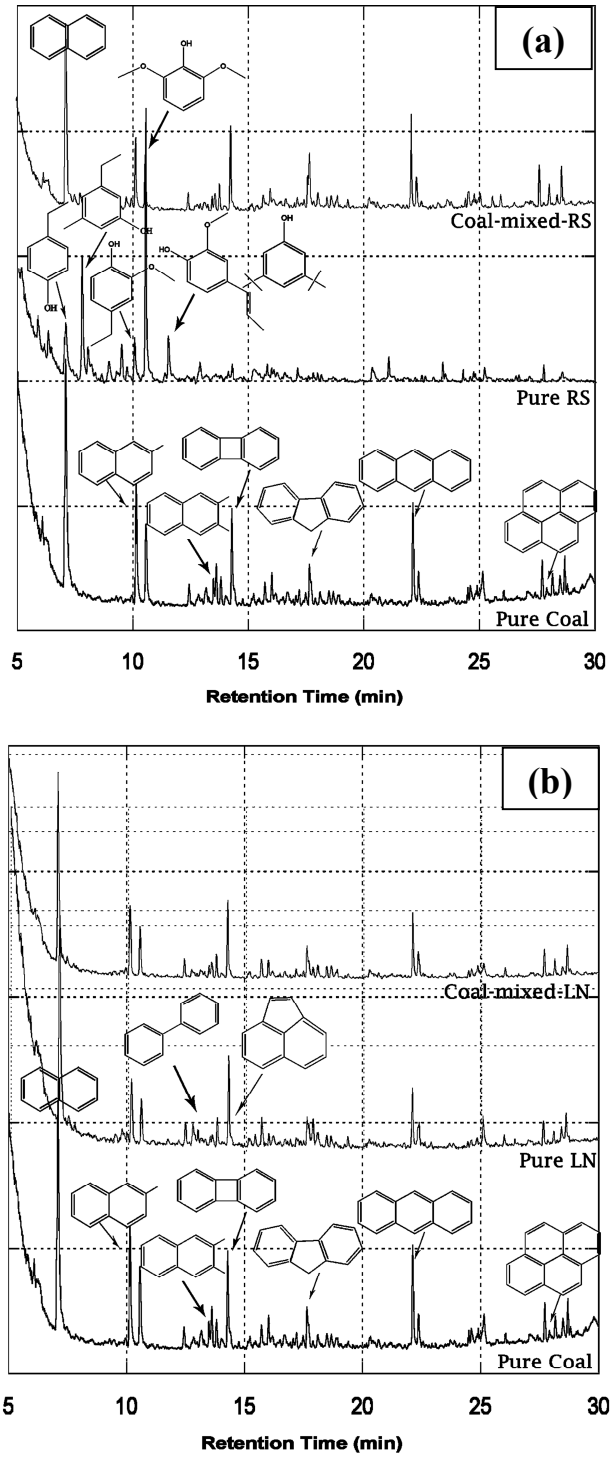

Figure 4.9 Chemical structure of pyrolytic tar derived from the pyrolysis of pure coal, pure biomass and Coal/biomass blend at 800 ^{O}C : for (a) coal/RS and (b) coal/LN

4.3 Synergetic effect during co-gasification

4.3.1 Effect of biomass to coal ratio

Co-gasification of coal and both types of biomass was also carried out in the drop-tube fixed bed reactor. As same as the co-pyrolysis test, the interaction of coal and biomass was determined by comparing the experimental values with the predicted values. Note that for steam gasification test, the product distribution was reported as the percentage of carbon conversion in order to neglect the H_2 production which might be generated from the dissociation of steam. Figure 4.10 shows carbon conversion of coal, biomass and coal/biomass blends from the steam gasification at 800 ^{O}C. The obtained carbon conversion into gas of coal/biomass blends was clearly higher whilst the carbon conversion into tar was evidently lower compared to the predicted values for both cases of coal/RS (Figure 4.10a) and coal/LN (Figure 4.10b) blends. It indicates that the synergetic effect between coal and biomass was manifested under this steam gasification condition. In addition, it was also noticed that the residual char was completely decomposed. It might be stated that the steam gasification of the produced char was a significant reaction step for generating the gaseous product for this experimental system.

The obvious synergetic effect was remarkable at biomass to coal ratio of 1:1 (w/w). When biomass weight ratio was increased to 3:1, the synergetic effect in terms of the increased gas and the decreased tar was not found. This result was different from the pyrolysis results, as mentioned in the section 4.2.1. For co-pyrolysis at a high biomass to coal ratio, the excess of volatiles influenced the synergy resulting in the decreased gas and increased char and tar yields. However, with the presence of external steam, the secondary tar and char formation was reduced by the progression of char steam gasification leading to the increase of gas product. In addition, the catalytic steam gasification of char with a presence of the AAEMs was promoted by the presence of external steam [19, 92]. Moreover, the biomass type was not influenced on the synergetic effect in terms of product distribution as can be seen the similar trends between coal/RS (Figure 4.10a) and coal/LN blends (Figure 4.10b). However, the effect of biomass type was slightly influenced on the composition of gas product that can be seen in Figure 4.11.

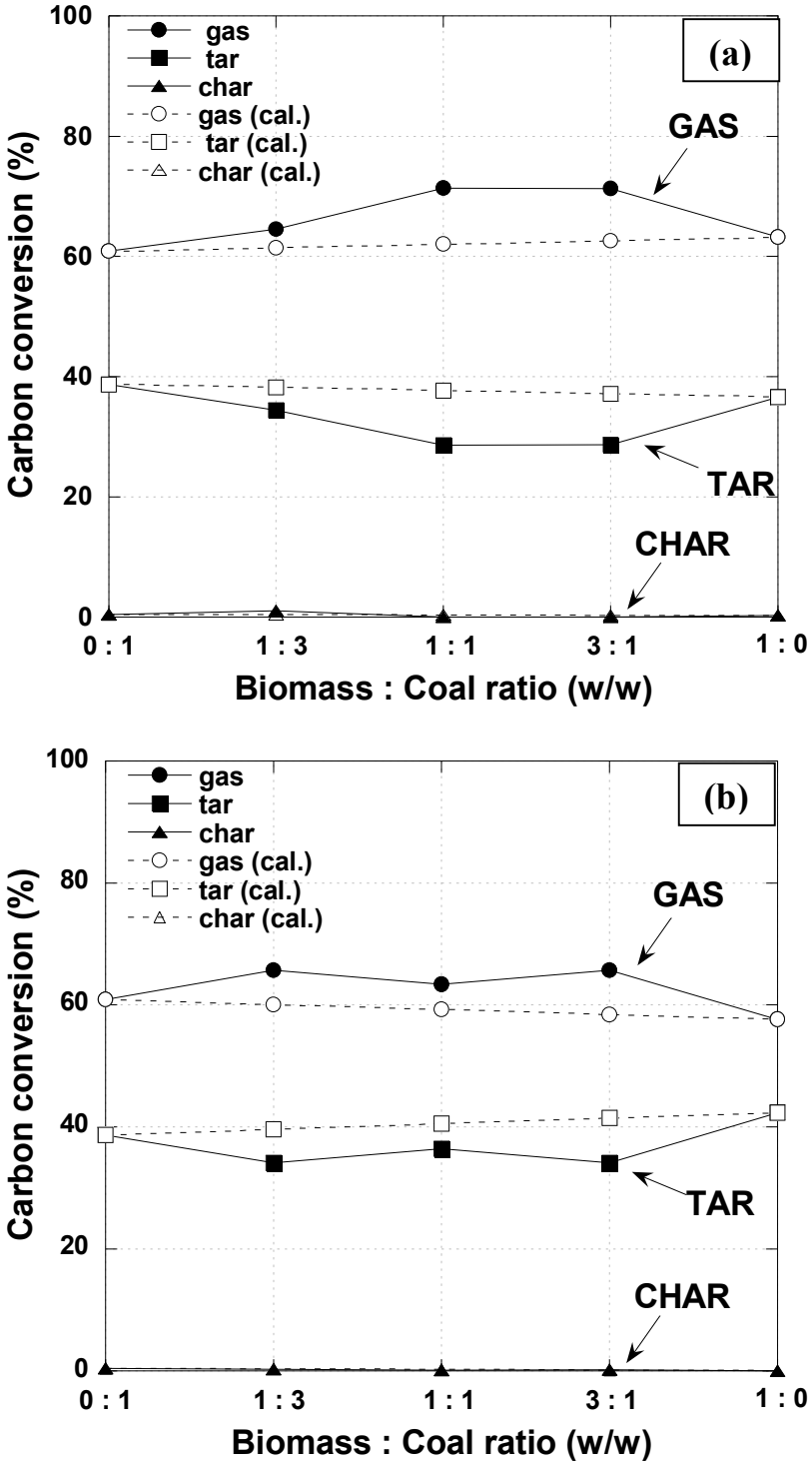

Figure 4.10 Carbon conversion from the steam gasification of the (a) coal/RS and (b) coal/LN blends at 800 ^{O}C

The gas production from co-gasification of coal/RS at RS and coal ratio of 1:1 and 3:1 showed that the production of H_2 and CO was slightly higher than the predicted values while CO_2 and CH_4 production was comparable to the predicted values. It was attributed to the production of gas in the steam gasification of coal/RS blend underwent along the tar steam reforming as shown in Eq. (4.1).

Tar steam reforming: $$C_nH_m + nH_2O \leftrightarrow nCO + (n + {}^{m}\!/_{2})H_2 \quad (4.1)$$

In case of the steam gasification of coal/LN blend, the production of H_2 and CO_2 was significantly higher than the predicted values (Figure 4.11b). It could be supposed that the gaseous product was preferential generated via water gas shift reaction following Eq. (4.2).

Water-gas shift: $$CO + H_2O \leftrightarrow CO_2 + H_2 \quad (4.2)$$

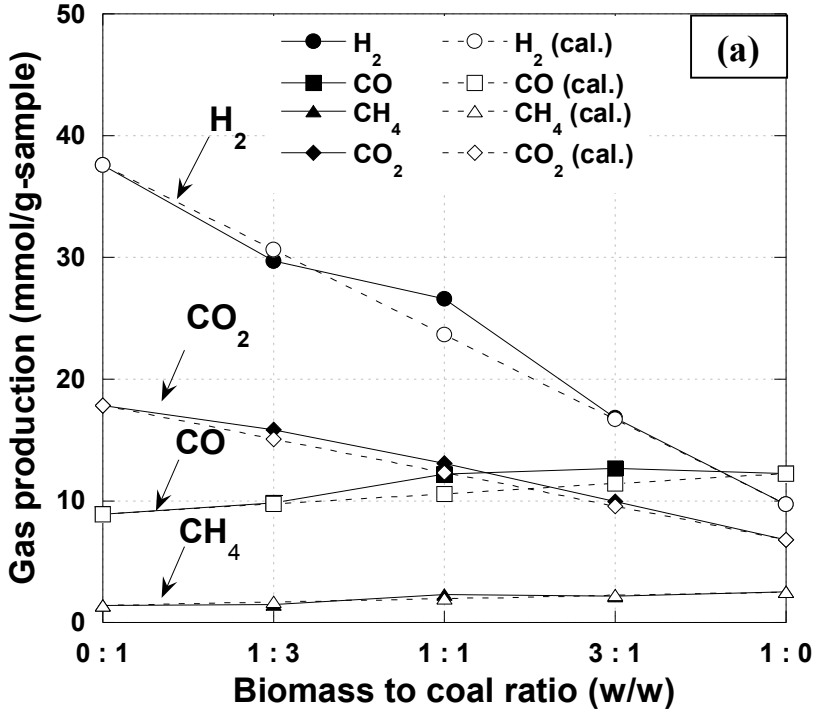

Figure 4.11 Gas production from the steam gasification of the (a) coal/RS and (b) coal/LN blends at 800 ^{O}C

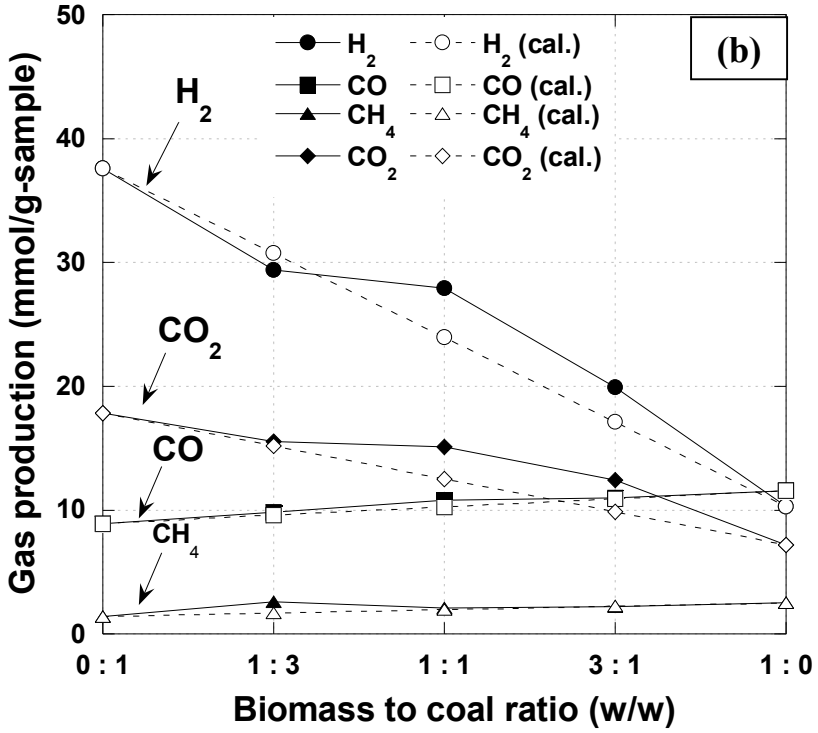

Figure 4.11 (cont.) Gas production from the steam gasification of the (a) coal/RS and (b) coal/LN blends at 800 ^{O}C

In steam gasification, the quality of syngas such as H_2/CO molar ratio and heating value of syngas is very important to determine the suitable application of syngas. The H_2/CO molar ratio and low heating values (LHV) of the produced gas obtained from the steam gasification of coal/biomass blend is shown in Figure 4.12. It was found that a lower H_2/CO molar ratio than the predicted values was found in the co-gasification of coal and RS at all RS to coal ratio. However, the higher H_2/CO molar ratio compared to the predicted values was found in cases of coal/LN blend at LN to coal ratio of 1:1 and 3:1. The LHV of gaseous product was related to the gas composition. The synergetic effect in terms of LHV of the produced gas was found only in the steam gasification of coal/RS blend with RS to coal ratio of 1:1 and coal/LN blend with LN to coal ratio of 1:3. For coal/LN blend, tar mostly converted to the gaseous product by the preferential water-gas shift reaction resulting in the increased H_2 and CO_2, in particular LN to coal ratio of 1:1 and 3:1.This is directly influenced on the higher H_2/CO and lower LHV, as can be seen in Figure 4.12b.

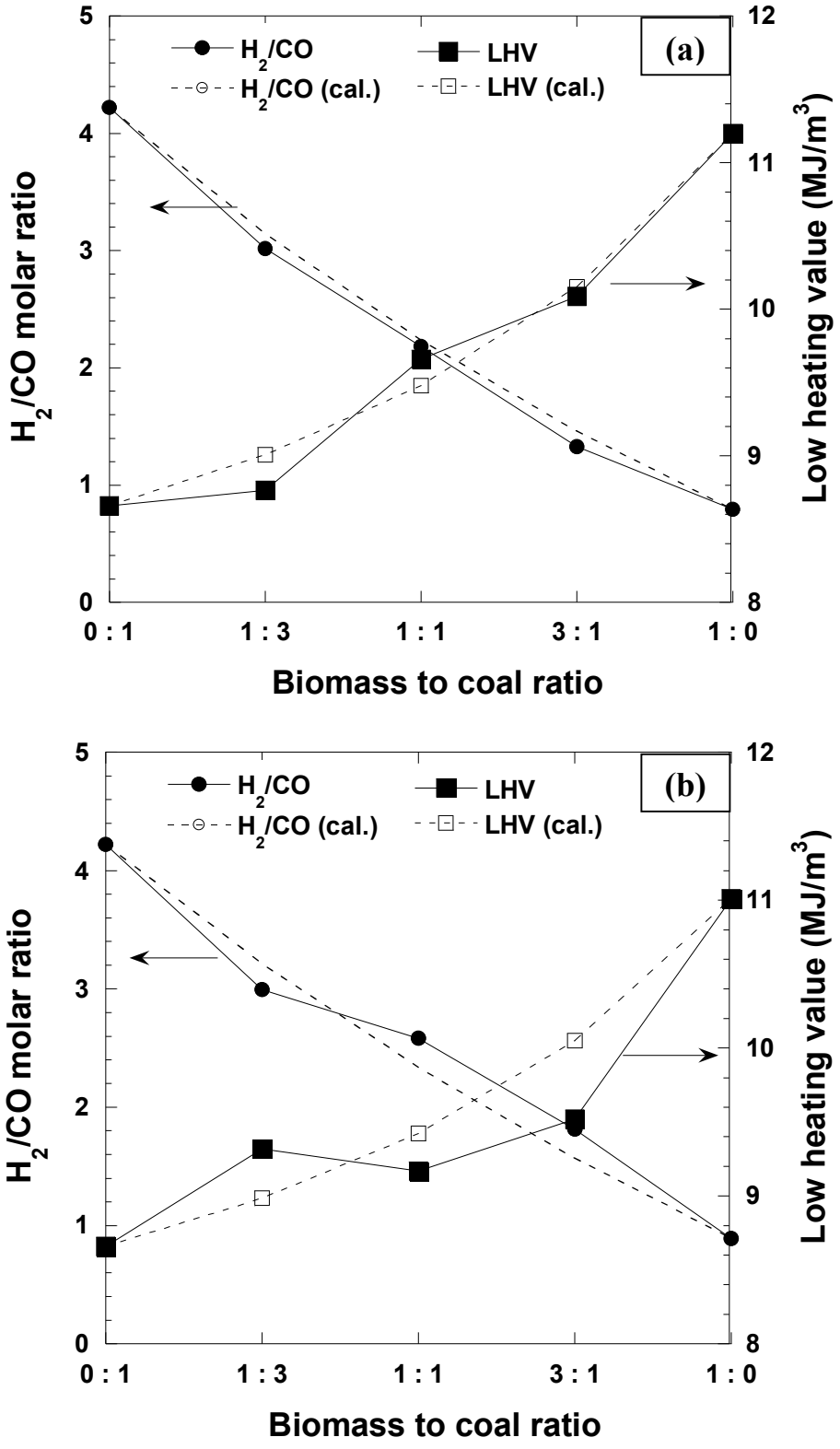

Figure 4.12 H_2/CO molar ratio and LHV of the produced gas obtained from the steam gasification of the (a) coal/RS and (b) coal/LN blends at 800 ^{O}C

4.3.2 Effect of reaction temperature

Effect of co-gasification temperature on carbon conversion for coal/RS and coal/LN at biomass to coal ratio of 1:1 (w/w) is shown in Figure 4.13. At lower reaction temperature (600 and 700 ^{O}C) the lower tar and gas and the higher char yield compared to the predicted yields were observed. It indicated that the synergetic effect on the product yield was not manifested at these gasification temperatures. The formation of secondary char was promoted by the released volatiles from the biomass leading to the increased char and decreased tar yields. At higher reaction temperature, the higher gas yield and lower tar and char yields compared to the predicted values were observed. This was because the suppression of the secondary char formation was promoted by the larger amount of active OH and H radicals and the volatile K which were released from the biomass at high temperature.

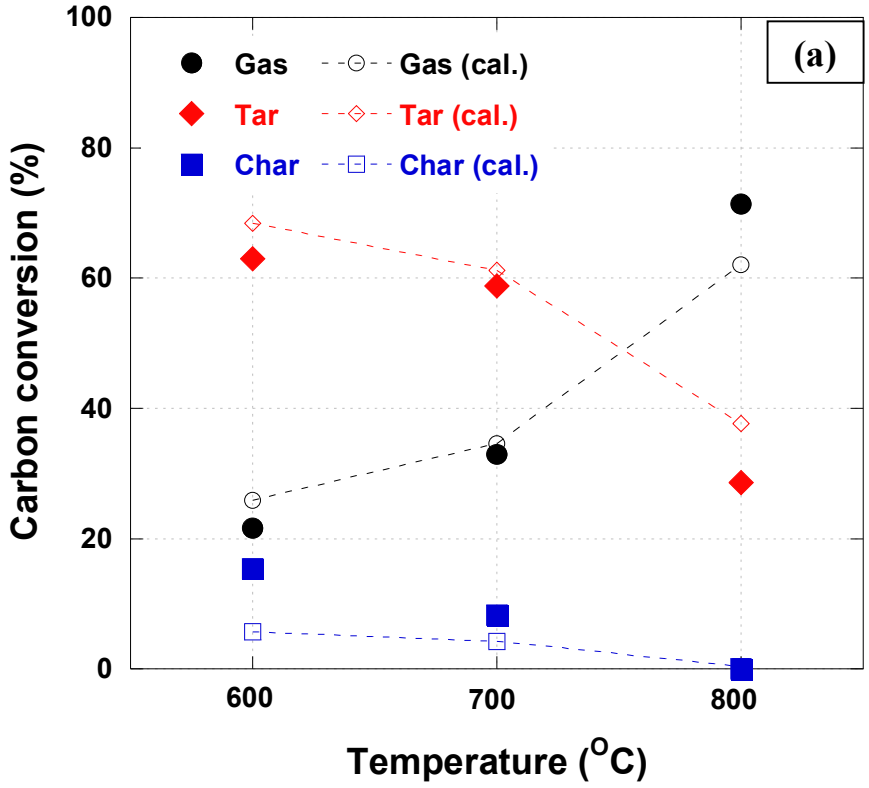

Figure 4.13 Effect of temperature on carbon conversion from the steam gasification of (a) coal/RS and (b) coal/LN blend with biomass to coal ratio of 1:1 (w/w)

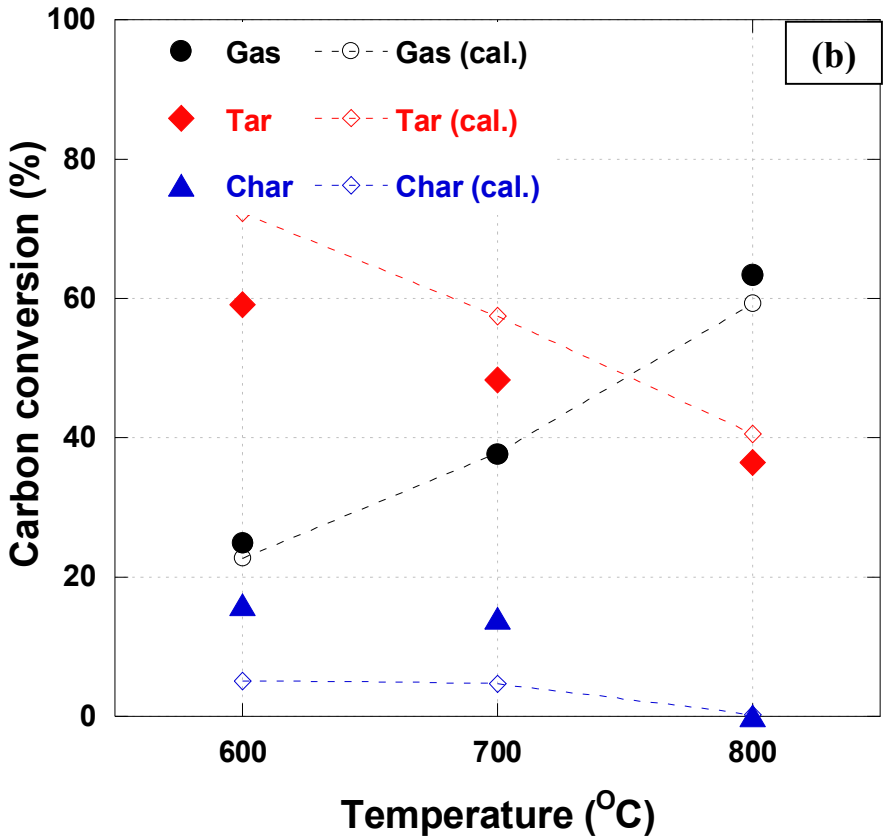

Figure 4.13 (cont.) Effect of temperature on carbon conversion from the steam gasification of (a) coal/RS and (b) coal/LN blend with biomass to coal ratio of 1:1 (w/w)

The effect of reaction temperature on the production of gas from the co-gasification of coal and biomass is showed in Figure 4.14. For coal/RS steam gasification at RS and coal ratio of 1:1 (Figure 4.14a), it can be seen that the CO and H_2 production was increased by the promotion of tar steam reforming (Eq. 4.1) at only the reaction temperature of 800^{O}C. For the steam gasification coal/LN blend at LN and coal ratio of 1:1, the increase in H_2 and CO_2 production was found at the reaction temperature of 700 and 800^{O}C (Figure 4.14b). It indicated that the water-gas shift reaction (Eq. 4.2) could be progressed from the relatively low temperature.

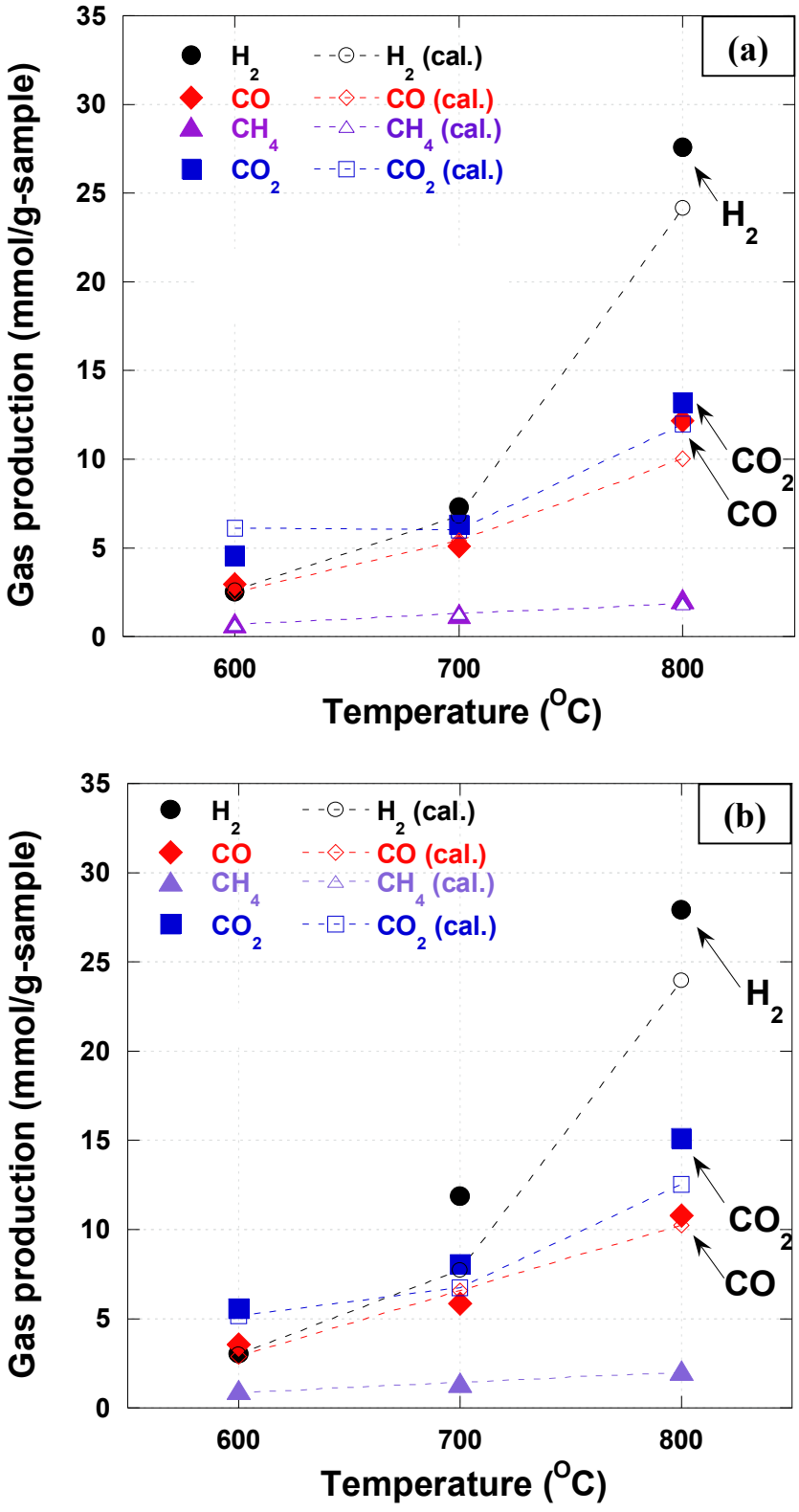

Figure 4.14 Effect of temperature on gas production from the steam gasification of (a) coal/RS and (b) coal/LN blend with biomass to coal ratio of 1:1 (w/w)

Table 4.6 Gas production from co-gasification of RS/coal and LN/Coal blends

Biomass/ coal (w/w)	Temperature (^{O}C)	H_2/CO molar ratio	LHV (MJ/m^3)
RS/Coal 1:1	600	0.853	8.525
	700	1.432	9.464
	800	2.264	9.582
RS/Coal 3:1	600	0.459	7.086
	700	0.865	9.812
	800	1.378	10.027
LN/Coal 1:1	600	0.854	8.673
	700	2.026	9.297
	800	2.445	9.252
LN/Coal 3:1	600	0.536	7.926
	700	1.112	10.104
	800	1.799	9.613

Moreover, the reaction temperature also influenced on the quality of the produced gas such as H_2/CO molar ratio and low heating value as presented in Table 4.6. It was found that the H_2/CO molar ratio was increased with the increase of reaction temperature. The steam gasification of coal/LN at LN and coal ratio of 1:1 gave the highest H_2/CO molar ratio of 2.445. This value might be suitable for the production of methanol which required the H_2/CO molar ratio of about 2. For dimethylether (DME) production or/and Fischer–Tropsch synthesis, the suitable H_2/CO molar ratio should be equal to 1. This H_2/CO molar ratio could be possibly produced from the co-gasification of coal and biomass at low temperature range (600 – 700^{O}C). In addition, the low heating value of the produced gas was increased with the reaction temperature and biomass blending ratio. For co-gasification of coal and biomass, the maximum low heating value of the produced gas was about 9 – 10 MJ/m^3 for coal/RS and coal/LN blends at biomass to coal ratio of 3:1.

CHAPTER V

VOLATILE-CHAR INTERACTION DURING CO-GASIFICATION : IN A THERMOBALANCE REACTOR

In this chapter, the interaction between coal char and biomass derived volatile was investigated in a rapid heating thermobalance reactor, as described in Chapter III. The interactions between three types of coal char (Ex-char, Ac-char and In-char) and three types of volatile sources (cellulose, xylan and rice straw) in terms of coal char reactivity and gas production rate were discussed. The results were divided into 5 sections; (i) characterization of the prepared coal chars and the volatile sources, (ii) steam gasification of coal char without the contact of volatiles, (iii) steam gasification of coal char with the contact of volatiles, (iv) decomposition of the volatile resource without coal char and (v) decomposition of the volatile resource with coal char**.**

5.1 Characterization of the prepared chars and volatile sources

Three types of coal chars were prepared i.e. Ex-char, Ac-char and In-char. The preparing conditions of each coal char was presented in Table 3.1. The BET surface area, pore volume and pore diameter of Ex-char and Ac-char are shown in Table 5.1. Comparing with Ex-char, the Ac-char has the 9.1 and 5.2 times lower BET surface area and pore volume, respectively whilst the average pore sized increased 1.75 times. This result indicates that the Ac-char structure was destroyed by the acid washing resulting in the less porosity structure with the larger pore diameter. The morphology of both coal chars was analyzed by SEM method and SEM images as shown in Figure 5.1. It was found that the surfaces of Ac-char have less porosity than that of the Ex-char. Moreover, the collapsed of carbon matrix was observed. This is an important confirmation for the destruction of the Ac-char. In addition, the mineral analysis of the chars was analyzed by XRF method and shown in Table 5.2. It was found that the AAEM on Ex-char surfaces was lost by acid washing. Unfortunately, the

characterization of the In-char could not be determined because the content of char formed inside the thermobalance reactor was not enough for the analysis by BET, SEM and XRF methods.

Table 5.1 BET surface area, pore volume and pore size of coal char

Coal char sample	Ex-char	Ac-char
BET surface area (m^2 g^{-1})	200.71	21.99
Pore volume (cm^3 g^{-1})	0.1389	0.0266
Average pore size (A^o)	27.68	48.33

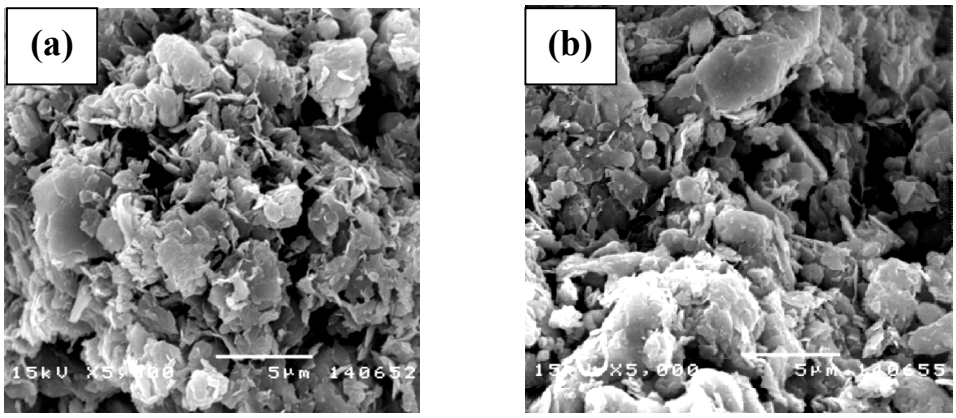

Figure 5.1 SEM images of (a) Ex-char and (b) Ac-char

Table 5.2 Element analysis of volatile sources and coal chars by XRF technique

Sample	Element content (wt%, as received)				
	Na	K	Mg	Ca	Si
Coal char bed					
Ex-char	0.31	0.59	0.41	9.56	10.90
Ac-char	0.02	0.17	0.28	0.82	5.55
Volatile source					
Xylan	0.73	0.17	<0.01	2.22	0.05
Rice straw	0.06	1.77	0.13	0.69	11.29

In this study, three types of volatile sources were used; cellulose, xylan and rice straw. The characterization of the tar derived from the pyrolysis of all volatile sources at 800 ^{O}C by GC-MS technique is shown in Figure 5.2. It was found that tar derived from rice straw mainly contained with aromatic compounds such as phenol, naphthalene, anthracene and pyrene. These compounds trended to form coke/soot over char surfaces easier than the saccharide units such as furfural in the tar derived from cellulose and xylan. In addition, the proximate and ultimate analyses of all volatile sources are shown in Table 5.3. It was found that cellulose had the highest of volatile matter content and lowest ash amount while rice straw contained the highest ash content. Xylan, the major component derived from the pyrolysis of hemicelluloses, has the similar level of volatile content with the rice straw which is about 63 wt%. This different composition of all volatile sources would be probably influenced on the reactivity of the coal char and the decomposition of them during the steam gasification which will be discussed in the next section.

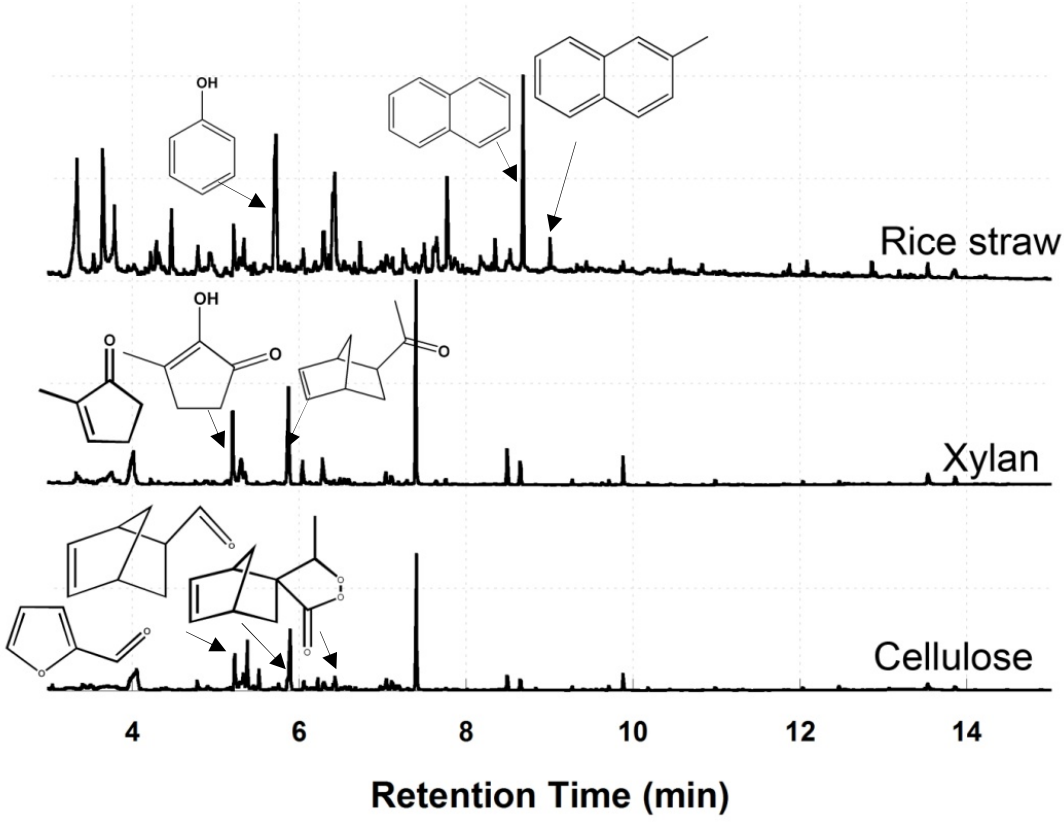

Figure 5.2 GC-MS patterns of the tar derived from the pyrolysis of cellulose, xylan and rice straw at 800 ^{O}C

Table 5.3 Proximate and ultimate analyses of the volatile sources

Sample	Proximate analysis (wt%)				Ultimate analysis (wt% dry ash-free basis)			
	Moisture	Ash	Volatile matter	Fixed carbon	C	H	N	O (diff.)
Rice straw	6.43	11.22	61.95	29.25	45.30	6.93	0.92	46.71
Cellulose	4.01	0.01	80.30	15.68	35.94	5.82	0.04	58.25
Xylan	12.88	8.01	63.95	15.16	37.50	7.15	0.10	55.25

5.2 Steam gasification of coal char without the contact of volatiles

Figure 5.3 shows the time-relative mass profile of all prepared coal chars during steam gasification at 800 ^{O}C without the contact of volatiles. Note that the initial time (0 s) was defined as the weight change of the raw sample during the initial pyrolysis before the temperature reached 800 ^{O}C. The time-relative mass profiles of all coal chars showed the similar patterns which rapidly decreased in the first stage and then slightly decreased to achieve the final weight at time of 5000 s. A summary of final char conversion ($X_{char,final}$) and the overall rate constant (k) of coal char during steam gasification is shown in Table 5.4. The overall rate constant (k) refers to the reactivity of coal char and it could be ordered as following: In-char > Ex-char > Ac-char. Among all coal chars, the Ac-char showed the lowest $X_{char,final}$ and k values of 0.831 and 3.22×10^{-4} s^{-1}, respectively. For char steam gasification under rapid heating rate, the catalytic gasification by alkali and alkaline earth metallic species (AAEMs) underwent in parallel with non-catalytic steam gasification [20]. As described in the previous section, the amount of AAEM species on the surfaces of the Ac-char was lower than those of the Ex-char, especially Na and Ca. Na and Ca were reported as the catalyst for steam gasification of carbon and coal [26]. Therefore, it could be stated that the loss of catalytic species in the Ac-char leading to the reduction of coal char reactivity with steam.

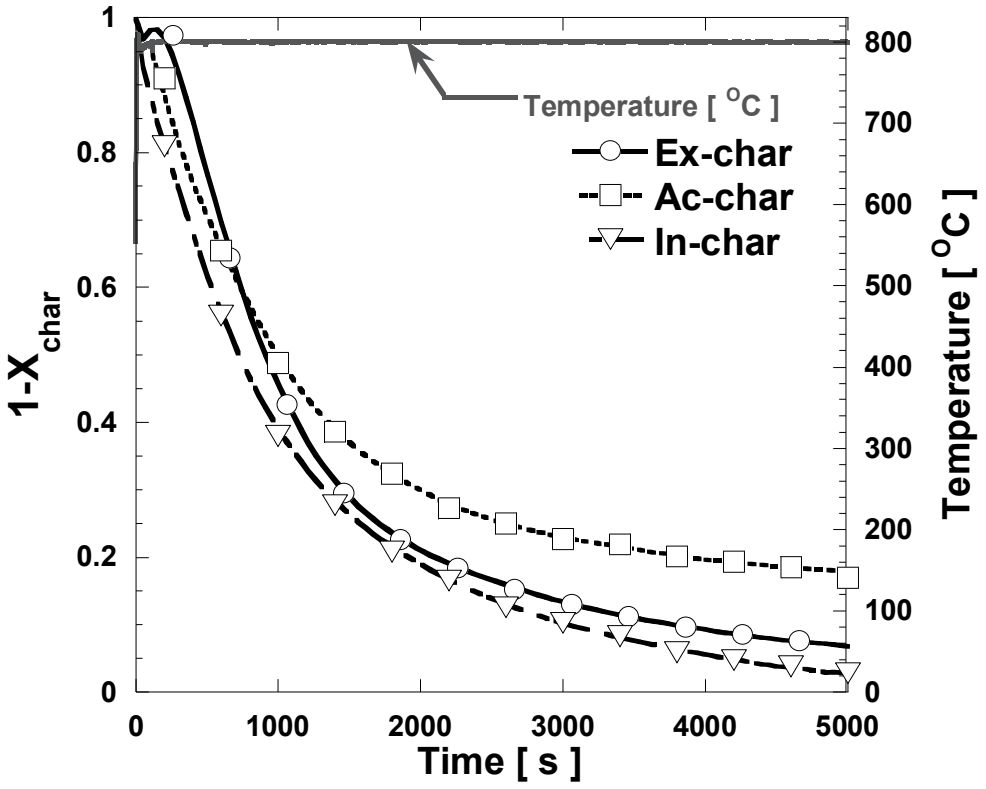

Figure 5.3 Time-relative mass profile of prepared coal chars in steam gasification at 800 ^{O}C without the contact of volatiles

Furthermore, the destruction of the Ac-char surfaces by acid washing is another reason to reduce the reactivity of coal char. This result agrees with Jamil et al. [93] which was stated that char reactivity depended on the catalytic activity of AAEMs and the char structure. The In-char showed the largest $X_{char,f}$ of 0.972 and the overall rate constant (k) of 6.76 × 10^{-4} s^{-1}. The overall rate constant of In-char was higher than that of Ac-char and Ex-char about 52% and 20%, respectively. The high reactivity of the In-char showed a good agreement with the reactivity of biomass char and coal char which was prepared with high heating rate [25, 80, 94]. The steam gasification rate of the coal char substantially increased under rapid heating because of the rapid evolution of volatile. This led to produce the high total porosity of char as well as large total surface area [95-97]. However, under rapid heating rate pyrolysis, the volatilization of AAEM species over char surfaces was promoted. Then, it caused the loss of catalytic species for char steam gasification [26, 88]. Hence, it could be

speculated that the high reactivity of the In-char was influenced by the improvement of char structure with the minor catalytic effect of AAEM on char surfaces.

Table 5.4 The final char conversion ($X_{char,final}$) and the overall rate constant (k) of char steam gasification at 800 ^{O}C

Coal char	Volatile sources	Char conversion at t=5000 s ($X_{char,final}$)	Overall rate constant, (k x10^4 s^{-1})	Regression coefficient (R^2)
Ex-char	-	0.932	5.44	0.95
Ex-char	Cellulose	0.883	4.14	0.94
Ex-char	Xylan	0.894	4.63	0.99
Ex-char	Rice straw	0.863	4.05	0.99
Ac-char	-	0.831	3.22	0.89
Ac-char	Cellulose	0.865	4.37	0.97
Ac-char	Xylan	0.730	2.50	0.90
Ac-char	Rice straw	0.842	3.99	0.99
In-char	-	0.972	6.76	0.99
In-char	Cellulose	0.866	3.62	0.91
In-char	Xylan	0.910	4.94	0.98
In-char	Rice straw	0.707	2.44	0.97

5.3 Steam gasification of coal char with the contact of volatiles

Figure 5.4 shows time-relative mass profiles of Ex-char with the contact of each volatile resource i.e. cellulose, xylan and rice straw. It was found that the relative mass profile of Ex-char with the contact of volatiles was dramatically higher than that of original Ex-char. It indicated that the steam gasification rate of the Ex-char was reduced by the contact of volatiles resulting in the lower $X_{char,final}$ and k values as can be seen in Table 5.4. It could be stated that the volatiles derived from all volatile sources caused the depletion of steam gasification rate of the Ex-char. In addition, it was found that the volatiles derived from rice straw seem to significantly reduce the steam gasification rate of Ex-char compared to those derived from cellulose and

xylan. It has been reported that cellulose, one of the major components in biomass, was H-donor species during pyrolysis [98]. A few studies reported about the inhibition effect of H-species on char reactivity [20, 24]. Fushimi et al. revealed that the higher hydrogen partial pressure greatly inhibited the gasification rate of biomass char via the reverse oxygen exchange and dissociative hydrogen adsorption reactions as expressed in Eqs. (5.1) and (5.2) [24]. Bayarsaikhan et al. also reported that the non-catalytic char steam gasification was greatly decelerated by the presence of H_2 due to its dissociative chemisorption onto free carbon sites (C) forming H-laden carbon (C(H)). It was also mentioned that the hydrogen radical dissociated from volatiles played more significant role on suppressing the char gasification than that from H_2. [20]. The dissociative chemisorption of hydrogen radical from the thermal cracking of volatile in the gas phase, following Eq. (5.3), could prevent the progress of char steam gasification.

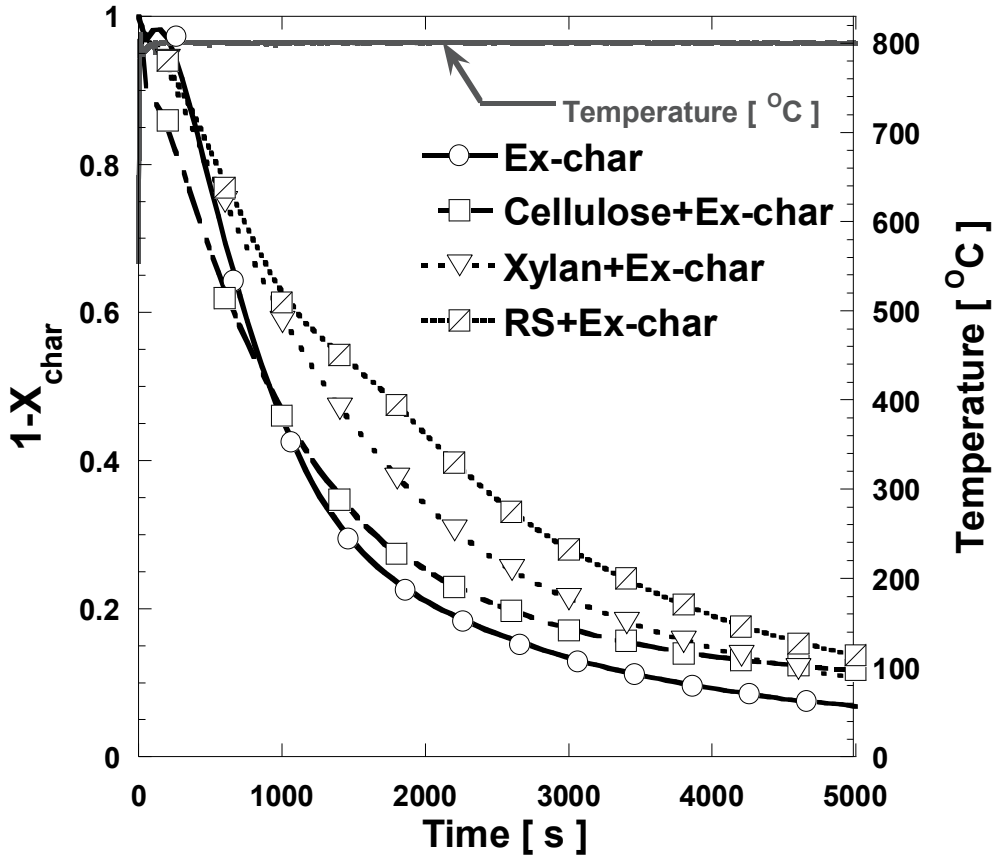

Figure 5.4 Time-relative mass profiles of Ex-char in steam gasification at 800^{O}C with the contact volatiles

Reverse oxygen exchange: $C(O)+H_2 \leftrightarrow C+H_2O$ (5.1)

Dissociative hydrogen adsorption: $C+\frac{1}{2}H_2 \leftrightarrow C(H)$ (5.2)

Dissociative H-radical from volatile chemisorption: $C+H \leftrightarrow C(H)$ (5.3)

In case of In-char, the time-relative mass profiles are shown in Figure 5.5. It was found that all volatile sources showed the crucial inhibition effect on In-char steam gasification rate. The order of $X_{char,final}$ and k values was shown as following: In-char > xylan+In-char > cellulose+In-char > rice straw+In-char (Table 5.4). The inhibition effect on In-char reactivity had the same trend with the Ex-char in Figure 5.4. However, the reduction of steam gasification rate of the In-char by the contact of volatiles was more significant.

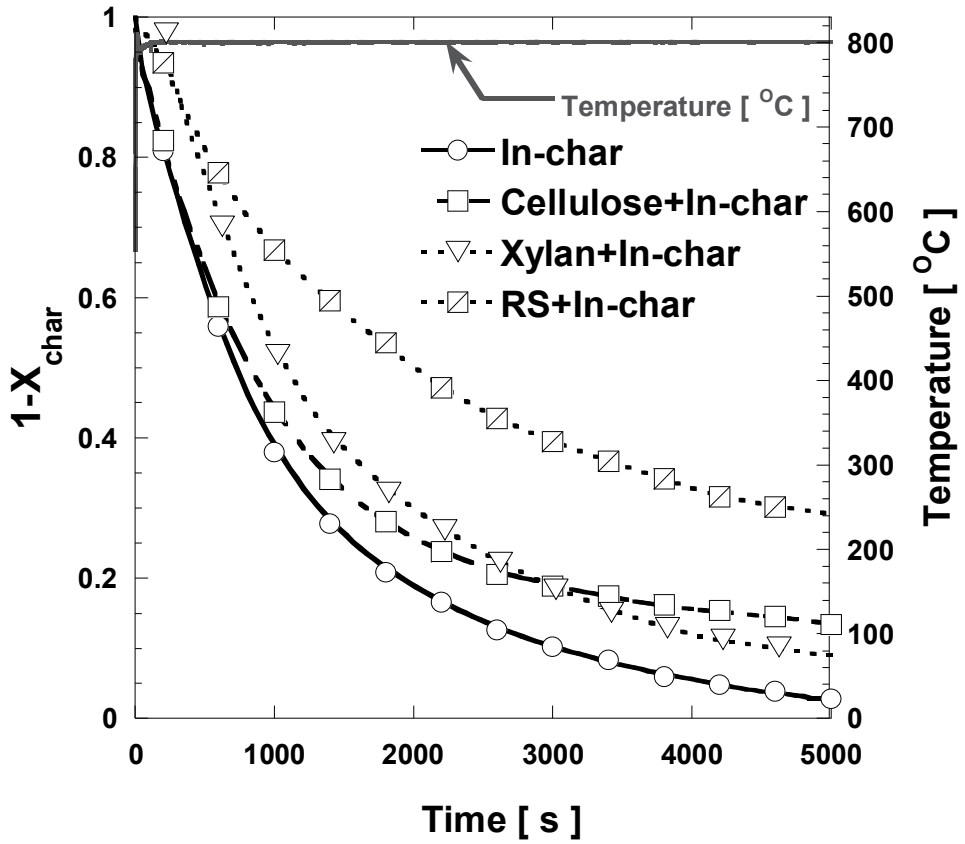

Figure 5.5 Time-relative mass profiles of In-char in steam gasification at 800 ^{O}C with volatile contacting

The difference of heating rate and holding time during char preparation step was influenced on the structure and reactivity of char. As mentioned in the previous section, the rapid release of volatiles during the rapid heating pyrolysis caused to obtain the highly porous char which mostly contained with mesopores (2-50 nm) and macropores (>50 nm). The mesopore and macropore surfaces of char were reported as the active sites for char gasification [96, 97, 99, 100] and the inductive sites for coke formation from the large molecular weight hydrocarbons [101]. Moreover, with the presence of volatiles, the competition between char steam gasification and carbon deposition by volatile occurred [20]. It could be supposed that the reactivity of the In-char was reduced by the contact of volatiles. It was because the coke formation might greater dominant than the char steam gasification leading to the higher solid residues as evidenced in Table 5.4. Another reason was the volatilization of the inherent catalyst species such as Na, K and Ca (Eq. (5.4)) was promoted by the presence of volatiles, resulting in the loss of catalytic effect for steam gasification of char [102].

Volatilization of AAEM by R radical $$R + CM - X \leftrightarrow CM - R + X \quad (5.4)$$

where R, CM and X represented to free radical from volatile (mainly H-radical), char matrix and AAEM species, respectively. Considering the type of volatile sources, the volatiles derived from rice straw showed the stronger inhibition effect on the reactivity of In-char compared to those derived from cellulose and xylan. The effect of volatile sources will be discussed accompanying with the result of gas production in the next section.

Time-relative mass profile of Ac-char with and without volatile contacting showed the similar patterns as can be seen in Figure 5.6. The final char conversion ($X_{char,final}$) and k values of all Ac-chars were close to the values of 0.8 and 4×10^{-4} s^{-1}, respectively (Table 5.4). This indicated that the volatiles derived from cellulose as well as rice straw do not affect the steam gasification rate of the Ac-char. It might be due to the non-active structure of the Ac-char after acid washing. However, in case of xylan contacting, the Ac-char showed the slightly small $X_{char,final}$ and k values compared to other volatile sources. It was supposed that the stronger inhibition of xylan on the Ac-char was attributed to the high possibility to form non-reactive carbon (coke) over the Ac-char. This hypothesis might be clarified by the result of gas production which showed the promotion of coking from methane, following Eq. (5.5),

leading to the decrease of CH_4 production and increase of H_2 production. The details of gas production from the decomposition of all volatile sources will be discussed later.

Coking from methane: $CH_4 \rightarrow C + 2H_2$ (5.5)

Coking from hydrocarbon: $C_nH_{2n+2} \leftrightarrow nC + (n+1)H_2$ (5.6)

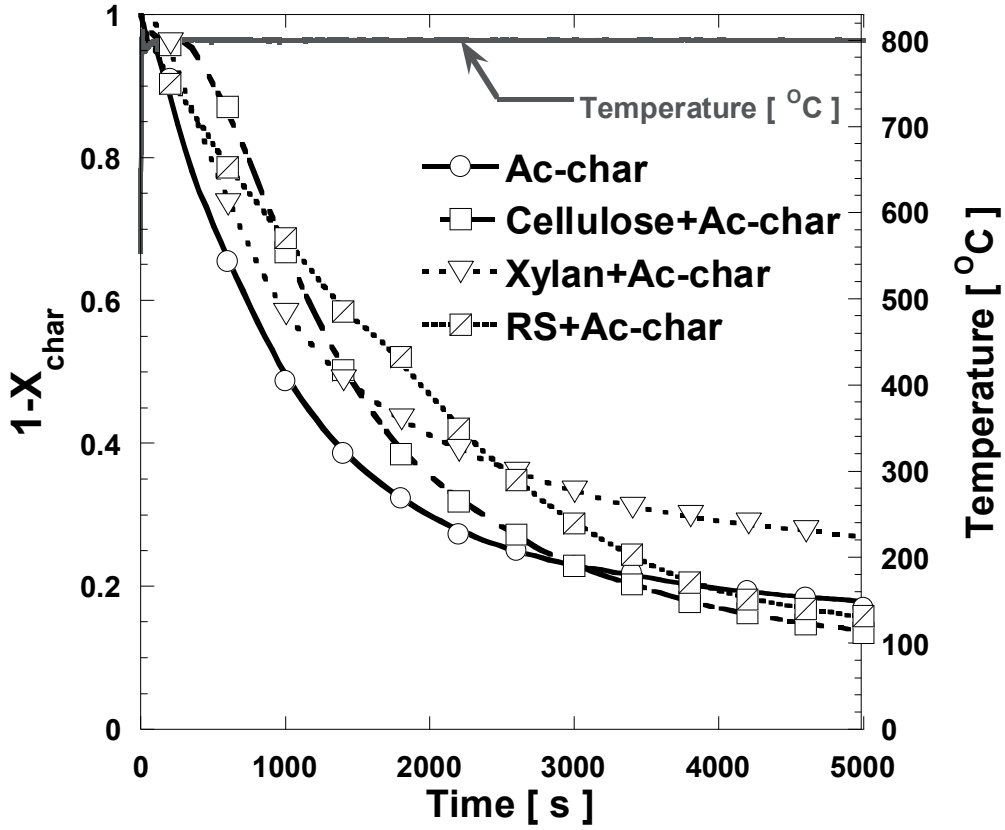

Figure 5.6 Time-relative mass profiles of Ac-char in steam gasification at 800 ^{O}C with volatile contacting

5.4 Decomposition of the volatile sources without coal char

The average gas production rate from the decomposition of pure volatile sources (cellulose, xylan and rice straw) without coal char during steam gasification at 800 ^{O}C is shown in Figure 5.7. It was found that cellulose favored the H_2 and CO production as the main products while H_2 and CO_2 were mostly generated from xylan decomposition. This result was consistent with the previous studies [103, 104]. They reported that, in the pyrolysis and air-steam gasification of cellulose and xylan, the

main gaseous products were H_2, CO and CO_2. Cellulose mostly produced the higher CO production than the other gaseous species whilst xylan produced the relatively high amount of CO_2. This is because cellulose molecules mainly contain with the ether (C-O-C) and carbonyl (C=O) group which can probably promote the CO production. In contrast, the release of CO_2 from hemicellulose (mainly xylan) was caused by the cracking and reforming of carboxyl (COOH) groups [104].

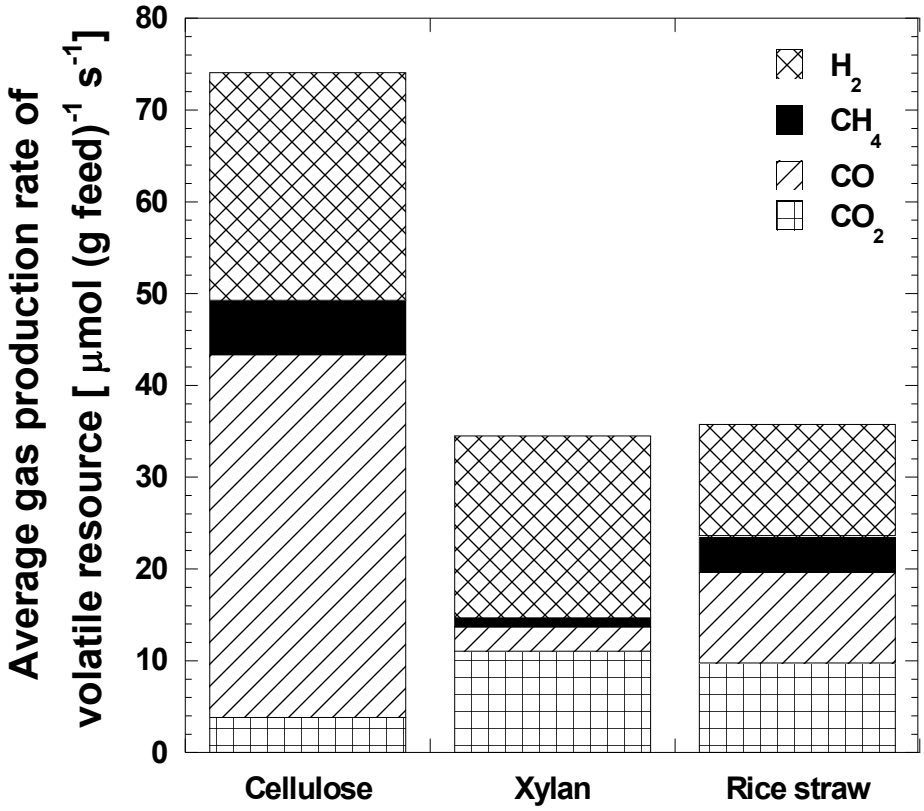

Figure 5.7 Averaged gas production rate from the decomposition of all volatile sources without coal char during steam gasification at 800 ^{O}C

5.5 Decomposition of the volatile sources with the presence of coal char

During the steam gasification of char with volatile feeding, the volatile decomposition took place simultaneously with the char steam gasification within the same reactor. The data represented the net gas production rate which derived from the volatile sources excluding gas evolution from coal char. Figure 5.8 shows the average gas production rate from the decomposition of cellulose with and without coal char during steam gasification at 800 ^{O}C. It was found that, with the presence of Ex-char,

the total gas production rate of cellulose dramatically increased. This provided the higher H_2 and CO production than the absence of coal char. This might be stated that the Ex-char performed as a catalyst for cellulose derived tar steam reforming following Eq. (5.7).

Tar steam reforming: $$C_nH_m + nH_2O \leftrightarrow nCO + (n + {}^{m}\!/_{2})H_2 \quad (5.7)$$

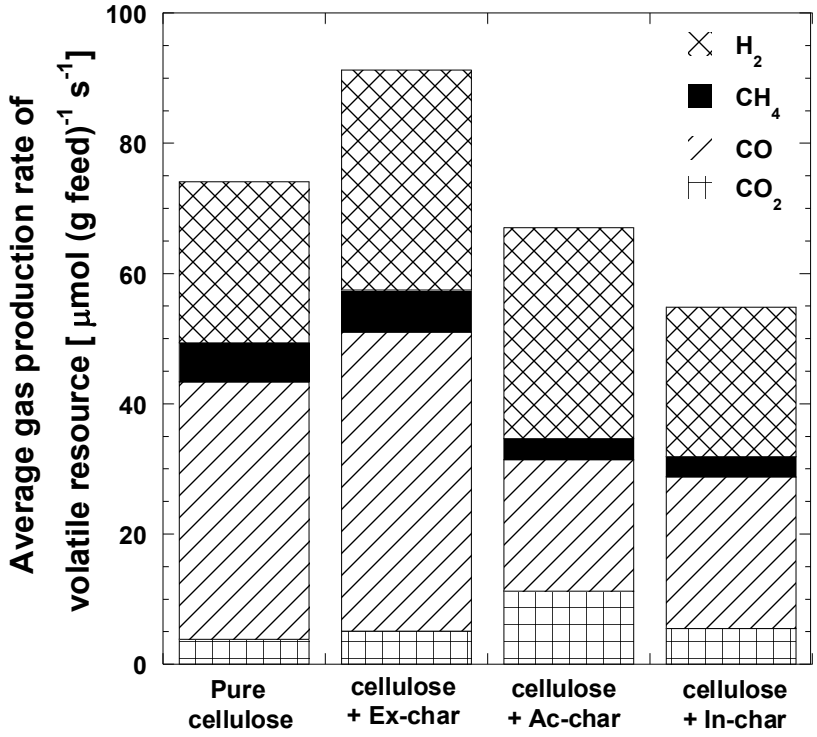

Figure 5.8 Averaged gas production rate from the decomposition of cellulose with inert and coal char beds during steam gasification at 800 ^{O}C

The catalytic effect of char, which derived from biomass as well as the low rank coal pyrolysis, on tar reduction has been paid attention in many studies [29, 31, 76, 77, 90]. Mechanism of the decomposition of nascent volatile and aromatics over charcoal was proposed by Hosokai et al. They reported that the nascent tars were deposited over the charcoal to form coke, subsequently, char/coke steam gasification to produce gas product [77, 105]. Therefore, the catalytic effect of Ex-char on the increase of gas production could be described in two ways; (i) the enhancement of coke formation due to the high porous structure, with surface area of 200.7 m^2 g^{-1} and (ii) the subsequent carbon steam gasification which was promoted by the AAEM

species over the Ex-char surfaces, especially Ca (see in Table 5.2). The retained Na and Ca in coal char was reported to be the active catalyst for the nascent tar/soot decomposition [76] as well as carbon steam gasification [26] .

Conversely, the presence of Ac-char and In-char gave the lower total gas production than the absence of coal char. This result indicates that the catalytic role of the Ac-char and In-char on tar reduction was not observed, the barrier of tar reduction was observed instead. Even though the Ac-char structure was not preferable to form coke alike the Ex-char, the higher H_2 and lower CH_4 production was observed. It could be supposed that coking over the Ac-char presumably occurred in this experimental system. The coke formation from methane and hydrocarbons underwent following Eq. (5.6) and (5.7). As mentioned above, the subsequence steam gasification of coke would be progressed and generated gas products. In this case, the rate of coke steam gasification was slower than coking due to the loss of AAEM species over char surfaces led to produce small gas product. Similarly with the case of In-char, the promotion of the volatilization of AAEM by volatiles resulted to reduce the rate of coke steam gasification. In the same time, the active structure of the In-char induced to form more coke over its surfaces. Therefore, the total gas production in case of In-char was lower than that in case of Ac-char.

Considering the effect of coal char on xylan and rice straw decomposition (Figure 5.9 and 5.10), it was found that the presence Ex-char gave the higher total gas production with higher H_2, CO and CO_2 production. It indicated that the Ex-char might act as the catalyst for rice straw derived tar steam reforming and also coke steam gasification because of its active surfaces as mentioned above. In addition, it can be noticed that the Ex-char also play a catalytic role on the decomposition of CH_4 resulting in the essential decrease of CH_4 as can be seen in Figure 5.9. This result was consistent with Bai et al. who reported that coal char could be a catalyst for methane decomposition [106]. They revealed that the catalytic methane decomposition over coal char mainly occurred within its micropores and the mineral on its ash had a little effect.

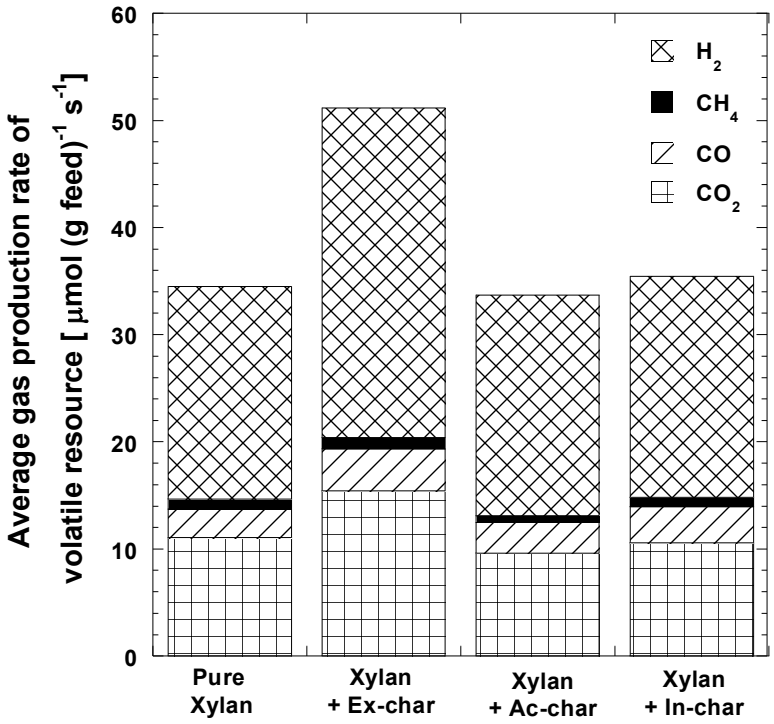

Figure 5.9 Averaged gas production rate from the decomposition of xylan with inert and coal char beds during steam gasification at 800 ^{O}C

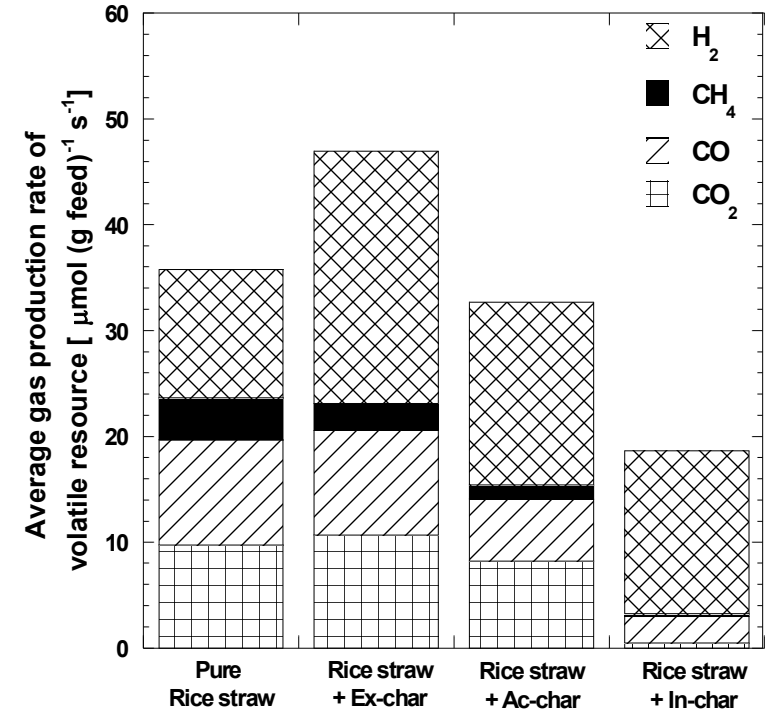

Figure 5.10 Averaged gas production rate from the decomposition of rice straw with inert and coal char beds during steam gasification at 800 ^{O}C

The effect of Ac-char and In-char on gas evolution of xylan and rice straw showed the similar results with the case of cellulose (Figure 5.8). However, it was noticeable that the gas evolution from rice straw with the presence of In-char had the lowest content among all experiments. It could be stated that the secondary reaction such as soot and coke formation in the case of rice straw derived tar with the presence of In-char was more significant than steam gasification of the forming coke. This result shows a good agreement with the reactivity of the In-char as mentioned in section 5.2. As describe in section 5.1, the composition of tar derived from rice straw mainly composed of the heavy aromatic hydrocarbons. Therefore, the coke formation from the heavy tar, via ring condensation and crosslink reaction, was more extensive on the carbonaceous material as well as the porous alumina [90]. On the other hand, the formed coke from the aromatics or high molecular weight hydrocarbon hardly to decompose by steam

Finally, interaction of volatile and three types of coal chars depended on the competitive reaction between coke formation (r_{ci}) and coke steam gasification (r_{si}) as illustrated in Figure 5.11. High porous structure and high AAEM contents of the Ex-char could be supposed that the rate of coke steam gasification would be faster than the rate of coke formation (Figure 5.11a). The loss of AAEM during the rapid heating during the preparation of the In-char and the presence of macropore surfaces induced to form coke more than converting into the gas products. It would be stated that in case of In-char the rate of coke formation would be higher than the rate of coke steam gasification. Lastly, in case of Ac-char which presence the less porosity and AAEM contents, the rate of coke formation would probably faster than the rate of coke steam gasification.

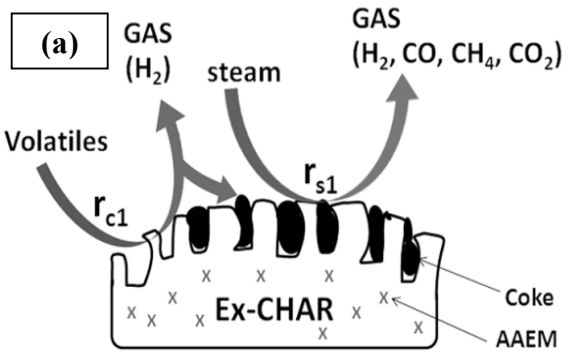

Ex-char : $r_{s1} > r_{c1}$

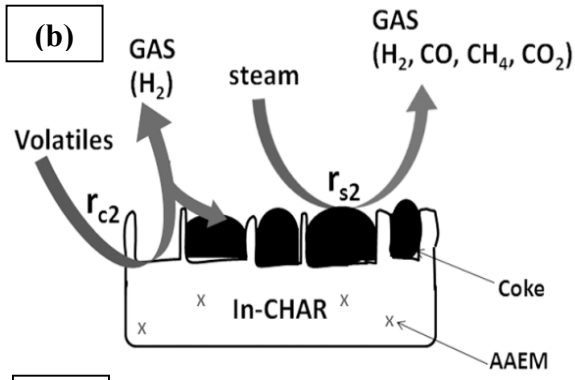

In-char : $r_{c2} >>> r_{s2}$

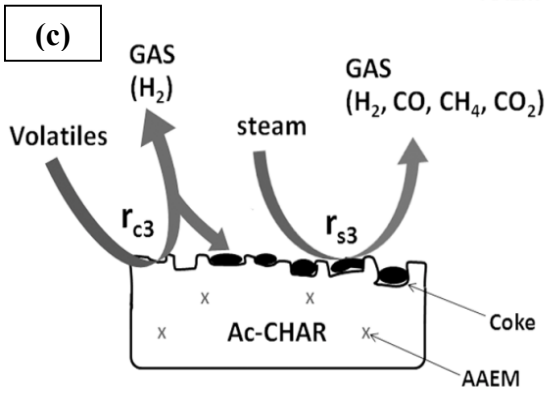

Ac-char : $r_{c3} > r_{s3}$

Rate of char steam gasification (r_g) = $r_{si} - r_{ci}$
r_{ci} = rate of coke formation of
r_{si} = rate of coke steam gasification
i = index of char type; 1=Ex-char, 2=In-char and 3= Ac-char

$$r_{g2} < r_{g3} < r_{g1}$$

Figure 5.11 Interaction between volatile and three types of coal char (a) Ex-char , (b) In-char and (c) Ac-char

CHAPTER VI

VOLATILE-CHAR INTERACTION DURING CO-PYROLYSIS/GASIFICATION : IN A TWO-STAGE FIXED BED REACTOR

In this chapter, the interaction between coal char and biomass derived volatile was investigated in a two-stage fixed bed reactor as described in Chapter III. The effect of two types of coal char; Ex-char and Ex-char800, on the product yield and gas composition during pyrolysis and steam gasification of rice straw was compared with the inert alumina bed. The effect of pyrolysis temperature on the catalytic effect of coal char was also explained in this chapter. The results were divided in 3 sections; (i) characterization of the prepared coal chars, (ii) the pyrolysis of rice straw and (iii) the steam gasification of rice straw with the presence of coal char.

6.1 Characterization of the prepared coal char

From proximate and ultimate analyses (Table 6.1), it was found that both prepared coal chars had the lower moisture content, volatile matter, H/C molar ratio and oxygen content whilst higher ash content and fixed carbon compared to the original coal. It was due to the release of volatile during the slow pyrolysis of coal at high temperature (600 – 800 ^{O}C) resulting in forming char via the secondary reactions those involve polymerization and/or thermal cracking of the heavier volatile products [107]. Comparing with Ex-char, the Ex-char800 had lower H/C molar ratio. This is because the char structure was naturally rearranged to become more dense surfaces at high temperature. The BET surface area, pore volume and average pore size of the prepared coal chars are shown in Table 6.2. It was found that BET surface area and pore volume of Ex-char were respectively 4 times and 2.8 times larger than those of Ex-char800. While, the average pore size of Ex-char800 was 1.4 times higher thanthat of Ex-char. It was attributable to the destruction of carbon matrix to form the larger

pore diameter at high temperature [108]. This result was confirmed by the SEM images as shown in Figure 6.1.

Table 6.1 Proximate and ultimate analyses of Indonesian coal and coal char samples

Sample	Indonesian coal (Coal)	Ex-char	Ex-char800
Proximate analysis (wt%, as received)			
Moisture	12.41	4.70	6.95
Ash	8.39	27.16	33.18
Volatile matter	36.38	5.64	5.07
Fixed carbon	42.36	62.50	54.80
Ultimate analysis (wt%, daf)			
Carbon	72.13	94.13	91.38
Hydrogen	6.67	2.39	1.83
Nitrogen	1.40	1.45	0.90
Sulfur[a]	0.22	n.d.	n.d.
Oxygen (by difference)	19.58	2.02[c]	5.89[c]
H/C molar ratio	1.11	0.30	0.24

[a] by Bomb washing method (ASTM 3177)

[b] n.d. = not determined

[c] O content including S content

Table 6.2 BET surface area, pore volume and pore size of coal char

Coal char sample	Ex-char	Ex-char800
BET surface area (m^2/g)	200.71	48.92
Pore volume (cm^3/g)	0.1389	0.0487
Average pore size (Å)	27.68	39.85

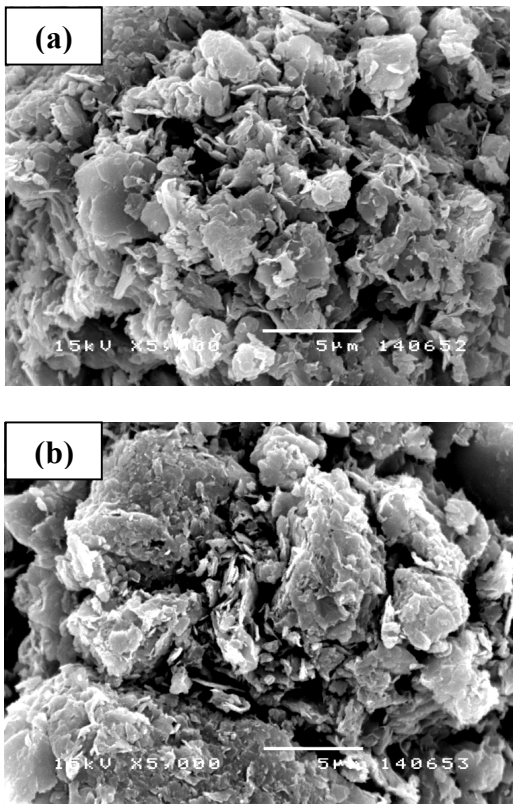

Figure 6.1 SEM images of coal char bed (a) Ex-char and (b) Ex-char800

The SEM result showed that the surfaces of Ex-char800 were occupied by the dense carbon matrix and the larger pores were observed. In contrast, the structure of Ex-char looked like the loosely packed of carbon with the smaller pores. This result agrees with the previous studies which revealed that the crystallite carbon structure increased accompanying with the decrease of micropores and the increase of macropores at high thermal treatment temperature [94, 97, 109]. In addition, the inherent AAEM species were reported as the catalyst for the decomposition of tar as well as char steam gasification [26, 76]. The AAEM contents of the prepared coal chars were characterized by XRF technique and the result is shown in Table 6.3. It was found that Ex-char had the slightly lower AAEM species than that of Ex-char800. However, the amount of retained AAEM on the spent Ex-char was largely different. The essential difference of char structure and the AAEM content between the Ex-char and the Ex-char800 was expected to play different catalytic roles on the decomposition of rice straw derived tar. The results will be discussed in next section.

Table 6.3 AAEM contents over coal chars by XRF technique

Sample	Element content (wt%, as received)				
	Na	K	Mg	Ca	Si
Fresh coal char					
Ex-char	0.082	0.373	0.169	2.207	3.422
Ex-char800	0.096	0.547	0.236	3.200	4.035
After used coal char					
Pyrolysis@800 ^{O}C					
Ex-char	0.045	0.523	0.235	2.386	7.700
Ex-char800	0.030	0.365	0.187	1.543	5.293
Gasification@800 ^{O}C					
Ex-char	0.022	0.191	0.175	1.543	2.988
Ex-char800	0.015	0.266	0.133	1.186	3.161

6.2. Pyrolysis of rice straw

6.2.1 Effect of coal char bed

The effect of coal char bed on product yield of rice straw pyrolysis at 800 ^{O}C is shown in Figure 6.2. Note that the product from coal char bed was already excluded. In this experiment, the pyrolysis temperature at the upper zone was set at 800 ^{O}C similar to the temperature at the lower zone. In case of inert alumina bed, rice straw was decomposed to produce tar as the main product (60 wt%). Besides, about 10 and 30 wt% of rice straw were respectively converted to char and gas products. In this case, the pyrolysis of rice straw totally underwent via the primary thermal decomposition. Comparing with the inert bed, tar yield decreased from 60 to 35 and 40wt% and gas yield increased from 30 to 55 and 50wt% with the presence of Ex-char and Ex-char800, respectively. It clearly indicates that coal char might play a catalytic role on rice straw derived tar decomposition leading to produce higher gaseous products. This result agreed with the previous studies [29, 31] that also reported the catalytic role of hot bed char (biomass char) on tar reduction.

Compared to the Ex-char800, the Ex-char gave the higher gas yield and lower tar yield evidently. It was probably due to its larger total surface area and pore

volume. The decomposition of tar over char surfaces underwent along with the deposition of nascent tar. The secondary char or coke was consequently formed and then the coke reacted with steam resulting in the gas production [27, 32]. For rice straw pyrolysis, the steam was presumably generated with the intensive amount, called pyrolytic steam [85, 110]. Hence, the high surface area of Ex-char might induce to promote the formation of coke. The generated coke was consecutively decomposed into gaseous product by reacting with the pyrolytic steam following Eq.(6.1).

$$C + H_2O \leftrightarrow CO + H_2 \quad (6.1)$$

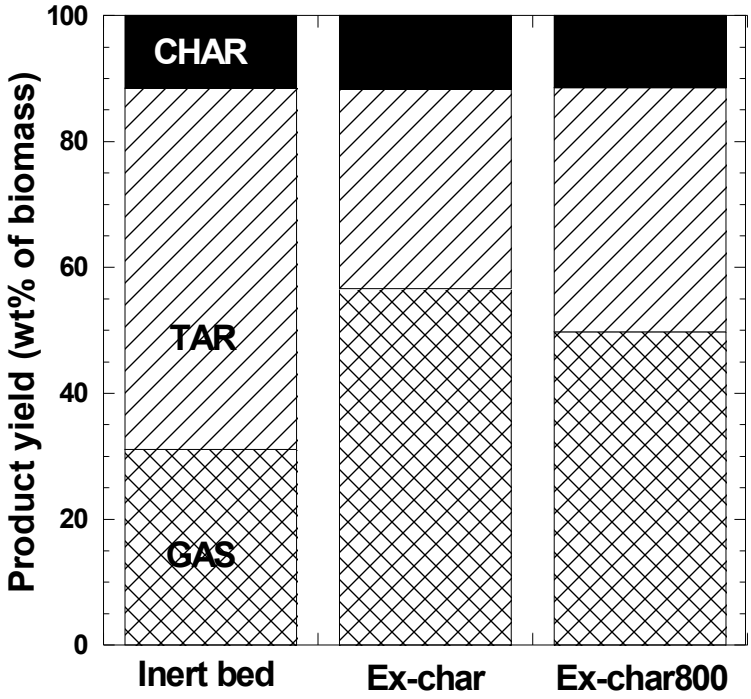

Figure 6.2 Effect of coal char on product yield of rice straw pyrolysis at 800 ^{O}C

Another explanation is the different of catalytic roles of AAEM over both coal chars. The content of AAEM over fresh and spent coal chars were compared (Table 6.3). It was found that the spent Ex-char had higher amount of AAEM species, especially K, compared to the fresh Ex-char. The increase of K content over the spent Ex-char might be due to the formation of phenolate group (K-O-C) between the volatile K released from rice straw, around 57 wt% of total K content in rice straw, and the carbon matrix of coal char [111, 112]. Moreover, the phenolate group was reported as the catalytic species for carbon and steam reaction [69, 81, 88]. Hence, the reaction between the generated coke over coal char surfaces and the pyrolytic steam

was enhanced by the catalytic role of K. In the same time, the loss of AAEM over coal char surfaces was also promoted by the contacting of H-radical from biomass derived volatiles following Eq. (6.2)

$$CM - M + H \leftrightarrow CM - H + M \quad (6.2)$$

where CM, M and H were char matrix, AAEMs and H-radical from volatile, respectively. In case of Ex-char, the formation of phenolate group was predominant as can be seen the increment of the retained K on the Ex-char surfaces. Conversely, the spent Ex-char800 had the retained K content 1.5 times lower than the original one. It could be speculated that the formation of phenolate group for the case of Ex-char800 was less dominant because of its lower porosity which inductive to form coke, as mentioned in section 6.1. Consequently, the loss of AAEM following Eq. 6.2 might be more important than the case of Ex-char.

The effect of coal char bed on gas production of rice straw pyrolysis at 800 ^{O}C is shown in Figure 6.3. In case of inert bed, it was found that rice straw pyrolysis generated CO as the main component of gaseous product. This might be attributed to the relatively high amount of cellulose in rice straw (~32 wt%) [85] which contains ether (C-O-C) and carbonyl (C=O) groups, leading to the formation of CO [85, 113]. With the presence of Ex-char, the production of H_2, CO and CO_2 was substantially higher than the presence of inert bed. It was possibly explained that the carbon steam gasification was promoted by the high active surfaces of Ex-char accompanying with the catalytic behavior of AAEMs as mentioned above. This result showed a good agreement with the previous report that mentioned that the carbon steam gasification (Eq. 6.1) was an additional reaction of tar decomposition with the presence of char [31]. The catalytic effect of the Ex-char was found to be more dominant than that of the Ex-char800. This is relevant to less AAEM content on the spent Ex-char800 (Table 6.3).

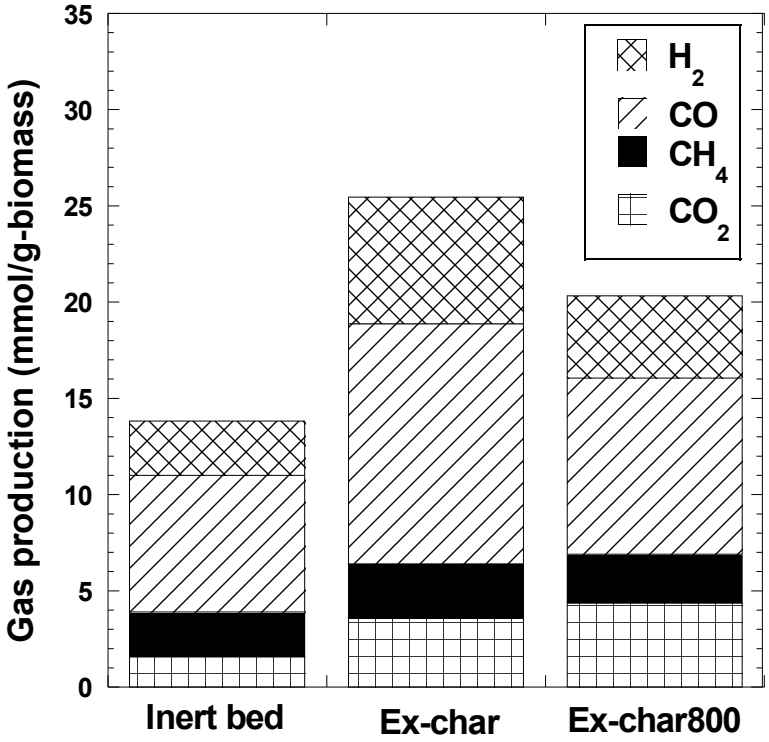

Figure 6.3 Effect of coal char on gas production of rice straw pyrolysis at 800 ^{O}C

6.2.2 Effect of pyrolysis temperature

The effect of pyrolysis temperature on product yield in cases of using inert bed and two types of coal char bed is shown in Figure 6.4a. The temperature of volatile-char contacting zone (lower part) was maintained at 800 ^{O}C. Whist the temperature of the pyrolysis zone (upper part) was changed to 600, 700 and 800 ^{O}C. With the increase of pyrolysis temperature, the decreased tar yield and increased gas yield were observed in all cases. The result also showed that the catalytic effect of both coal chars on tar reduction was more significant when the pyrolysis temperature increased. Moreover, the Ex-char exhibited more effectively for tar reduction than the Ex-char800 at all pyrolysis temperatures. The effect of pyrolysis temperature on gas production from the pyrolysis of rice straw is shown in Figure 6.4b. In case of inert bed, the higher H_2, CO and CH_4 production increased with pyrolysis temperature. It was probably due to the promotion of tar cracking into gas product at high pyrolysis temperature. In cases of coal char beds, the significantly increased CO, H_2 and CO_2 production was observed. The increment of those gaseous species was dominant when the pyrolysis temperature increased.

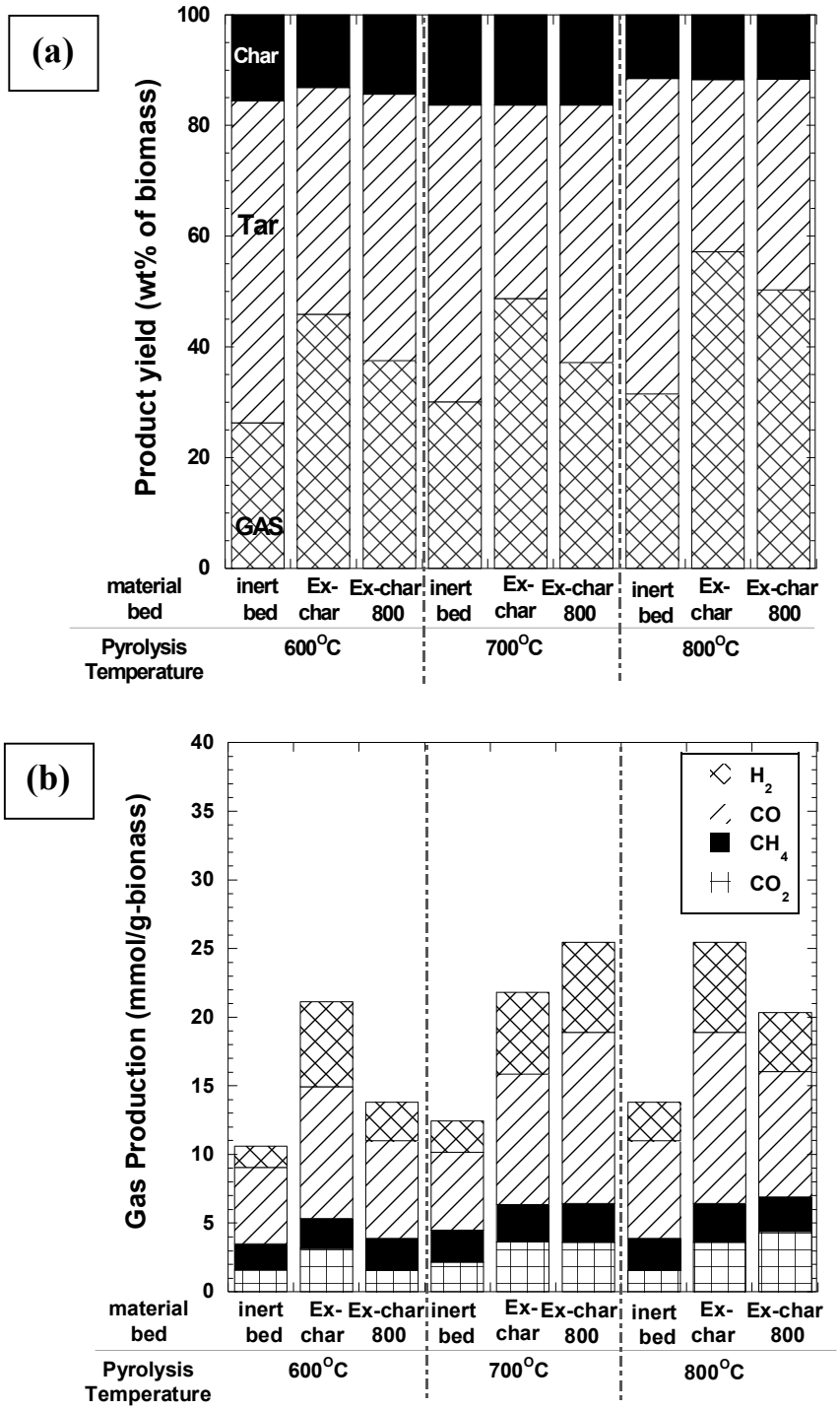

Figure 6.4 Effect of pyrolysis temperature on (a) product yield and (b) gas production of the pyrolysis of rice straw with the temperature at lower zone of 800 ^{O}C, with an inert and coal char beds

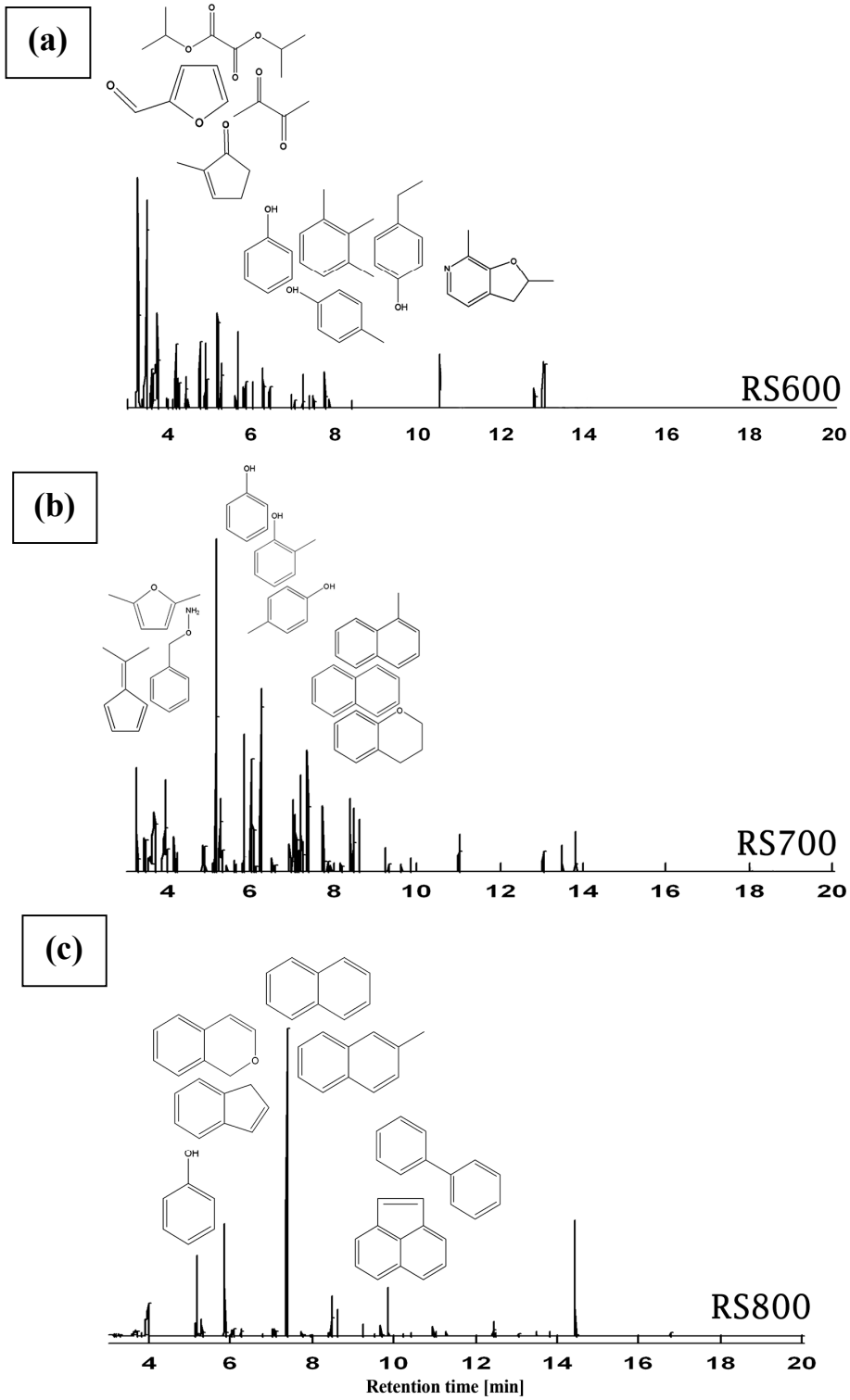

Figure 6.5 Effect of pyrolysis temperature on GC-MS patterns of rice straw derived tar at (a) 600 ^{O}C (b) 700 ^{O}C and (c) 800 ^{O}C

Figure 6.5 shows the structure of tar derived from rice straw pyrolysis at 600, 700 and 800 ^{O}C. At pyrolysis temperature of 600 ^{O}C (Figure 6.5a), the result showed that tar mainly contains the oxygenated compounds (ketones and esters), phenols and some of benzene derivatives. These components were the major components of tar which derived from cellulose and hemicelluloses decomposition at 600 ^{O}C during the pyrolysis of rice straw [114, 115]. At the pyrolysis temperature of 700 ^{O}C, the oxygenated compounds disappeared but phenolic compounds and some light aromatics such as benzene and naphthalene appeared instead (Fig. 6b). With the increase of pyrolysis temperature up to 800 ^{O}C, the phenol content trended to decrease whilst the heavy aromatic compounds such as naphthalene and anthracene became predominant (Fig. 6c). This result was consistent with tar structure derived from the pyrolysis of pine wood in the previous literature [29]. It revealed that tar derived from the pyrolysis at 600 ^{O}C contained mostly phenolic compounds, while the heavy aromatic compounds such as anthracene and fluorene began to observe at the pyrolysis temperature above 700 ^{O}C.

According to the result of product yield and gas production (Figure 6.4), it is suggested that the catalytic activity of coal char on tar reduction significantly depended on tar structure which derived from the different pyrolysis temperature. Heavy aromatic compounds in tar were preferentially decomposed over coal chars in comparison with the oxygenated compounds and light hydrocarbons. Hosokai et al. also reported that the aromatics, especially naphthalene, were almost completely decomposed on charcoal [77].

6.3. Steam gasification of rice straw

6.3.1 Effect of coal char bed

The effect of coal char bed on product yield of rice straw steam gasification is shown in Figure 6.6. Note that the product distribution which reported here based on the total carbon of feed (rice straw) and the gas production from coal char was completely subtracted. Compared to the inert bed, the presence of Ex-char gave the lower carbon conversion into tar and the higher carbon conversion into gas.

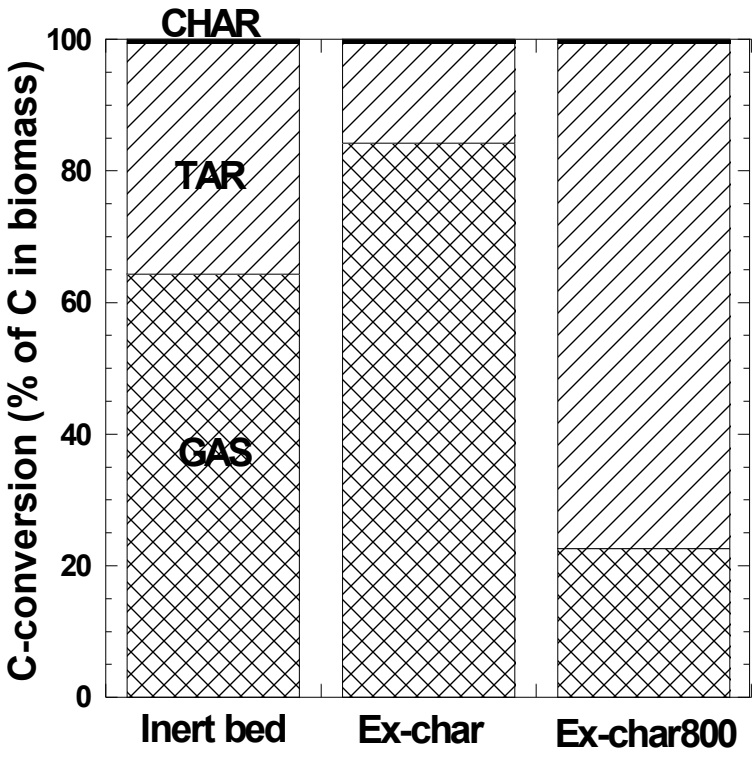

Figure 6.6 Effect of coal char on Carbon conversion of rice straw steam gasification at 800 ^{O}C

The result indicated that the catalytic effect of Ex-char was also found in the steam gasification of rice straw. This is due to the promotion of tar steam reforming by the added steam. At the same time, catalytic carbon/coke steam gasification by AAEMs on char surfaces significantly took place following Eqs. (6.3) – (6.6)

$$M + H_2O \leftrightarrow M(O) + H_2 \quad (6.3)$$

$$M(O) + C \leftrightarrow C(O) + M \quad (6.4)$$

$$C(O) \leftrightarrow CO \quad (6.5)$$

$$C(O) + M(O) \leftrightarrow M + CO_2 \quad (6.6)$$

where M, M(O) and C(O) were AAEMs, alkali-oxygen bond on carbon surfaces and carbon-oxygen bond on carbon surfaces, respectively [88]. However, it could be seen that AAEM content on the spent coal char obtained from gasification was lower than that obtained from pyrolysis (Table 6.3). Therefore, it demonstrated that external steam also induced the loss of AAEMs.

In steam gasification, the presence of Ex-char800 gave the higher carbon conversion into tar and lower carbon conversion into gas, compared to the presence of inert bed. This result showed somewhat different from the presence of Ex-char800 in the pyrolysis condition. It could be assumed that the formation of secondary tar (soot or carbon substrate) from light hydrocarbons was more dominant than the steam reforming of tar. Equations (6.7) - (6.10) show the possible gas-gas reactions which involving to the generated carbon associated with tar steam reforming at high temperature [116].

$$2CO \leftrightarrow C + CO_2 \tag{6.7}$$

$$CH_4 \leftrightarrow C + 2H_2 \tag{6.8}$$

$$CO + H_2 \leftrightarrow C + H_2O \tag{6.9}$$

$$C_nH_{2n+2} \rightarrow nC + (n+1)H_2 \tag{6.10}$$

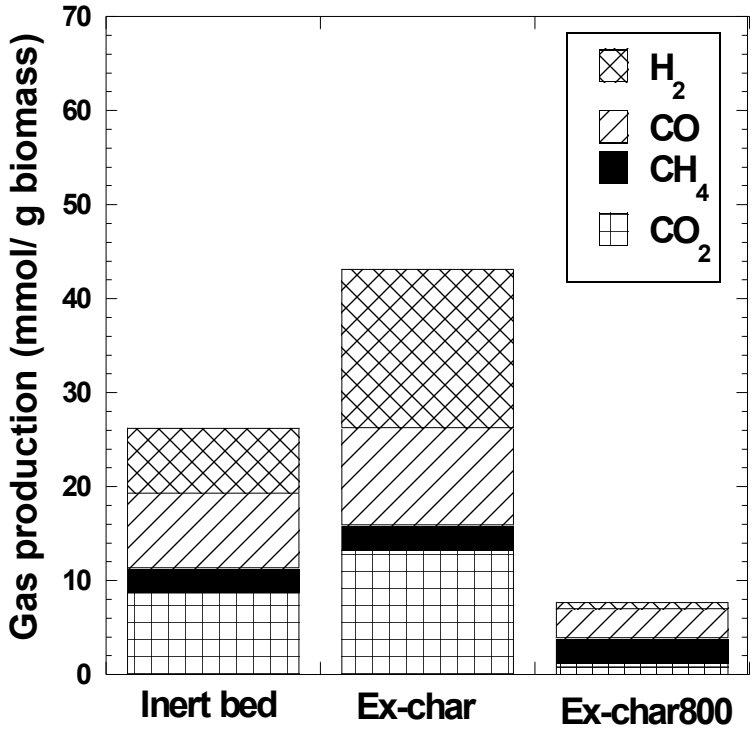

Figure 6.7 Effect of coal char on gas production of rice straw steam gasification at 800 ^{O}C

The effect of coal char bed on gas production of rice straw steam gasification at 800 ^{O}C is shown in Figure 6.7. It was found that, with the presence of Ex-char, the H_2 and CO_2 production was dramatically increased. It could be supposed that the Ex-char presumably played the catalytic role on the steam reforming of rice straw derived tar followed by the water gas shift reactions. In contrast, the decrease of all gas products was clearly evidenced with the presence of Ex-char800. It indicated that the Ex-char800 inhibited the tar conversion into gaseous product, as can be seen in Figure 6.6.

6.3.2 Effect of pyrolysis temperature

The effect of pyrolysis temperature on the carbon conversion of the steam gasification of rice straw with an inert bed and coal char beds is shown in Figure 6.8a. With the presence of inert bed, the carbon conversion into gas increased and the carbon conversion into tar decreased with the pyrolysis temperature. This was because the large amount of the tar released at higher pyrolysis temperature could be reacted with steam leading to generate more gas products. With the presence of Ex-char, carbon conversion into gas increased and carbon conversion into tar decreased with pyrolysis temperature. It indicated that the Ex-char could be exhibited as the catalyst for tar steam reforming for all pyrolysis temperatures and showed the best performance for the steam reforming of tar which released at 800^{O}C. As mentioned in section 6.2, the tar released at 800^{O}C mostly contained with the heavy aromatic hydrocarbons such as naphthalene, anthracene and pyrene (Figure 6.5). Therefore, it could be concluded that the Ex-char exhibited as a good catalyst for the thermal cracking and steam reforming of the heavy aromatic hydrocarbons which released at the high pyrolysis temperature. As mentioned above, coke formation over Ex-char800 surfaces was less significant than Ex-char surfaces, therefore the formation of coke in this experimental condition might mostly underwent in the gas phase

Interestingly, Figure 6.8a showed that Ex-char800 induced the higher carbon conversion into gas at only the pyrolysis temperature of 600 ^{O}C. At the pyrolysis temperature of 700^{O}C, the carbon conversion into gas of this case was comparable with the case of inert bed and then it became lower when the pyrolysis temperature was increased to 800^{O}C. It implied that the catalytic effect of the Ex-char800 on tar

steam reforming was diminished when the pyrolysis temperature increased. From Figure 6.5, tar mostly composed of the saccharide units which released from the decomposition of hemicelluloses and partly cellulose at 600^{O}C. The non active structure (less porosity) of the Ex-char800 could be suitable for the decomposition of the saccharide compounds with the presence of steam. However, the non-active structure of the Ex-char was not proper for decomposition of the aromatic hydrocarbon which was produced at high pyrolysis temperature.

Considering the gas production, at the pyrolysis temperature of 600 ^{O}C, Ex-char gave a higher CO_2 than the inert bed while the Ex-char800 gave the higher H_2 and CO. It was speculated that the catalytic roles of both coal chars on tar decomposition was different. The Ex-char might performed as a good catalyst for water-gas shift reaction while the Ex-char800 might be a good catalyst for tar steam reforming. However, when the pyrolysis temperature increased to 700 ^{O}C, the catalytic role of coal char was dramatically changed. The Ex-char showed the best catalytic performance on tar steam reforming at this pyrolysis temperature, resulting in the highest CO and H_2 production. For the pyrolysis temperature of 800^{O}C, the Ex-char the catalytic effect of the Ex-char was less but still gave the higher H_2, CO and CO_2 production than the inert bed. In contrast, the Ex-char800 was not performed the catalytic activity on tar steam reforming but exhibited as the inhibitor for tar reduction in the presence of steam.

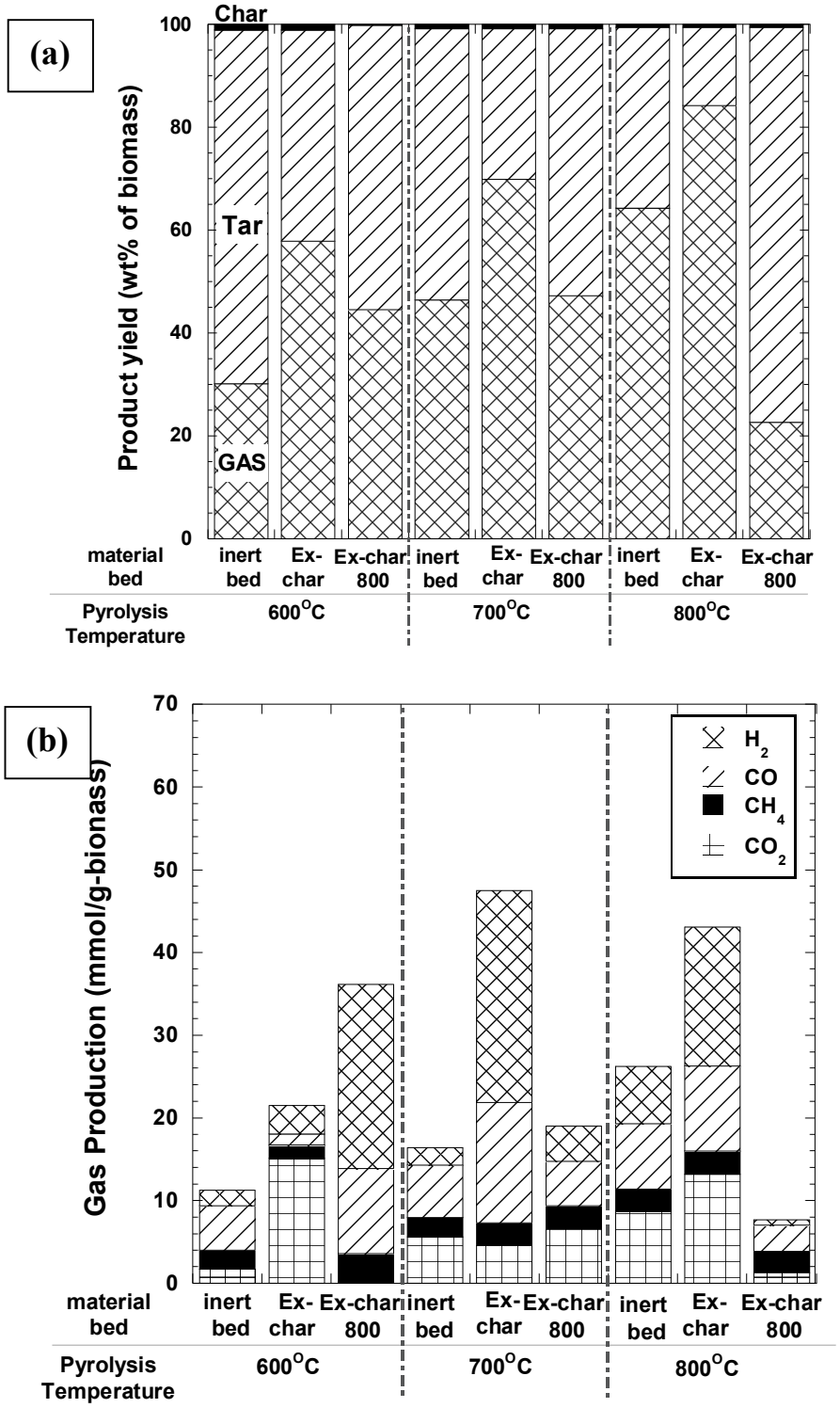

Figure 6.8 Effect of pyrolysis temperature on (a) carbon conversion and (b) gas production of the steam gasification of rice straw with the temperature at lower zone of 800 ^{O}C, with an inert and coal char beds

CHAPTER VII

CONCLUSIONS AND RECOMMANDATIONS

7.1 Conclusions

All of the results from Chapter IV to VI can be separately concluded in each part as shown below;

1. Synergetic effect during co-pyrolysis and co-gasification of coal and biomass

The synergetic effect during co-pyrolysis and co-gasification of Indonesian coal (sub-bituminous) and biomass (RS and LN) was carried out in a drop-tube fixed bed reactor. Results showed that the synergetic effect, in terms of higher gas and lower tar and char yields, was observed under these pyrolysis and steam gasification experimental conditions.

The synergetic effect could be described by the transferring of OH and H radicals. The radicals were generated from the biomass and transferred to the coal structure. This phenomenon accompanied with the potential catalytic effect of AAEM species, especially K which also released from the biomass. In addition, the secondary char formation was suppressed by the H-transferring during the pyrolysis of coal and biomass. The magnitude of the synergetic results was dramatically depended on biomass to coal ratio, reaction temperature and biomass type.

In co-pyrolysis, the improvement of char structure and the increase of the retained K in the chars obtained from co-pyrolysis were observed. These directly influenced on the enhancement of steam gasification rate of the chars produced during the *in situ* co-pyrolysis of coal and biomass in a thermobalance reactor, resulting in the obvious synergetic effect.

2. Volatile-char interaction during co-gasification: in a thermobalance reactor

The interaction between coal chars, prepared by three different conditions, and volatiles from xylan, cellulose and rice straw was examined in a rapid heating thermobalance reactor. Results showed that the reactivity of char in steam gasification

was dependent upon its preparation condition. The reactivity could be ordered as following: In-char > Ex-char > Ac-char. This order is likely relevant to the differences in their structures and the contents of inherent AAEM catalytic species. The volatiles derived from all three volatile sources inhibited the reactivity of the Ex-char as well as the In-char. On the other hand, the non-active structure of the Ac-char showed no significant inhibition of its otherwise low char reactivity. The volatiles derived from rice straw seem to significantly hinder the steam gasification rate of coal char more than that derived from cellulose and xylan.

Moreover, the Ex-char showed a strong catalytic effect on tar decomposition, resulting in the increases in H_2, CO and CO_2 production rates. The catalytic effect was not observed in the presence of either Ac-char or In-char but rather secondary reactions such as coke formation were dominant instead.

3. Volatile-char interaction during co-pyrolysis/gasification: in a two-stage fixed bed reactor

The catalytic activity of coal char on rice straw derived tar decomposition was examined in a two-stage reactor. Results showed that coal char exhibited as a good catalyst for thermal cracking of rice straw derived tar as well as tar steam reforming. The catalytic activity of coal char could be described by its high porosity of char structure and the catalytic behavior of AAEM species on coal char surfaces. Coal char, which was prepared at lower pyrolysis temperature (Ex-char), showed better catalytic activity for tar decomposition than the char, which was prepared at higher pyrolysis temperature (Ex-char800). In case of rice straw pyrolysis, both Ex-char and Ex-char800 preferentially performed the catalytic activity on heavy aromatic hydrocarbons which was generated at high pyrolysis temperature.

Moreover, in steam gasification of rice straw, only Ex-char showed the catalytic roles on tar steam reforming, leading to the increase of H_2 and CO production. It also suggested that coal char might be an attractive catalyst for tar reduction in the gasification process because of its effective activity and economic advantage. In addition, the interaction between coal char and biomass derived tar should be a useful information in co-processing design and operation of coal and biomass.

7.2 Recommendation and future works

Although the comprehensive results can be obtained from this study, some recommendations were proposed for further investigation about co-pyrolysis and co-gasification as followed.

1. Selection of biomass to coal ratio as well as type of coal and biomass should be regarding to the supply of biomass and coal in each region. For example, the ratio of biomass and coal for energy production is about 30 to 70 [117] for Thailand which is agricultural based country. In case of Industrial countries, amount of energy crop/biomass is too low compared to the supply of coal. Therefore, the lower biomass blending, such as 1 – 10 wt% of biomass should be investigated in the future.

2. The low heating value of the syngas obtained from co-gasification in this study is relatively low (8 – 10 MJ/m^3), whilst, the H_2/CO molar ratio is quit high (1 – 2.5). That will be effective for methanol production or liquid fuel synthesis rather than using as the fuel. However, the syngas with higher heating value can be produced from the co-gasification of coal and biomass by adjusting some operating conditions, such as increasing reaction temperature and biomass content in the blend.

3. From the results of volatile-char interaction, it revealed that tar structure and the content of volatile AAEM releasing from the biomass are significantly influenced on the gasification of coal char. In the future, the effect of tar which is released from the various types of biomass, on the gasification of char should be investigated.

4. Since the catalytic effect of AAEM on char surfaces is very important, the way to increase AAEM content over coal char surfaces, such as adsorption from the biomass sources or the addition of AAEM metal from the other sources should be studied.

5. For the effective co-gasification of coal and biomass process, the ratio of coal char and biomass derived volatile which are produced inside the reactor is very important. The negative interaction of biomass volatile on the gasification of coal char simultaneously occurs with the positive interaction of coal char on the reduction of biomass derived tar. The suitable process should be designed in order to control these two contradict interactions. One of the designs for co-gasification in a dual-bed circulating fluidized-bed reactor is proposed as shown in Figure 7.1. The dual bed circulating fluidized-bed reactor is divided into two units: combustor (part A) and

gasifier (part B). In part A, the combustion of fuel with air takes place in order to generate heat. Then the heat is transferred into the upper zone of gasifier by sand particles. In the upper zone of gasifier (zone BI), the temperature is higher than the lower zone (BII). Coal is fed into zone BI, the pyrolysis of coal take place leading the production of coal char and coal derived volatiles. The coal char drops into zone BII whilst coal volatiles convert into gaseous product. On the other hand, biomass is fed into the lower zone (BII) along with steam and then steam gasification of biomass takes place. Biomass derived volatiles move up to zone BI and crack into the product gas with the presence of coal char. Concurrently, biomass char is transferred to part A and uses as a fuel for combustion. The concept of this co-gasification design is that the catalytic effect of coal char on biomass derived tar steam reforming is presumably significant compared to the inhibition effect of gasification of char by volatiles.

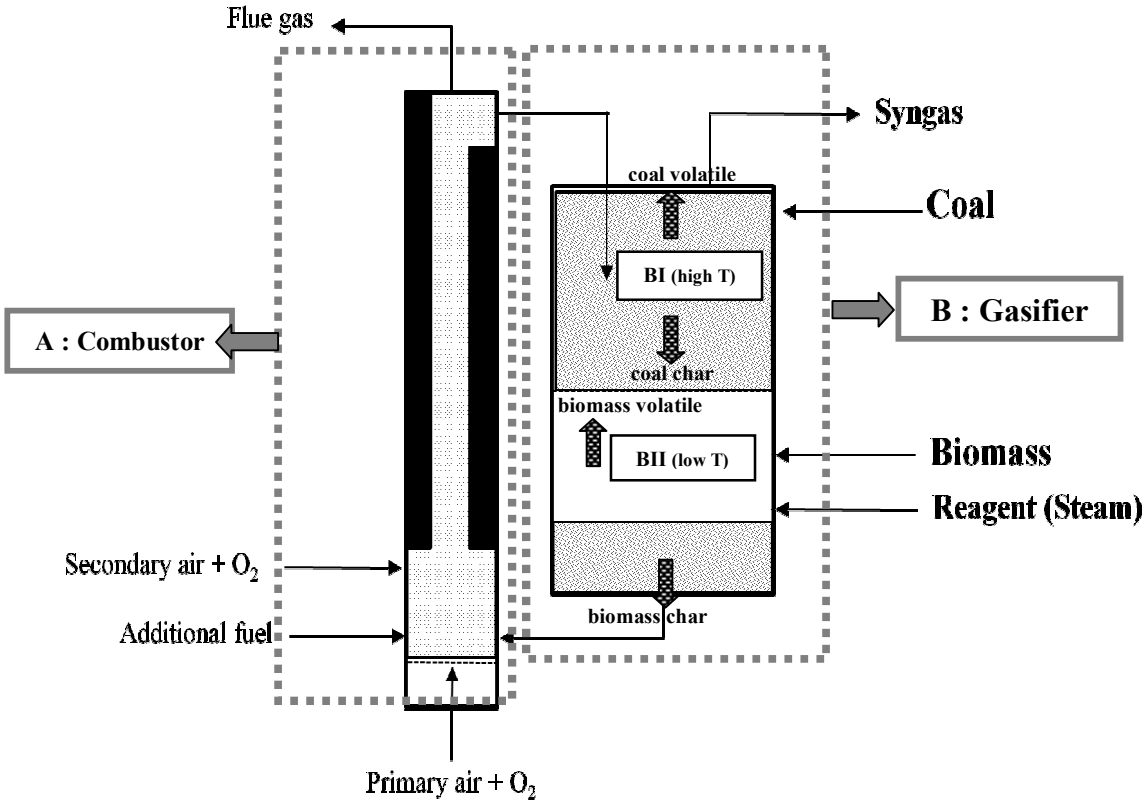

Figure 7.1 The proposed design for co-gasification in a dual-bed circulating fluidized-bed gasifier

REFERENCES

[1] Pipatmanomai, S. Overview and Experiences of biomass fluidized bed gasification in Thailand. Journal of Sustainable Energy and Environment 1 (2011): 29-33.

[2] Zhang, L., Xu, S.P., Zhao, W. and Liu, S.Q. Co-pyrolysis of biomass and coal in a free fall reactor. Fuel 86 (2007): 353-359.

[3] Sonobe, T., Worasuwannarak, N. and Pipatmanomai, S. Synergies in co-pyrolysis of Thai lignite and corncob. Fuel Processing Technology 89 (2008): 1371-1378.

[4] Kumabe, K., Hanaoka, T., Fujimoto, S., Minowa, T. and Sakanishi, K. Co-gasification of woody biomass and coal with air and steam. Fuel 86 (2007): 684-689.

[5] Alzate, C.A., Chejne, F., Valdes, C.F., Berrio, A., De La Cruz, J. and Londono, C.A. CO-gasification of pelletized wood residues. Fuel 88 (2009): 437-445.

[6] Blesa, M.J., Miranda, J.L., Moliner, R., Izquierdo, M.T. and Palacios, J.M. Low-temperature co-pyrolysis of a low-rank coal and biomass to prepare smokeless fuel briquettes. Journal of Analytical and Applied Pyrolysis 70 (2003): 665-677.

[7] Zhu, W.K., Song, W.L. and Lin, W.G. Catalytic gasification of char from co-pyrolysis of coal and biomass. Fuel Processing Technology 89 (2008): 890-896.

[8] Pan, Y.G., Velo, E., Roca, X., Manyà, J.J. and Puigjaner, L. Fluidized-bed co-gasification of residual biomass/poor coal blends for fuel gas production. Fuel 79 (2000): 1317-1326.

[9] Park, D.K., Kim, S.D., Lee, S.H. and Lee, J.G. Co-pyrolysis characteristics of sawdust and coal blend in TGA and a fixed bed reactor. Bioresource Technology 101 (2010): 6151-6156.

[10] Haykiri-Acma, H. and Yaman, S. Synergy in devolatilization characteristics of lignite and hazelnut shell during co-pyrolysis. Fuel 86 (2007): 373-380.

[11] Idris, S.S., Rahman, N.A., Ismail, K., Alias, A.B., Rashid, Z.A. and Aris, M.J. Investigation on thermochemical behaviour of low rank Malaysian coal, oil palm biomass and their blends during pyrolysis via thermogravimetric analysis (TGA). Bioresource Technology 101 (2010): 4584-4592.

[12] Moghtaderi, B., Meesri, C. and Wall, T.F. Pyrolytic characteristics of blended coal and woody biomass. Fuel 83 (2004): 745-750.

[13] Kastanaki, E., Vamvuka, D., Grammelis, P. and Kakaras, E. Thermogravimetric studies of the behavior of lignite-biomass blends during devolatilization. Fuel Processing Technology 77 (2002): 159-166.

[14] Collot, A.G., Zhuo, Y., Dugwell, D.R. and Kandiyoti, R. Co-pyrolysis and co-gasification of coal and biomass in bench-scale fixed-bed and fluidised bed reactors. Fuel 78 (1999): 667-679.

[15] Yilgin, M., Duranay, N.D. and Pehlivan, D. Co-pyrolysis of lignite and sugar beet pulp. Energy Conversion and Management 51 (2010): 1060-1064.

[16] Yuan, S., Dai, Z.H., Zhou, Z.J., Chen, X.L., Yu, G.S. and Wang, F.C. Rapid co-pyrolysis of rice straw and a bituminous coal in a high-frequency furnace and gasification of the residual char. Bioresource Technology 109 (2012): 188-197.

[17] Sjostrom, K., Chen, G., Yu, Q., Brage, C. and Rosen, C. Promoted reactivity of char in co-gasification of biomass and coal: synergies in the thermochemical process. Fuel 78 (1999): 1189-1194.

[18] Zhang, S., Min, Z., Tay, H.-L., Asadullah, M. and Li, C.-Z. Effects of volatile–char interactions on the evolution of char structure during the gasification of Victorian brown coal in steam. Fuel 90 (2011): 1529-1535.

[19] Zhang, S., Hayashi, J.-i. and Li, C.-Z. Volatilisation and catalytic effects of alkali and alkaline earth metallic species during the pyrolysis and gasification of Victorian brown coal. Part IX. Effects of volatile-char interactions on char–H_2O and char–O_2 reactivities. Fuel 90 (2011): 1655-1661.

[20] Bayarsaikhan, B., Sonoyama, N., Hosokai, S., Shimada, T., Hayashi, J.-i., Li, C.-Z. and Chiba, T. Inhibition of steam gasification of char by volatiles in a fluidized bed under continuous feeding of a brown coal. Fuel 85 (2006): 340-349.

[21] Marcilla, A., Asensio, M. and Martín-Gullón, I. Influence of the carbonization heating rate on the physical properties of activated carbons from a sub-bituminous coal. Carbon 34 (1996): 449-456.

[22] Cai, H.Y., Güell, A.J., Chatzakis, I.N., Lim, J.Y., Dugwell, D.R. and Kandiyoti, R. Combustion reactivity and morphological change in coal chars: Effect of pyrolysis temperature, heating rate and pressure. Fuel 75 (1996): 15-24.

[23] Wang, X., He, R. and Chen, Y. Evolution of porous fractal properties during coal devolatilization. Fuel 87 (2008): 878-884.

[24] Fushimi, C., Wada, T. and Tsutsumi, A. Inhibition of steam gasification of biomass char by hydrogen and tar. Biomass & Bioenergy 35 (2011): 179-185.

[25] Cetin, E., Gupta, R. and Moghtaderi, B. Effect of pyrolysis pressure and heating rate on radiata pine char structure and apparent gasification reactivity. Fuel 84 (2005): 1328-1334.

[26] Hayashi, J.-I., Iwatsuki, M., Morishita, K., Tsutsumi, A., Li, C.-Z. and Chiba, T. Roles of inherent metallic species in secondary reactions of tar and char during rapid pyrolysis of brown coals in a drop-tube reactor. Fuel 81 (2002): 1977-1987.

[27] Zhang, L.-x., Matsuhara, T., Kudo, S., Hayashi, J.-i. and Norinaga, K. Rapid pyrolysis of brown coal in a drop-tube reactor with co-feeding of char as a promoter of in situ tar reforming. Fuel (2011).

[28] Min, Z., Yimsiri, P., Asadullah, M., Zhang, S. and Li, C.-Z. Catalytic reforming of tar during gasification. Part II. Char as a catalyst or as a catalyst support for tar reforming. Fuel 90 (2011): 2545-2552.

[29] Sun, Q., Yu, S., Wang, F. and Wang, J. Decomposition and gasification of pyrolysis volatiles from pine wood through a bed of hot char. Fuel 90 (2011): 1041-1048.

[30] Abu El-Rub, Z., Bramer, E.A. and Brem, G. Experimental comparison of biomass chars with other catalysts for tar reduction. Fuel 87 (2008): 2243-2252.

[31] Gilbert, P., Ryu, C., Sharifi, V. and Swithenbank, J. Tar reduction in pyrolysis vapours from biomass over a hot char bed. Bioresource Technology 100 (2009): 6045-6051.

[32] Brandt, P., Larsen, E. and Henriksen, U. High tar reduction in a two-stage gasifier. Energy & Fuels 14 (2000): 816-819.

[33] López, D., Acelas, N. and Mondragón, F. Average structural analysis of tar obtained from pyrolysis of wood. Bioresource Technology 101 (2010): 2458-2465.

[34] Xiao, R. and Yang, W. Influence of temperature on organic structure of biomass pyrolysis products. Renewable Energy 50 (2013): 136-141.

[35] Sadaka, S. Department of Agricultural and Biosystems Engineering Iowa State University, USA. [online]. Gasification. Available from: http://bioweb.sungrant.org/NR/rdonlyres/F4AE220B-0D98-442C-899F-177CFD725ADD/0/Gasification.pdf [4 September 2011]

[36] Department of Energy, Natianal Energy Technology Laboratory. USA [online]. Gasification world databases 2010. Available from: http://www.netl.doe.gov/technologies/coalpower/gasification/worlddatabase/2010_Worldwide_Gasification_Database.pdf [29 Mar 2013]

[37] Croft, P. [online]. A global coal production forecast. Available from: http://qmunty.com/blog/2011/03/02/el-mercado-mundial-de-carbon-se-encuentra-al-borde-del-abismo/ [29 Mar 2013]

[38] Higman, C. and Burgt, M.v.d. Gasification. Elsevier, Massachusetts, USA, 2008.

[39] Macedo, I.C. InterAcademy Council [online]. Biomass as a source of Energy. Available from: http://www.interacademycouncil.net/ [28 Mar 2013]

[40] Slade, R., Suanders, R., Gross, R. and Bauen, A. Imperial College Centre for Energy Policy, the UK Energy Research Centre. UK [online]. Energy form biomass: the size of the global resource. Available from: www.ukerc.ac.uk/support/tiki-download_file.php?fileId=2095 [30 Mar 2013]

[41] Slade, R., Gross, R. and Bauen, A. Estimating bio-energy resource potentials to 2050: learning from experience. Energy & Environmental Science 4 (2011): 2645-2657.

[42] Hoogwijk, M., Faaij, A., van den Broek, R., Berndes, G., Gielen, D. and Turkenburg, W. Exploration of the ranges of the global potential of biomass for energy. Biomass and Bioenergy 25 (2003): 119-133.

[43] Smeets, E.M.W., Faaij, A.P.C., Lewandowski, I.M. and Turkenburg, W.C. A bottom-up assessment and review of global bio-energy potentials to 2050. Progress in Energy and Combustion Science 33 (2007): 56-106.

[44] Hamelinck, C.N., Faaij, A.P.C., den Uil, H. and Boerrigter, H. Production of FT transportation fuels from biomass; technical options, process analysis and optimisation, and development potential. Energy 29 (2004): 1743-1771.

[45] Department of Alternative Energy Development and Efficientcy (DEDE), Ministry of Energy. Thailand [online]. Thailand Energy Statistics, 2010. Available from: www.dede.go.th [28 Mar 2013]

[46] Department of Alternative Energy Development and Efficientcy (DEDE), Ministry of Energy. Bangkok, Thailand [online]. Sittuation of Coal consumption in Thai Industry. Available from: http://www.dede.go.th/ [28 Mar 2013]

[47] Kessels, J. IEA clean coal centre, UK. [online]. Prospects for coal and clean coal technologies in Thailand. Available from: http://www.iea-coal.org.uk/ [28 Mar 2013]

[48] Energy Policy and Planning Office, Ministry of Energy, Thailand. [online]. Thailand's Energy situation in 2010 and trend in 2011. Available from: www.eppo.go.th [29 Mar 2013]

[49] Department of Alternative Energy Development and Efficientcy (DEDE), Ministry of Energy. Thailand [online]. Thailand alternative energy situation 2011. Available from: www.dede.go.th [28 Mar 2013]

[50] Ciferno, J.P. and Marano, J.J. U.S. Department of Energy, National Energy Technology Laboratory. [online]. Benchmarking Biomass Gasification Technologies for Fuels, Chemicals and Hydrogen Production. Available from: http://www.netl.doe.gov/ [4 September 2012]

[51] Reimert, R. and Schaub, G. Gas production. in, Ullmaan's Encyclopedia of Inductrial Chemistry, pp. 215. VCH Verlagsgesellschaft: Weinheim, 1989.

[52] Smooth, L.D. and Smith, P.J. Coal combustion and gasification. Plenum, New York, US, 1985.

[53] Ricketts, B., Hotchkiss, R., Livingston, B. and Hall, M. Technology status review of Waste/biomass Co-gasification with coal. Proceeding of IChemE 5th Gasification conference (2002).

[54] Technical research center of Finland, ESPOO. [online]. Review of Finnish biomass gasification technologies. Available from: http://www.ieatask33.org/ [4 September 2011]

[55] Simbeck, D.R., Korens, D.R., Biasca, C.F., Vejtasa, S. and Dickkenson, R.L. Coal gasification Guidbook: Status, Applications and Technologies. Electric power research and institue (EPRI), Palo Alto, 1993.

[56] Whiting, K.J. Solid waste gasification perspectives. Paper presented at Waste Gasification Seminar (S594) (24 November 1998).

[57] Xiao, B., Sun, X.F. and Sun, R.C. Chemical, structural, and thermal characterizations of alkali-soluble lignins and hemicelluloses, and cellulose from maize stems, rye straw, and rice straw. Polymer Degradation and Stability 74 (2001): 307-319.

[58] The energy lab, U.S. Depeartment of Energy. [online]. Methanol synthesis. Available from: http://www.netl.doe.gov/ [30 Mar 2013]

[59] Spath, P.L. and Dayton, D.C. National Renewable Energy Laboratory. [online]. Technical and economic assessment of synthesis gas to fuels and chemicals with emphasis on the potential for biomass-derived syngas. Available from: http://www.nrel.gov/docs/fy04osti/34929.pdf

[60] Jones, J.M., Kubacki, M., Kubica, K., Ross, A.B. and Williams, A. Devolatilisation characteristics of coal and biomass blends. Journal of Analytical and Applied Pyrolysis 74 (2005): 502-511.

[61] Meesri, C. and Moghtaderi, B. Lack of synergetic effects in the pyrolytic characteristics of woody biomass/coal blends under low and high heating rate regimes. Biomass & Bioenergy 23 (2002): 55-66.

[62] Seo, M.W., Goo, J.H., Kim, S.D., Lee, S.H. and Choi, Y.C. Gasification Characteristics of Coal/Biomass Blend in a Dual Circulating Fluidized Bed Reactor. Energy & Fuels 24 (2010): 3108-3118.

[63] Aigner, I., Pfeifer, C. and Hofbauer, H. Co-gasification of coal and wood in a dual fluidized bed gasifier. Fuel 90 (2011): 2404-2412.

[64] Pan, Y.G., Velo, E., Roca, X., Manya, J.J. and Puigjaner, L. Fluidized-bed co-gasification of residual biomass/poor coal blends for fuel gas production. Fuel 79 (2000): 1317-1326.

[65] Li, K., Zhang, R. and Bi, J. Experimental study on syngas production by co-gasification of coal and biomass in a fluidized bed. International Journal of Hydrogen Energy 35 (2010): 2722-2726.

[66] Fermoso, J., Arias, B., Plaza, M.G., Pevida, C., Rubiera, F., Pis, J.J., García-Peña, F. and Casero, P. High-pressure co-gasification of coal with biomass and petroleum coke. Fuel Processing Technology 90 (2009): 926-932.

[67] McLendon, T.R., Lui, A.P., Pineault, R.L., Beer, S.K. and Richardson, S.W. High-pressure co-gasification of coal and biomass in a fluidized bed. Biomass and Bioenergy 26 (2004): 377-388.

[68] Joly, J.P., Cazorla-Amoros, D., Charcosset, H., Linares-Solano, A., Marcilio, N.R., Martinez-Alonso, A. and de Lecea, C.S.-M. The state of calcium as a char gasification catalyst — a temperature-programmed reaction study. Fuel 69 (1990): 878-884.

[69] Wang, J., Jiang, M., Yao, Y., Zhang, Y. and Cao, J. Steam gasification of coal char catalyzed by K_2CO_3 for enhanced production of hydrogen without formation of methane. Fuel 88 (2009): 1572-1579.

[70] Li, X.J., Wu, H.W., Hayashi, J.I. and Li, C.Z. Volatilisation and catalytic effects of alkali and alkaline earth metallic species during the pyrolysis and gasitication of Victorian brown coal. Part VI. Further investigation into the effects of volatile-char interactions. Fuel 83 (2004): 1273-1279.

[71] Wu, H.W., Quyn, D.M. and Li, C.Z. Volatilisation and catalytic effects of alkali and alkaline earth metallic species during the pyrolysis and gasification of Victorian brown coal. Part III. The importance of the interactions between volatiles and char at high temperature. Fuel 81 (2002): 1033-1039.

[72] Jiang, M.-Q., Zhou, R., Hu, J., Wang, F.-C. and Wang, J. Calcium-promoted catalytic activity of potassium carbonate for steam gasification of coal char: Influences of calcium species. Fuel 99 (2012): 64-71.

[73] Huang, Z., Zhang, J., Zhao, Y., Zhang, H., Yue, G., Suda, T. and Narukawa, M. Kinetic studies of char gasification by steam and CO_2 in the presence of H_2 and CO. Fuel Processing Technology 91 (2010): 843-847.

[74] Kajitani, S., Tay, H.-L., Zhang, S. and Li, C.-Z. Mechanisms and kinetic modelling of steam gasification of brown coal in the presence of volatile–char interactions. Fuel 103 (2013): 7-13.

[75] Dufour, A., Celzard, A., Fierro, V., Martin, E., Broust, F. and Zoulalian, A. Catalytic decomposition of methane over a wood char concurrently activated by a pyrolysis gas. Applied Catalysis a-General 346 (2008): 164-173.

[76] Masek, O., Sonoyama, N., Ohtsubo, E., Hosokai, S., Li, C.Z., Chiba, T. and Hayashi, J. Examination of catalytic roles of inherent metallic species in steam reforming of nascent volatiles from the rapid pyrolysis of a brown coal. Fuel Processing Technology 88 (2007): 179-185.

[77] Hosokai, S., Kumabe, K., Ohshita, M., Norinaga, K., Li, C.Z. and Hayashi, J.I. Mechanism of decomposition of aromatics over charcoal and necessary condition for maintaining its activity. Fuel 87 (2008): 2914-2922.

[78] Sathe, C., Pang, Y.Y. and Li, C.Z. Effects of heating rate and ion-exchangeable cations on the pyrolysis yields from a Victorian brown coal. Energy & Fuels 13 (1999): 748-755.

[79] He, M.Y., Xiao, B., Hu, Z.Q., Liu, S.M., Guo, X.J. and Luo, S.Y. Syngas production from catalytic gasification of waste polyethylene: Influence of temperature on gas yield and composition. International Journal of Hydrogen Energy 34 (2009): 1342-1348.

[80] Sinha, S., Jhalani, A., Ravi, M.R. and Ray, A. Modeling of pyrolysis in Wood: A Review. Journal of the Solar Energy Society of India 10 (2000): 41-62.

[81] Wu, Y., Wang, J., Wu, S., Huang, S. and Gao, J. Potassium-catalyzed steam gasification of petroleum coke for H2 production: Reactivity, selectivity and gas release. Fuel Processing Technology 92 (2011): 523-530.

[82] Ulloa, C.A., Gordon, A.L. and Garcia, X.A. Thermogravimetric study of interactions in the pyrolysis of blends of coal with radiata pine sawdust. Fuel Processing Technology 90 (2009): 583-590.

[83] Howaniec, N., Smolinski, A., Stanczyk, K. and Pichlak, M. Steam co-gasification of coal and biomass derived chars with synergy effect as an innovative way of hydrogen-rich gas production. International Journal of Hydrogen Energy 36 (2011): 14455-14463.

[84] Kajitani, S., Zhang, Y., Umemoto, S., Ashizawa, M. and Hara, S. Co-gasification Reactivity of Coal and Woody Biomass in High-Temperature Gasification. Energy & Fuels 24 (2010): 145-151.

[85] Worasuwannarak, N., Sonobe, T. and Tanthapanichakoon, W. Pyrolysis behaviors of rice straw, rice husk, and corncob by TG-MS technique. Journal of Analytical and Applied Pyrolysis 78 (2007): 265-271.

[86] Wannapeera, J., Fungtammasan, B. and Worasuwannarak, N. Effects of temperature and holding time during torrefaction on the pyrolysis behaviors of woody biomass. Journal of Analytical and Applied Pyrolysis 92 (2011): 99-105.

[87] Sonoyama, N., Okuno, T., Mašek, O., Hosokai, S., Li, C.-Z. and Hayashi, J.-i. Interparticle Desorption and Re-adsorption of Alkali and Alkaline Earth Metallic Species within a Bed of Pyrolyzing Char from Pulverized Woody Biomass. Energy & Fuels 20 (2006): 1294-1297.

[88] Okuno, T., Sonoyama, N., Hayashi, J., Li, C.Z., Sathe, C. and Chiba, T. Primary release of alkali and alkaline earth metallic species during the pyrolysis of pulverized biomass. Energy & Fuels 19 (2005): 2164-2171.

[89] Worasuwannarak, N., Wannapeera, J. and Fungtammasan, B., Pyrolysis behaviors of woody biomass torrefied at temperatures below 300^{O}C, in: Clean Energy and Technology (CET), 2011 IEEE First Conference on, 2011, pp. 287-290.

[90] Hosokai, S., Hayashi, J.I., Shimada, T., Kobayashi, Y., Kuramoto, K., Li, C.Z. and Chiba, T. Spontaneous Generation of Tar Decomposition Promoter in a Biomass Steam Reformer. Chemical Engineering Research and Design 83 (2005): 1093-1102.

[91] Rouzaud, J.N., Vogt, D. and Oberlin, A. Coke properties and their microtexture Part I: Microtextural analysis: A guide for cokemaking. Fuel Processing Technology 20 (1988): 143-154.

[92] Yip, K., Tian, F.J., Hayashi, J. and Wu, H.W. Effect of Alkali and Alkaline Earth Metallic Species on Biochar Reactivity and Syngas Compositions during Steam Gasification. Energy & Fuels 24 (2010): 173-181.

[93] C.Z., J.K.a.L. Volatilisation and Catalytic Effects of AAEM species on Reactivity of char from Pyrolysis and Gasification of Victorian Brown Coal. Journal of Energy and Environment 5 (2006): 31-44.

[94] Zanzi, R., Sjöström, K. and Björnbom, E. Rapid high-temperature pyrolysis of biomass in a free-fall reactor. Fuel 75 (1996): 545-550.

[95] Chaiprasert, P. and Vitidsant, T. Effects of promoters on biomass gasification using nickel/dolomite catalyst. Korean Journal of Chemical Engineering 26 (2009): 1545-1549.

[96] Fushimi, C., Araki, K., Yamaguchi, Y. and Tsutsumi, A. Effect of heating rate on steam gasification of biomass. 1. Reactivity of char. Industrial & Engineering Chemistry Research 42 (2003): 3922-3928.

[97] Onay, O. Influence of pyrolysis temperature and heating rate on the production of bio-oil and char from safflower seed by pyrolysis, using a well-swept fixed-bed reactor. Fuel Processing Technology 88 (2007): 523-531.

[98] Hosoya, T., Kawamoto, H. and Saka, S. Solid/liquid- and vapor-phase interactions between cellulose- and lignin-derived pyrolysis products. Journal of Analytical and Applied Pyrolysis 85 (2009): 237-246.

[99] Krerkkaiwan, S., Yamamoto, H., Fushimi, C., Tsutsumi, A. and Kuchonthara, P. Co-gasification of Indonesian coal and Thai biomass : Investigation of experimental conditions. Prodeeding of coal science conference (2011): 114-115.

[100] Mermoud, F., Salvador, S., Van de Steene, L. and Golfier, F. Influence of the pyrolysis heating rate on the steam gasification rate of large wood char particles. Fuel 85 (2006): 1473-1482.

[101] Carter, S.D., Taulbee, D.N. and Robl, T.L. The relative coke-inducing tendencies of pyrolysed, gasified and combusted Devonian oil shales. Fuel 72 (1993): 851-854.

[102] Wu, H., Quyn, D.M. and Li, C.-Z. Volatilisation and catalytic effects of alkali and alkaline earth metallic species during the pyrolysis and gasification of Victorian brown coal. Part III. The importance of the interactions between volatiles and char at high temperature. Fuel 81 (2002): 1033-1039.

[103] Hanaoka, T., Inoue, S., Uno, S., Ogi, T. and Minowa, T. Effect of woody biomass components on air-steam gasification. Biomass & Bioenergy 28 (2005): 69-76.

[104] Wu, C., Wang, Z., Huang, J. and Williams, P.T. Pyrolysis/gasification of cellulose, hemicellulose and lignin for hydrogen production in the presence of various nickel-based catalysts. Fuel.

[105] Hosokai, S., Norinaga, K., Kimura, T., Nakano, M., Li, C.Z. and Hayashi, J. Reforming of Volatiles from the Biomass Pyrolysis over Charcoal in a Sequence of Coke Deposition and Steam Gasification of Coke. Energy & Fuels 25 (2011): 5387-5393.

[106] Bai, Z., Chen, H., Li, W. and Li, B. Hydrogen production by methane decomposition over coal char. International Journal of Hydrogen Energy 31 (2006): 899-905.

[107] Zhang, D. Thermal Decompostion of Coal in, Coal, Oil shale, Natural bitumen, Heavy oil and Peat, pp. Encyclopedia of life Support System.

[108] Singla, P.K., Miura, S., Hudgins, R.R. and Silveston, P.L. Pore development during carbonization of coals. Fuel 62 (1983): 645-648.

[109] Wang, J., Du, J., Chang, L. and Xie, K. Study on the structure and pyrolysis characteristics of Chinese western coals. Fuel Processing Technology 91 (2010): 430-433.

[110] Tsai, W.T., Lee, M.K. and Chang, Y.M. Fast pyrolysis of rice straw, sugarcane bagasse and coconut shell in an induction-heating reactor. Journal of Analytical and Applied Pyrolysis 76 (2006): 230-237.

[111] Hashimoto, K., Miura, K., Xu, J.-J., Watanabe, A. and Masukami, H. Relation between the gasification rate of carbons supporting alkali metal salts and the amount of oxygen trapped by the metal. Fuel 65 (1986): 489-494.

[112] Wigmans, T., Elfring, R. and Moulijn, J.A. On the mechanism of the potassium carbonate catalysed gasification of activated carbon: the influence of the catalyst concentration on the reactivity and selectivity at low steam pressures. Carbon 21 (1983): 1-12.

[113] Yang, H., Yan, R., Chen, H., Lee, D.H. and Zheng, C. Characteristics of hemicellulose, cellulose and lignin pyrolysis. Fuel 86 (2007): 1781-1788.

[114] Fu, P., Yi, W., Bai, X., Li, Z., Hu, S. and Xiang, J. Effect of temperature on gas composition and char structural features of pyrolyzed agricultural residues. Bioresource Technology 102 (2011): 8211-8219.

[115] Shi, L., Yu, S., Wang, F.-C. and Wang, J. Pyrolytic characteristics of rice straw and its constituents catalyzed by internal alkali and alkali earth metals. Fuel 96 (2012): 586-594.

[116] Trimm, D.L. Coke formation and minimisation during steam reforming reactions. Catalysis Today 37 (1997): 233-238.

[117] Ministry of Energy. Thailand [online]. THAILAND'S ENERGY SITUATION IN 2010 AND TREND IN 2011. Available from: http://www.dede.go.th [12 Mar 2013]

APPENDICES

APPENDIX A

DATA FROM DROP TUBE FIXED-BED REACTOR

A1 Co-pyrolysis data

Co-pyrolysis experiments were carried out in a drop tube fixed-bed reactor mentioned in Chapter III. All experiments were examined with 2 or 3 replicates. The average gas production with an acceptable standard deviation (SD) was reported in Chapter IV and the raw data are shown in Table A.1.

Table A1 Gas production of the co-pyrolysis of coal/RS and coal/LN at various reaction temperatures and biomass to coal ratios

No.	Sample / temp. (^{O}C)	Biomass : coal ratio (w/w)	No. replicate	Gas production (mmol/g-sample)				Char yield (wt%)
1	RS/Coal 600	1 : 0		H_2	CO	CH_4	CO_2	
			1	1.545	4.059	1.150	3.543	24.389
			2	1.538	4.927	1.458	2.537	26.887
			average	1.541	4.493	1.304	3.040	25.638
			SD	0.005	0.614	0.218	0.711	1.767
2	RS/Coal 600	1 : 1		H_2	CO	CH_4	CO_2	Char yield (wt%)
			1	1.560	2.571	0.773	3.012	32.989
			2	1.790	2.932	0.872	2.900	32.139
			average	1.675	2.752	0.822	2.956	32.564
			SD	0.163	0.255	0.070	0.079	0.601
3	RS/Coal 600	0 : 1		H_2	CO	CH_4	CO_2	Char yield (wt%)
			1	1.986	1.130	0.553	2.675	43.806
			2	2.116	1.777	0.753	2.318	44.450
			average	2.051	1.454	0.653	2.496	44.128
			SD	0.092	0.457	0.141	0.253	0.456

Table A1 (cont.) Gas production of the co-pyrolysis of coal/RS and coal/LN

No.	Sample / temp.	Biomass : coal ratio (w/w)	No. replicate	Gas production (mmol/g-sample)				Char yield (wt%)
4	RS/Coal 700	1 : 0		H_2	CO	CH_4	CO_2	
			1	2.631	5.893	1.483	3.259	24.479
			2	2.578	6.347	1.609	3.046	23.234
			average	2.604	6.120	1.546	3.152	23.857
			SD	0.038	0.321	0.089	0.150	0.881
5	RS/Coal 700	1 : 1		H_2	CO	CH_4	CO_2	Char yield (wt%)
			1	4.157	4.735	1.731	3.239	29.787
			2	3.831	5.226	1.330	2.879	29.641
			average	3.994	4.980	1.531	3.059	29.714
			SD	0.230	0.347	0.283	0.254	0.103
6	RS/Coal 700	0 : 1		H_2	CO	CH_4	CO_2	Char yield (wt%)
			1	4.497	3.058	0.917	4.312	33.941
			2	4.925	4.144	1.296	3.188	35.251
			average	4.711	3.601	1.107	3.750	34.596
			SD	0.303	0.768	0.268	0.795	0.927
7	RS/Coal 800	1 : 0		H_2	CO	CH_4	CO_2	Char yield (wt%)
			1	4.966	13.539	2.613	4.039	21.184
			2	6.378	13.309	3.288	3.812	-
			average	5.672	13.424	2.951	3.925	21.184
			SD	0.998	0.162	0.477	0.160	-
8	RS/Coal 800	1 : 3		H_2	CO	CH_4	CO_2	Char yield (wt%)
			1	9.186	10.442	1.878	2.677	29.25
			2	6.636	10.167	1.661	3.025	-
			average	7.911	10.305	1.769	2.851	29.25
			SD	1.803	0.194	0.154	0.246	-

Table A1 (cont.) Gas production of the co-pyrolysis of coal/RS and coal/LN

No.	Sample / temp.	Biomass : coal ratio (w/w)	No. replicate	Gas production (mmol/g-sample)				Char yield (wt%)
9	RS/Coal 800	1 : 1		H_2	CO	CH_4	CO_2	
			1	6.949	12.796	2.012	4.782	27.500
			2	6.251	12.101	1.933	4.525	-
			average	6.315	12.263	1.965	4.804	27.500
			SD	0.605	0.473	0.042	0.290	-
10	RS/Coal 800	3 : 1		H_2	CO	CH_4	CO_2	Char yield (wt%)
			1	7.306	11.521	2.304	3.152	24.260
			2	5.462	10.931	2.043	3.460	24.260
			average	6.384	11.226	2.173	3.306	24.260
			SD	1.303	0.417	0.185	0.218	0
11	RS/Coal 800	0 : 1		H_2	CO	CH_4	CO_2	Char yield (wt%)
			1	7.392	7.910	1.466	2.549	36.912
			2	7.213	6.199	1.754	3.575	34.377
			average	7.303	7.055	1.610	3.062	35.644
			SD	0.127	1.210	0.203	0.725	1.792
12	LN/Coal 600	1 : 0		H_2	CO	CH_4	CO_2	Char yield (wt%)
			1	1.430	4.507	1.174	3.632	20.199
			2	1.873	6.966	1.655	2.838	23.364
			average	1.652	5.736	1.414	3.235	21.781
			SD	0.314	1.738	0.340	0.561	2.239
13	LN/Coal 600	1 : 1		H_2	CO	CH_4	CO_2	Char yield (wt%)
			1	2.307	3.931	1.160	2.988	29.596
			2	1.891	3.886	1.050	3.196	30.887
			average	2.099	3.909	1.105	3.092	30.242
			SD	0.294	0.031	0.078	0.147	0.912

Table A1 (cont.) Gas production of the co-pyrolysis of coal/RS and coal/LN

No.	Sample / temp.	Biomass : coal ratio (w/w)	No. replicate	Gas production (mmol/g-sample)				Char yield (wt%)
14	LN/Coal 600	0 : 1		H_2	CO	CH_4	CO_2	
			1	1.986	1.130	0.553	2.675	43.806
			2	2.116	1.777	0.753	2.318	44.450
			average	2.051	1.454	0.653	2.496	44.128
			SD	0.092	0.457	0.141	0.253	0.456
15	LN/Coal 700	1 : 0		H_2	CO	CH_4	CO_2	Char yield (wt%)
			1	3.658	10.859	2.914	2.478	10.219
			2	3.481	9.407	2.440	2.395	17.892
			average	3.570	10.133	2.677	2.437	14.055
			SD	0.125	1.027	0.335	0.058	5.426
16	LN/Coal 700	1 : 1		H_2	CO	CH_4	CO_2	Char yield (wt%)
			1	5.060	7.450	2.145	3.768	23.712
			2	4.724	6.412	1.894	3.377	26.145
			average	4.892	6.931	2.019	3.572	24.929
			SD	0.237	0.734	0.177	0.277	1.720
17	LN/Coal 700	0 : 1		H_2	CO	CH_4	CO_2	Char yield (wt%)
			1	4.497	3.058	0.917	4.312	33.941
			2	4.925	4.144	1.296	3.188	35.251
			average	4.711	3.601	1.107	3.750	34.596
			SD	0.303	0.768	0.268	0.795	0.927
18	LN/Coal 800	1 : 0		H_2	CO	CH_4	CO_2	Char yield (wt%)
			1	3.657	11.340	2.526	4.231	21.025
			2	5.153	12.643	2.396	3.330	-
			average	4.405	11.992	2.461	3.781	21.025
			SD	1.058	0.921	0.092	0.637	-

Table A1 (cont.) Gas production of the co-pyrolysis of coal/RS and coal/LN

No.	Sample / temp.	Biomass : coal ratio (w/w)	No. replicate	Gas production (mmol/g-sample)				Char yield (wt%)
19	LN/Coal 800	1 : 3		H_2	CO	CH_4	CO_2	
			1	8.190	10.256	1.808	2.882	20.965
			2	6.913	11.009	1.673	2.894	-
			average	7.551	10.633	1.741	2.888	20.965
			SD	0.903	0.532	0.095	0.008	-
20	LN/Coal 800	1 : 1		H_2	CO	CH_4	CO_2	Char yield (wt%)
			1	7.052	14.322	1.974	4.113	25.030
			2	6.836	14.039	2.086	4.158	-
			average	6.944	14.181	2.030	4.136	25.030
			SD	0.152	0.200	0.079	0.032	-
21	LN/Coal 800	3 : 1		H_2	CO	CH_4	CO_2	Char yield (wt%)
			1	7.072	12.273	2.375	3.260	30.708
			2	5.797	13.629	2.214	2.958	-
			average	6.435	12.951	2.295	3.109	30.708
			SD	0.902	0.958	0.113	0.214	-
22	LN/Coal 800	0 : 1		H_2	CO	CH_4	CO_2	Char yield (wt%)
			1	7.392	7.910	1.466	2.549	36.912
			2	7.213	6.199	1.754	3.575	34.377
			average	7.303	7.055	1.610	3.062	35.644
			SD	0.127	1.210	0.203	0.725	1.792

A2 Co-gasification data

Co-gasification experiments were carried out in a drop tube fixed-bed reactor. All experiments were examined with 2 or 3 replicates. The average gas productions with an acceptable standard deviation (SD) were reported in Chapter IV and the raw data are shown in Table A-2. Steam content was about 60 % by volume.

Table A2 Gas production of the co-gasification of coal/RS and coal/LN at various reaction temperatures and biomass to coal ratios

No.	Sample / temp. (^{O}C)	Biomass : coal ratio (w/w)	No. replicate	Gas production (mmol/g-sample)				Char yield (wt%)
1	RS/Coal 600	1 : 0		H_2	CO	CH_4	CO_2	
			1	0.882	3.849	0.772	7.022	16.86
			2	0.711	2.990	0.599	7.234	-
			average	0.797	3.419	0.685	7.128	16.86
			SD	0.121	0.608	0.123	0.150	-
2	RS/Coal 600	1 : 3		H_2	CO	CH_4	CO_2	Char yield (wt%)
			1	3.259	2.822	0.751	6.389	25.395
			2	4.210	2.845	1.014	6.257	-
			average	3.735	2.834	0.882	6.323	25.395
			SD	0.672	0.017	0.186	0.094	-
3	RS/Coal 600	1 : 1		H_2	CO	CH_4	CO_2	Char yield (wt%)
			1	3.270	3.058	0.823	4.384	27.95
			2	1.820	2.908	0.711	4.762	-
			average	2.545	2.983	0.767	4.573	27.95
			SD	1.025	0.106	0.080	0.267	-

Table A2 (cont.) Gas production of the co-gasification of coal/RS and coal/LN

No.	Sample / temp. (^{O}C)	Biomass : coal ratio (w/w)	No. replicate	Gas production (mmol/g-sample)				Char yield (wt%)
4	RS/Coal 600	3 : 1		H_2	CO	CH_4	CO_2	
			1	1.685	3.005	0.693	7.216	20.21
			2	1.575	4.098	0.913	6.566	-
			average	1.630	3.551	0.803	6.891	20.21
			SD	0.078	0.773	0.155	0.460	-
5	RS/Coal 600	0 : 1		H_2	CO	CH_4	CO_2	Char yield (wt%)
			1	4.490	1.454	0.612	5.203	9.15
			2	4.330	1.760	0.707	5.011	-
			average	4.410	1.607	0.659	5.107	9.15
			SD	0.113	0.217	0.067	0.136	-
6	RS/Coal 700	1 : 0		H_2	CO	CH_4	CO_2	Char yield (wt%)
			1	3.688	7.619	1.575	4.863	13.145
			2	2.967	7.715	1.647	4.348	-
			average	3.327	7.667	1.611	4.606	13.145
			SD	0.510	0.068	0.051	0.364	-
7	RS/Coal 700	1 : 3		H_2	CO	CH_4	CO_2	Char yield (wt%)
			1	10.990	3.901	1.245	7.393	15.68
			2	9.018	4.078	1.255	6.086	-
			average	10.004	3.990	1.250	6.740	15.68
			SD	1.394	0.125	0.007	0.924	-
8	RS/Coal 700	1 : 1		H_2	CO	CH_4	CO_2	Char yield (wt%)
			1	7.298	5.097	1.282	6.307	15.24
			2	3.613	4.899	1.526	4.540	-
			average	5.456	4.998	1.404	5.423	15.24
			SD	2.605	0.140	0.172	1.249	-

Table A2 (cont.) Gas production of the co-gasification of coal/RS and coal/LN

No.	Sample / temp. (^{O}C)	Biomass : coal ratio (w/w)	No. replicate	Gas production (mmol/g-sample)				Char yield (wt%)
9	RS/Coal 700	3 : 1		H_2	CO	CH_4	CO_2	
			1	5.615	5.536	1.226	5.232	16.51
			2	3.963	5.534	1.163	5.247	-
			average	4.789	5.535	1.195	5.240	16.51
			SD	1.168	0.001	0.044	0.010	-
10	RS/Coal 700	0 : 1		H_2	CO	CH_4	CO_2	Char yield (wt%)
			1	11.703	2.907	1.018	7.755	7.98
			2	8.839	3.363	0.965	7.125	-
			average	10.271	3.135	0.992	7.440	7.98
			SD	2.026	0.322	0.038	0.446	-
11	RS/Coal 800	1 : 0		H_2	CO	CH_4	CO_2	Char yield (wt%)
			1	10.701	11.889	2.219	5.835	8.00
			2	10.357	10.670	2.285	6.956	-
			average	10.529	11.280	2.252	6.395	8.00
			SD	0.244	0.862	0.046	0.793	-
12	RS/Coal 800	1 : 3		H_2	CO	CH_4	CO_2	Char yield (wt%)
			1	29.729	9.848	1.494	15.855	8.613
			2	32.206	9.028	1.533	16.542	-
			average	30.967	9.438	1.514	16.198	8.613
			SD	1.751	0.580	0.027	0.485	-
13	RS/Coal 800	1 : 1		H_2	CO	CH_4	CO_2	Char yield (wt%)
			1	26.602	12.198	2.288	13.095	8.613
			2	28.557	12.161	1.955	13.283	-
			average	27.579	12.180	2.121	13.189	8.613
			SD	1.382	0.026	0.235	0.133	-

Table A2 (cont.) Gas production of the co-gasification of coal/RS and coal/LN

No.	Sample / temp. (^{O}C)	Biomass : coal ratio (w/w)	No. replicate	Gas production (mmol/g-sample)				Char yield (wt%)
14	RS/Coal 800	3 : 1		H_2	CO	CH_4	CO_2	
			1	16.283	12.175	2.145	9.559	9.287
			2	17.359	13.133	2.224	10.333	7.367
			3	18.381	12.434	2.113	10.598	-
			average	17.341	12.581	2.161	10.165	8.327
			SD	1.049	0.496	0.057	0.583	1.358
15	RS/Coal 800	0 : 1		H_2	CO	CH_4	CO_2	Char yield (wt%)
			1	37.466	8.904	1.396	17.207	4.944
			2	38.079	8.703	1.487	18.020	3.905
			average	37.773	8.804	1.442	17.614	4.425
			SD	0.433	0.142	0.065	0.575	0.735
16	LN/Coal 600	1 : 0		H_2	CO	CH_4	CO_2	Char yield (wt%)
			1	1.521	4.431	1.063	4.823	8.19
			2	1.604	3.893	0.981	5.660	-
			average	1.562	4.162	1.022	5.242	8.19
			SD	0.059	0.380	0.058	0.592	-
17	LN/Coal 600	1 : 3		H_2	CO	CH_4	CO_2	Char yield (wt%)
			1	2.341	2.237	0.962	5.226	25.395
			2	3.339	2.633	0.897	4.654	-
			average	2.840	2.435	0.929	4.940	25.395
			SD	0.706	0.280	0.046	0.405	-

Table A2 (cont.) Gas production of the co-gasification of coal/RS and coal/LN

No.	Sample / temp. (^{O}C)	Biomass : coal ratio (w/w)	No. replicate	Gas production (mmol/g-sample)				Char yield (wt%)
18	LN/Coal 600	1 : 1		H_2	CO	CH_4	CO_2	Char yield (wt%)
			1	3.235	3.757	1.027	5.403	24.955
			2	2.825	3.340	1.021	5.732	-
			average	3.030	3.548	1.024	5.567	24.955
			SD	0.290	0.295	0.004	0.232	-
19	LN/Coal 600	3 : 1		H_2	CO	CH_4	CO_2	
			1	2.369	3.694	0.922	5.685	25.395
			2	1.565	3.648	0.895	6.495	-
			average	1.967	3.671	0.908	6.090	25.395
			SD	0.569	0.032	0.019	0.573	-
20	LN/Coal 600	0 : 1		H_2	CO	CH_4	CO_2	Char yield (wt%)
			1	4.490	1.454	0.612	5.203	8.19
			2	4.330	1.760	0.707	5.011	-
			average	4.410	1.607	0.659	5.107	8.19
			SD	0.113	0.217	0.067	0.136	-
21	LN/Coal 700	1 : 0		H_2	CO	CH_4	CO_2	Char yield (wt%)
			1	5.385	9.804	1.902	6.513	7.37
			2	5.011	10.249	1.949	5.579	-
			average	5.198	10.026	1.925	6.046	7.37
			SD	0.264	0.315	0.034	0.661	-
22	LN/Coal 700	1 : 3		H_2	CO	CH_4	CO_2	Char yield (wt%)
			1	10.767	3.972	1.183	7.251	14.00
			2	9.421	4.422	1.334	6.517	-
			average	10.094	4.197	1.258	6.884	14.00
			SD	0.951	0.318	0.106	0.519	-

Table A2 (cont.) Gas production of the co-gasification of coal/RS and coal/LN

No.	Sample / temp. (^{O}C)	Biomass : coal ratio (w/w)	No. replicate	Gas production (mmol/g-sample)				Char yield (wt%)
23	LN/Coal 700	1 : 1		H_2	CO	CH_4	CO_2	Char yield (wt%)
			1	11.843	5.844	1.416	8.048	22.67
			2					-
			average	11.843	5.844	1.416	8.048	22.67
				SD				-
24	LN/Coal 700	3 : 1		H_2	CO	CH_4	CO_2	
			1	8.307	7.471	1.815	7.063	14.93
			2	-	-	-	-	-
			average	8.307	7.471	1.815	7.063	14.93
			SD	-	-	-	-	-
25	LN/Coal 700	0 : 1		H_2	CO	CH_4	CO_2	Char yield (wt%)
			1	11.703	2.907	1.018	7.755	7.98
			2	8.839	3.363	0.965	7.125	-
			average	10.271	3.135	0.992	7.440	7.98
			SD	2.026	0.322	0.038	0.446	-
26	LN/Coal 800	1 : 0		H_2	CO	CH_4	CO_2	Char yield (wt%)
			1	7.077	10.556	2.283	6.954	13.973
			2	10.311	11.586	2.528	7.206	13.199
			average	8.694	11.071	2.405	7.080	13.586
			SD	2.287	0.729	0.173	0.178	0.547

Table A2 (cont.) Gas production of the co-gasification of coal/RS and coal/LN

No.	Sample / temp. (^{O}C)	Biomass : coal ratio (w/w)	No. replicate	Gas production (mmol/g-sample)				Char yield (wt%)
27	LN/Coal 800	1 : 3		H_2	CO	CH_4	CO_2	Char yield (wt%)
			1	29.392	10.052	2.672	15.552	8.723
			2	32.114	10.581	1.691	16.236	9.282
			average	30.753	10.317	2.182	15.894	8.066
			SD	1.925	0.374	0.694	0.484	0.395
28	LN/Coal 800	1 : 1		H_2	CO	CH_4	CO_2	Char yield (wt%)
			1	23.407	9.723	1.870	13.870	14.056
			2	26.635	10.745	2.089	13.345	13.143
			average	25.021	10.234	1.980	13.608	13.850
			SD	2.282	0.723	0.155	0.371	0.646
29	LN/Coal 800	3 : 1		H_2	CO	CH_4	CO_2	
			1	19.643	11.010	2.204	11.438	15.749
			2	19.932	10.989	2.222	12.421	16.617
			average	19.787	11.000	2.213	11.929	16.183
			SD	0.205	0.015	0.013	0.695	0.614
30	LN/Coal 800	0 : 1		H_2	CO	CH_4	CO_2	Char yield (wt%)
			1	37.466	8.904	1.396	17.207	4.944
			2	38.079	8.703	1.487	18.020	3.905
			average	37.773	8.804	1.442	17.614	4.425
			SD	0.433	0.142	0.065	0.575	0.735

A3 Calculation of the predicted values

In co-pyrolysis and co-gasification, the calculation yield (Y_{cal}) of coal/biomass blend was obtained by following equation;

$$Y_{cal} = X_b \times Y_b + (1 - X_b) \times Y_c \quad (3.1)$$

,where X_b is the mass fraction of biomass in the mixture, Y_b and Y_c are the yield of coal and biomass individually. All predicted values are calculated from the average values obtained from the experiment of individual feeds. The predicted values of co-pyrolysis and co-gasification are shown in Table A-3 and Table A-4, respectively.

Table A3 Predicted gas productions obtained from the pyrolysis of coal, RS and LN at various reaction temperatures

No.	Sample / temp.	Biomass : coal ratio (w/w)	Gas production (mmol/g-sample)				Char yield (wt%)
			H_2	CO	CH_4	CO_2	
1	RS/Coal 600	1 : 1	1.796	2.973	0.978	2.768	34.883
2	RS/Coal 700	1 : 1	3.658	4.861	1.326	3.451	31.649
3	RS/Coal 800	1 : 3	6.895	8.647	1.945	3.278	32.364
4	RS/Coal 800	1 : 1	6.488	10.239	2.280	3.494	28.585
5	RS/Coal 800	3 : 1	6.080	11.832	2.615	3.710	24.805
6	LN/Coal 600	1 : 1	1.851	3.595	1.033	2.866	37.185
7	LN/Coal 700	1 : 1	4.802	5.266	1.563	3.661	36.693
8	LN/Coal 800	1 : 3	6.578	8.289	1.823	3.242	33.186
9	LN/Coal 800	1 : 1	5.854	9.523	2.035	3.421	30.227
10	LN/Coal 800	3 : 1	5.130	10.757	2.248	3.601	27.269

Table A4 Predicted gas productions obtained from the steam gasification of coal, RS and LN at various reaction temperatures

No.	Sample / temp.	Biomass : coal ratio (w/w)	Gas production (mmol/g-sample)			
			H_2	CO	CH_4	CO_2
1	RS/Coal 600	1 : 3	3.507	2.060	0.666	5.612
2	RS/Coal 600	1 : 1	2.603	2.513	0.672	6.117
3	RS/Coal 600	3 : 1	1.700	2.966	0.679	6.623
4	RS/Coal 700	1 : 3	8.535	4.268	1.146	6.731
5	RS/Coal 700	1 : 1	6.799	5.401	1.301	6.023
6	RS/Coal 700	3 : 1	5.063	6.534	1.456	5.314
7	RS/Coal 800	1 : 3	30.962	9.423	1.644	14.809
8	RS/Coal 800	1 : 1	24.151	10.042	1.847	12.005
9	RS/Coal 800	3 : 1	17.340	10.661	2.050	9.200
10	LN/Coal 600	1 : 3	3.698	2.246	0.750	5.141
11	LN/Coal 600	1 : 1	2.986	2.885	0.841	5.174
12	LN/Coal 600	3 : 1	2.240	3.523	0.931	5.208

Table A4 (cont.) Predicted gas productions obtained from the steam gasification of coal, RS and LN at various reaction temperatures

No.	Sample / temp.	Biomass : coal ratio (w/w)	Gas production (mmol/g-sample)			
			H_2	CO	CH_4	CO_2
10	LN/Coal 700	1 : 3	9.003	4.858	1.225	7.091
11	LN/Coal 700	1 : 1	7.735	6.581	1.458	6.743
12	LN/Coal 700	3 : 1	5.801	8.303	1.692	6.394
13	LN/Coal 800	1 : 3	60.053	30.503	9.371	1.683
14	LN/Coal 800	1 : 1	59.233	23.233	9.937	1.924
15	LN/Coal 800	3 : 1	58.414	15.964	10.504	2.164

APPENDIX B

DATA FROM THERMOBALANCE REACTOR

B1 Evaluation of relative mass of char over time during steam gasification

The steam gasification of char was explored in a thermobalance reactor which mentioned in Chapter III. The relative mass ($1\text{-}X_{char}$) of char, which presented in Chapter IV and V, was evaluated from the deviation of weight during char steam gasification and char steam gasification blank (no char placed in the ceramic basket). The example of net weight loss during steam gasification is shown in Figure B1. Note that W_p and W referred to the weight of char after pyrolysis and weight of char at any experiment time, respectively.

After char steam gasification, the remained char was combusted with O_2/Ar atmosphere and then the char combustion blank was explored. The weight difference during char combustion and char combustion blank was determined the weight of residues after steam gasification.

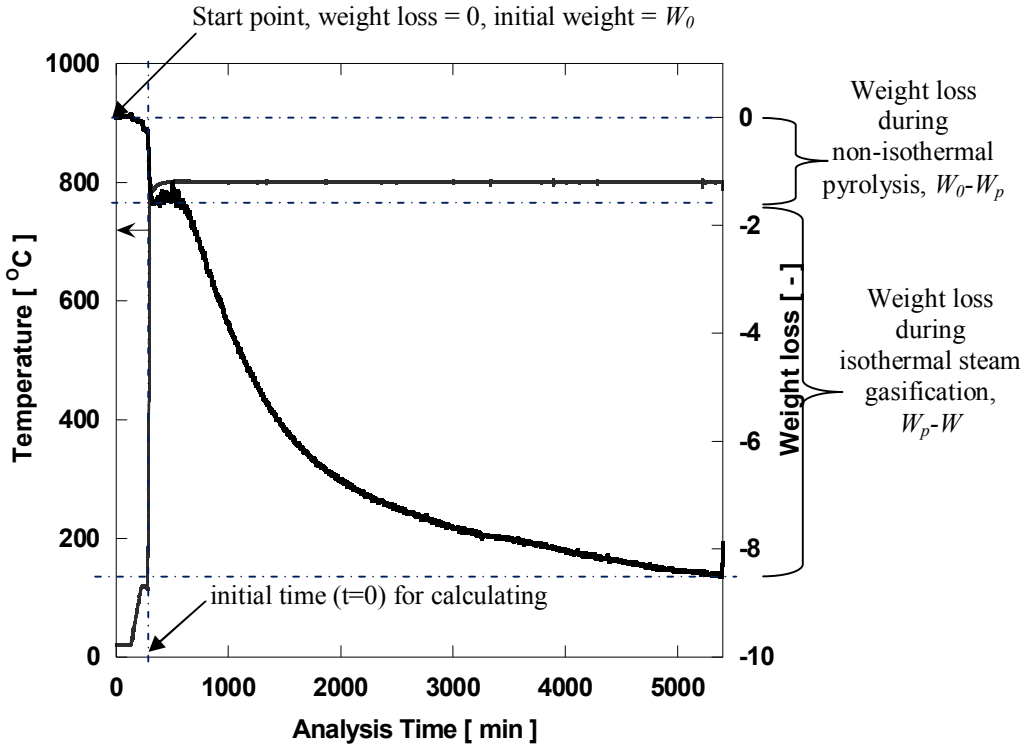

Figure B1 Net weight loss of the Ex-char during steam gasification at 800 °C

B2 Evaluation of overall rate constant (k_i) of char steam gasification

From the profile of weigh loss with time as described in section B1., the char conversion (X_{char}) was calculated by following equation:

$$X_{char} = \frac{X - X_p}{1 - X_p},$$

where X and X_p are the conversion of char at any time and the conversion of char during pyrolysis, respectively. The conversion of char (X) can be defined following equation:

$$X = 1 - \frac{W}{W_0},$$

where W and W_0 represented weight of sample at any experiment time and initial weight of sample, respectively.

The rate of char steam gasification was determined by assuming to obey the first-order kinetics and expressed in the equation below,

$$\frac{dX_{char}}{dt} = -k_i(1 - X_{char})$$

A linear relationship between ln(1-X_{char}) vs time (t) was generated with the correlation coefficient (R^2) almost unity, as expressed in the following equation:

$$\ln(1 - X_{char}) = -k_i t + C$$

,where C is constant. The overall rate constant (k_i) was defined as a slope of the linear equation.

B3 Determination of the overall rate constant (k_i) of all samples during steam gasification

B3.1 Coal/biomass mixtures

In Chapter IV, the steam gasification of char derived from the *in situ* pyrolysis of coal, RS, LN and coal/biomass blends was explored in a thermobalance reactor. The reactivity of char derived from the pyrolysis of the blends was compared with char derived from biomass and coal alone. The overall rate constant (k_i) was determined by plotting ln(1-X_{char}) vs time (t). A slope (-k), intercept and correlation coefficient (R^2) of the relationship are summarized in Table B1.

Table B1 Slope ($-k_i$), intercept and correlation coefficient (R^2) of the char derived from the *in situ* pyrolysis of coal, RS, LN and coal/biomass blends

No.	Sample	Biomass : coal (w/w)	Slope ($-k_i$)	Intercept	R^2
1	Pure Coal	-	-0.493×10^{-4}	-0.204	0.94
2	Coal/RS	1 : 3	-9.687×10^{-4}	0.069	0.99
3	Coal/RS	1 : 1	-10.362×10^{-4}	-0.036	0.99
4	Coal/LN	1 : 3	-8.021×10^{-4}	-0.472	0.90
5	Coal/LN	1 : 1	-12.767×10^{-4}	0.155	0.78
6	Pure RS	-	-6.892×10^{-4}	-0.496	0.73
7	Pure LN	-	-21.32×10^{-4}	-0.757	0.75

B3.2 Coal chars without the contact of volatiles

The overall rate constant of all prepared coal char during steam gasification at 800 ^{O}C were determined. The relationship between $\ln(1-X_{char})$ vs time (t) was plotted as shown in Figure B3. A slope ($-k$), intercept and correlation coefficient (R^2) of the relationship are summarized in Table B2.

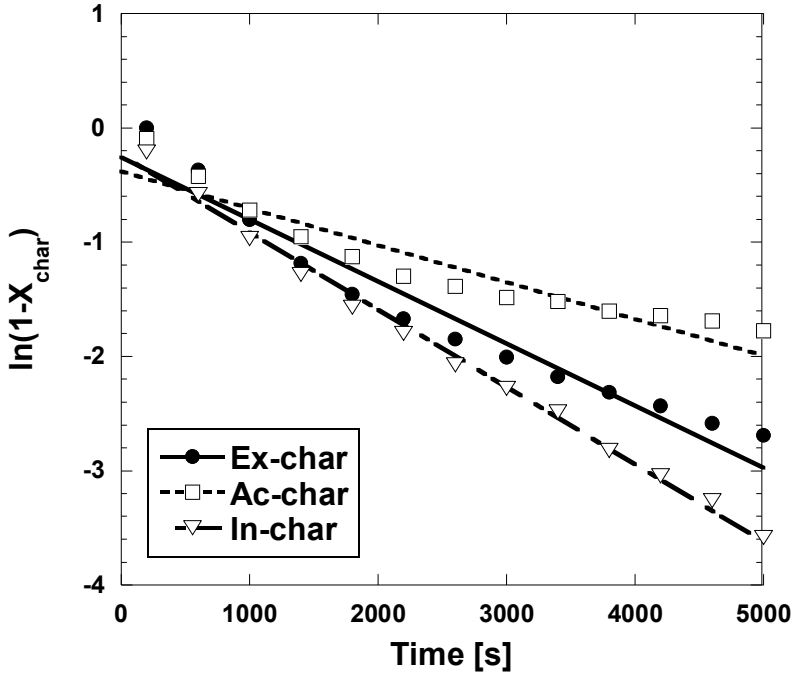

Figure B2 $\ln(1-X_{char})$ vs time (t) of Ex-char, Ac-char and In-char during steam gasification at 800 ^{O}C without the contact of volatiles

Table B2 Slope ($-k_i$), intercept and correlation coefficient (R^2) of the coal chars without the contact of volatiles

No.	Sample	Slope ($-k_i$)	Intercept	R^2
1	Ex-char	-5.436×10^{-4}	-0.258	0.95
2	Ac-char	-3.222×10^{-4}	-0.380	0.89
3	In-char	-6.758×10^{-4}	-0.238	0.99

B3.3 Coal chars with the contact of volatiles

The overall rate constant of all prepared coal char during steam gasification at 800 ^{O}C were determined. The relationship between ln(1-X_{char}) vs time (t) of the Ex-char, Ac-char and In-char with volatiles contacting are shown in Figure B4, B5 and B6, respectively. In addition, the slope (-k), intercept and correlation coefficient (R^2) of the relationship are summarized in Table B3.

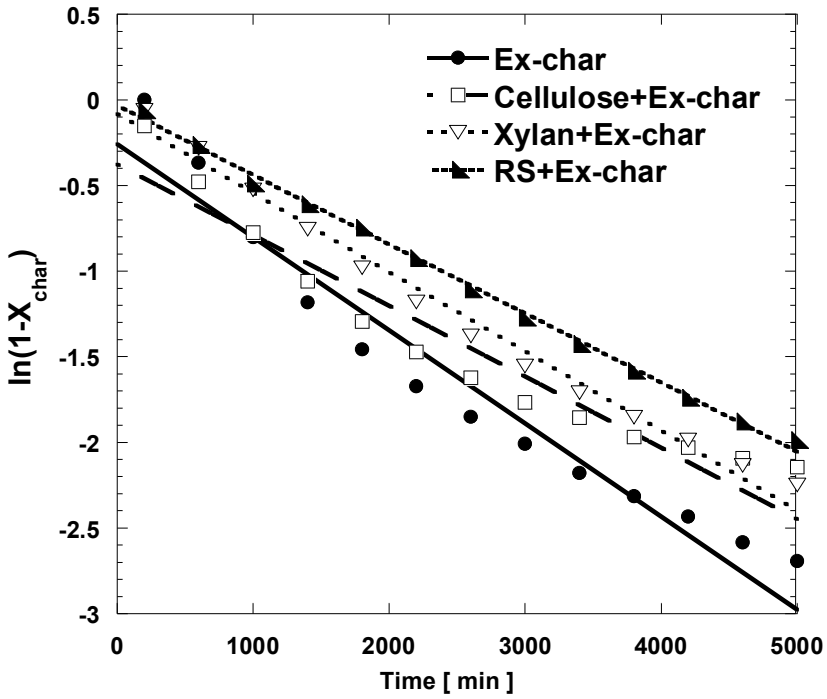

Figure B3 ln(1-X_{char}) vs time (t) of Ex-char during steam gasification at 800 ^{O}C with the contact of the different volatiles

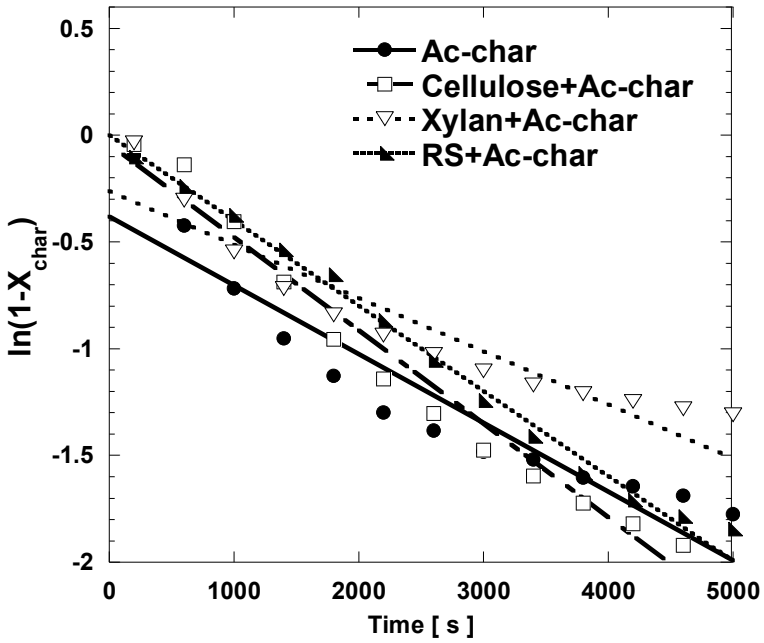

Figure B4 ln(1-X_{char}) vs time (t) of Ac-char during steam gasification at 800 ^{O}C with the contact of the different volatiles

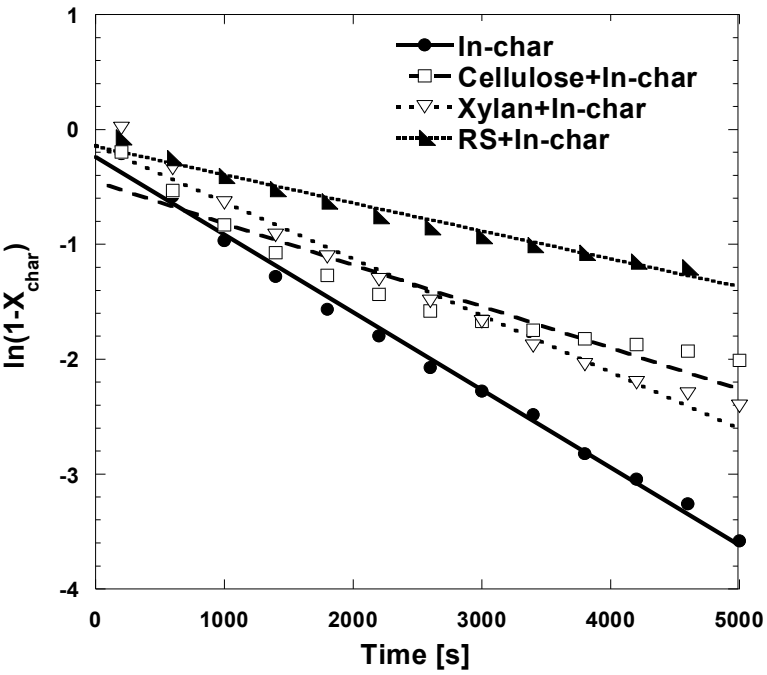

Figure B5 ln(1-X_{char}) vs time (t) of In-char during steam gasification at 800^{O}C with the contact of the different volatiles

Table B3 Slope ($-k_i$), intercept and correlation coefficient (R^2) of the prepared coal chars with the contact of the different types of volatiles

No.	Sample	Slope ($-k_i$)	Intercept	R^2
1	Ex-char	-5.436×10^{-4}	-0.258	0.95
2	Ex-char + cellulose	-4.143×10^{-4}	-0.3765	0.93
3	Ex-char + Xylan	-4.626×10^{-4}	-0.0839	0.99
4	Ex-char + rice straw	-5.436×10^{-4}	-0.0332	0.99
5	Ac-char	-3.222×10^{-4}	-0.380	0.89
6	Ac-char + cellulose	-4.372×10^{-4}	-0.041	0.97
7	Ac-char + Xylan	-2.503×10^{-4}	-0.261	0.90
8	Ac-char + rice straw	-3.991×10^{-4}	0.001	0.90
9	In-char	-6.758×10^{-4}	-0.238	0.99
10	In-char + cellulose	-3.617×10^{-4}	-0.452	0.91
11	In-char + Xylan	-4.934×10^{-4}	-0.137	0.98
12	In-char + rice straw	-2.441×10^{-4}	-0.146	0.97

B4 Evaluation of gas derived from the steam gasification of different types of volatile sources

As mentioned in Chapter III, the reactivity of coal char was detected simultaneously with the evolution of gas derived from the volatile sources (cellulose, xylan and rice straw). The reported gas evolution in Chapter V was determined by the evolution of gas which obtained from 3 types of experiment; experiment A (pure coal char and no feeding), experiment B (no coal char and volatile feeding) and experiment C (coal char presenting with volatile feeding). The image of three types of experiment is illustrated in Figure B7. With the presence of coal char (Exp. C), gas evolution from volatile sources was calculated from the deviation between gas production rate derived from experiment C and experiment A. Gas evolution rate over the steam gasification time derived from the steam gasification of all prepared coal chars are shown in Figures B8 to B10.

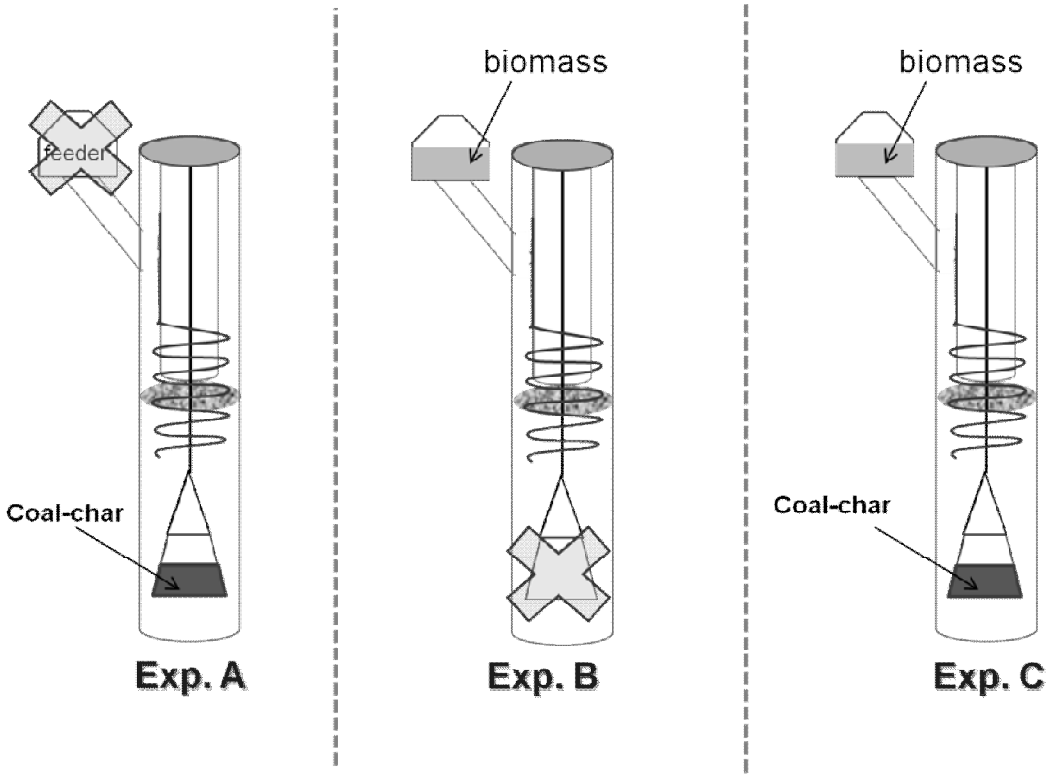

Figure B6 Three types of experiment of the steam gasification by using a thermobalance reactor

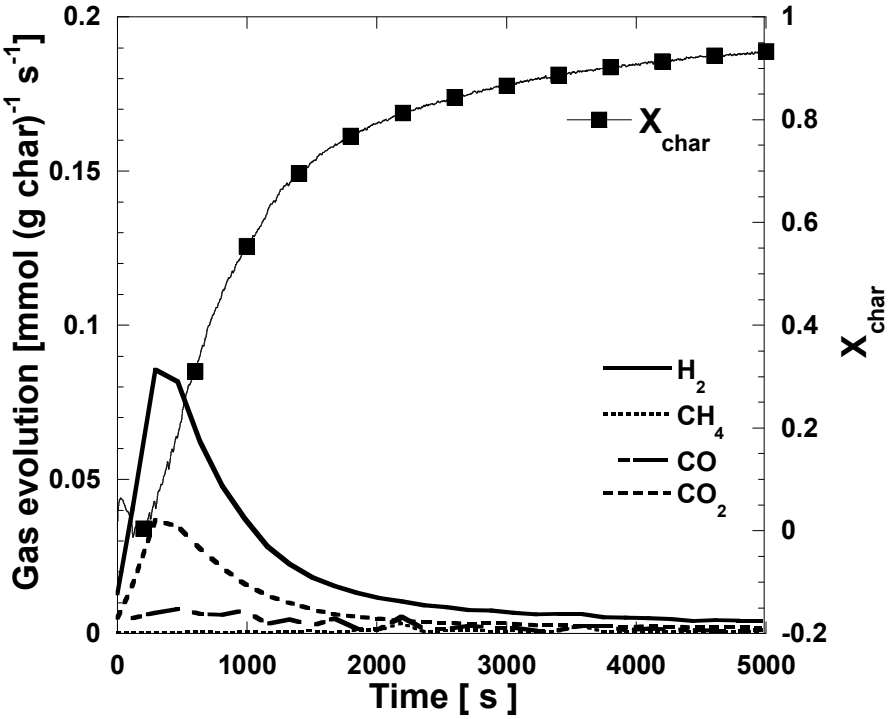

Figure B7 Gas evolution rate over time and char conversion (Xchar) during steam gasification of Ex-char

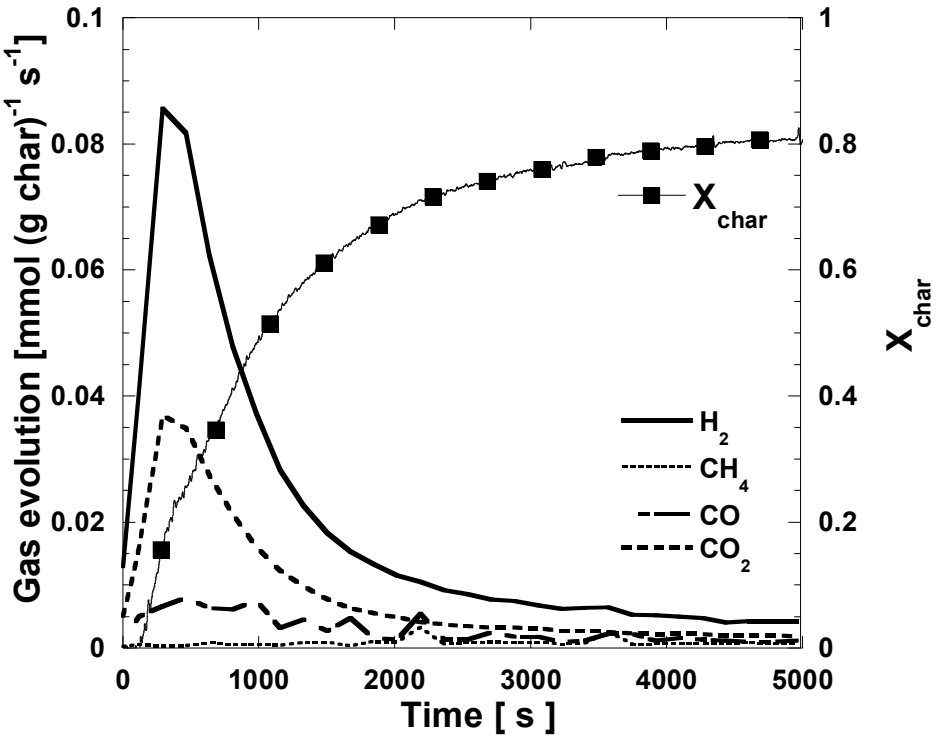

Figure B8 Gas evolution rate over time and char conversion (X_{char}) during steam gasification of Ac-char

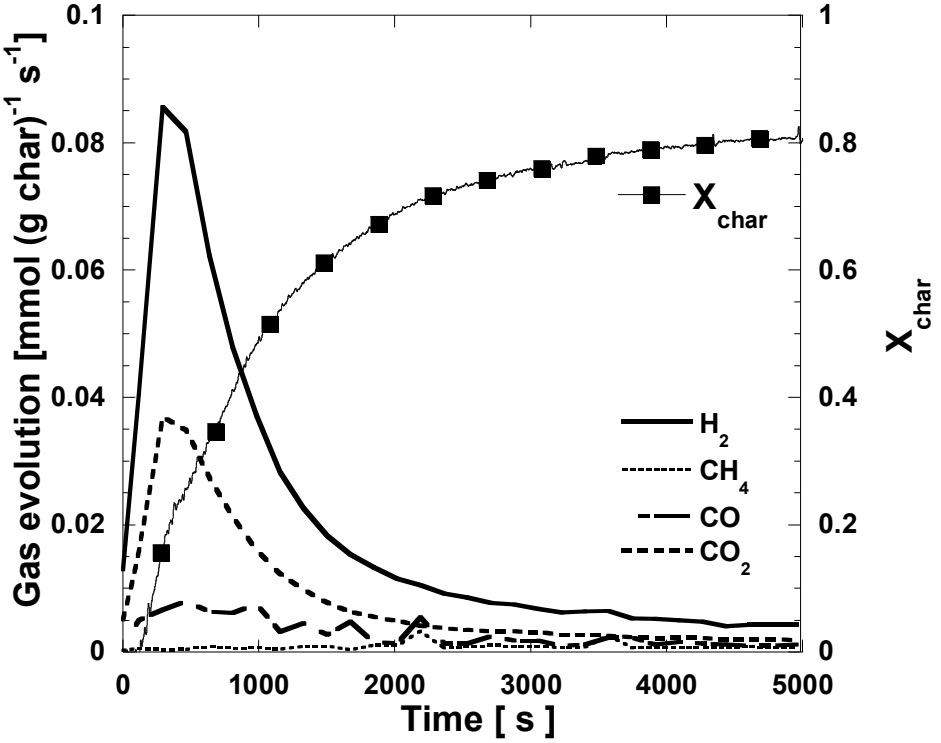

Figure B9 Gas evolution rate over time and char conversion (X_{char}) during steam gasification of In-char

APPENDIX C

DATA FROM TWO-STAGE FIXED BED REACTOR

C1 Evaluation of gas production from the two-stage fixed bed reactor

The data obtained from a two-stage fixed bed reactor was calculated from two types of experiments as shown in Figure C1. In chapter VI, the gas production of rice straw pyrolysis and steam gasification was calculated by the deviation gas production obtained from experiment A and B.

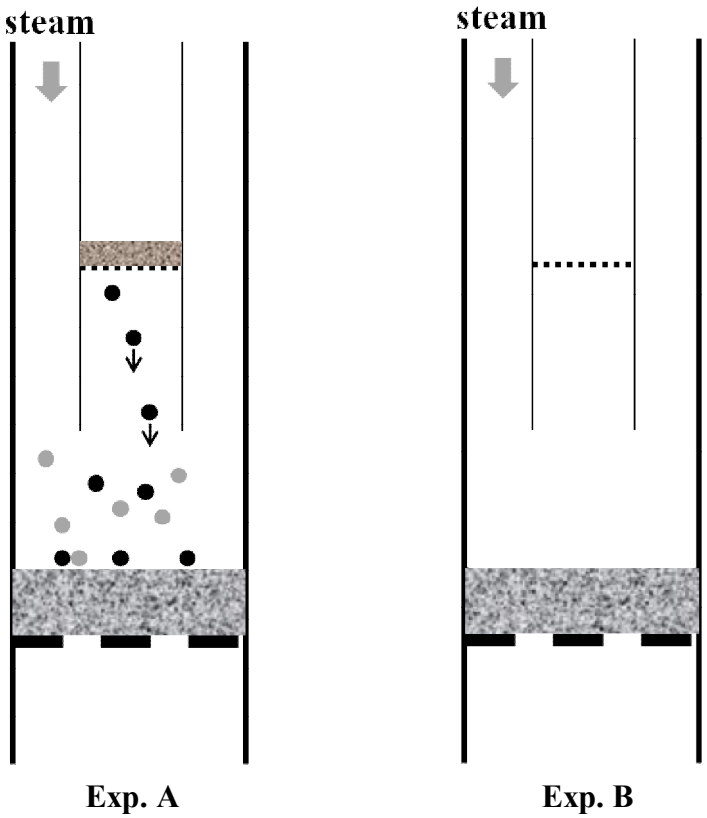

Figure C1 Two types of experiment of rice straw pyrolysis and steam gasification by using a two-stage fixed bed reactor

C2 Gas production obtained from the pyrolysis and steam gasification of prepared coal chars at 800^{O}C

Gas production rate obtained from the pyrolysis and steam gasification of the prepared coal chars at the temperature of volatile-char contacting zone of 800^{O}C is shown in Table C1.

Table C1 Gas production obtained from the pyrolysis and steam gasification of the prepared coal char at 800 ^{O}C

No.	Coal char bed	atmosphere	Gas production (mmol/min)			
			H_2	CO	CH_4	CO_2
1	Ex-char	inert Ar	0.0687	0.0760	0	0.0210
2	Ex-char800	inert Ar	0.0681	0.0951	0	0.0325
3	Ex-char	steam/Ar	0.1454	0.0318	0.000725	0.0495
4	Ex-char800	steam/Ar	0.1394	0.0212	0.000271	0.0555

BIOGRAPHY

Miss Supachita Krerkkaiwan was born on September 20th, 1985 at Chiangmai, Thailand. She received the bachelor degree of engineering in field of petrochemical and polymeric materials from faculty of engineering and industrial technology, Silpakorn University, and graduated the master degree of Sciences in chemical engineering from faculty of science, Chulalongkorn University. Supachita joined the Department of Chemical Technology, Chulalongkorn University, as a doctoral student in 2009. She has received the Royal Golden Jubilee Scholarship from Thailand Research Fund (2009 – 2012).

During graduate study, Supachita spent 9 months (2011) for doing research in Tsutsumi Laboratory at Collaborative Research Center for Energy Engineering in The University of Tokyo, Japan. Her first paper entitled "Synergetic effect during co-pyrolysis/gasification of biomass and sub-bituminous coal" has been accepted for publication in "Fuel processing technology". The second paper entitled "Biomass derived-tar decomposition over coal char bed" has been accepted for publication in "ScienceAsia". The third paper entitled "Volatile-char interaction during co-gasification of coal and biomass" is under reviewing for publication in "Fuel processing technology". She also presented her works at 1 conference in Japan (48^{th} Coal science conference at Tokimase Conventional hall, Niigata, Japan), 1 conference in Singapore (14^{th} Asia Pacific Confederation of Chemical Engineering Congress, APCChE 2012 at Suntec conventional hall) and 3 conferences in Thailand (The first is oral presentation at 3^{rd} Research Symposium on Petrochemical and Materials Technology, Queen Sirikit National Convention Center, The second is poster presentation at RGJ-Ph.D. Congress XIII in Pattaya and the last is poster presentation at 8^{th} Mathematics and Physical Sciences Graduate congress in Bangkok).